จุฬาลงกรณ์มหาวิทยาลัย
ทุนวิจัย
กองทุนรัชดาภิเษกสมโภช

รายงานผลการวิจัย

ปฏิกิริยาเอธีลีนออกไซด์บนตัวเร่งปฏิกิริยาโลหะเงิน ภายใต้ระบบพลาสมาอุณหภูมิต่ำแบบโคโรนาดีสชาร์จ

โดย
สุเมธ ชวเดช
ธรรมนูญ ศรีทะวงศ์
อโนทัย ตันสุวรรณ
ธนภูมิ สุวรรณบาตร์

ตุลาคม 2552

Acknowledgement

This research work was financially supported by the Ratchadapisek Somphot Fund, Chulalongkorn University.

ชื่อโครงการวิจัย	ปฏิกิริยาเอธีลีนออกไซด์บนตัวเร่งปฏิกิริยาโลหะเงินภายใต้ระบบพลาสมาอุณหภูมิต่ำแบบโคโรนาดีสชาร์จ
ชื่อผู้วิจัย	รศ. ดร. สุเมธ ชวเดช, ผศ. ดร. ธรรมนูญ ศรีทะวงศ์, นายอโนทัย ตันสุวรรณ, และ นายธนภูมิ สุวรรณบาตร์
เดือนและปีที่ทำการวิจัยเสร็จ	ตุลาคม 2552

บทคัดย่อ

ส่วนที่ 1: ในงานวิจัยนี้ กระบวนการอีพอกซิเดชันของเอธีลีนไปเป็นเอธีลีนออกไซด์ถูกทำการทดลองในเครื่องปฏิกรณ์พลาสมาอุณหภูมิต่ำแบบโคโรนาดีสชาร์จร่วมกับตัวเร่งปฏิกิริยา 3 ชนิด ได้แก่ โลหะเงินบนอลูมินาเฟสแอลฟาชนิดพื้นที่ผิวต่ำ โลหะเงินบนอลูมินาเฟสแอลฟาชนิดพื้นที่ผิวสูง และโลหะเงิน-โลหะทองบนอลูมินาเฟสแอลฟาชนิดพื้นที่ผิว จากผลการทดลองพบว่า ตัวเร่งปฏิกิริยาโลหะเงินบนอลูมินาเฟสแอลฟาชนิดพื้นที่ผิวต่ำให้ความเฉพาะเจาะจงในการเกิดเอธีลีนออกไซด์สูงที่สุด ขณะเดียวกัน ให้ความเฉพาะเจาะจงในการเกิดคาร์บอนไดออกไซด์และคาร์บอนมอนอกไซด์ต่ำที่สุด การเพิ่มความต่างศักย์ช่วยเพิ่มความเฉพาะเจาะจงในการเกิดเอธีลีนออกไซด์ ขณะที่ความเฉพาะเจาะจงในการเกิดเอธีลีนออกไซด์ค่อนข้างคงที่เมื่อใช้ความถี่ในช่วง 300-500 เฮิรตซ์ อย่างไรก็ตาม ที่ความถี่มากกว่า 500 เฮิรตซ์ ความเฉพาะเจาะจงในการเกิดเอธีลีนออกไซด์ลดลง ปริมาณโลหะเงินบนอลูมินาเฟสแอลฟาชนิดพื้นที่ผิวต่ำที่ให้ความเฉพาะเจาะจงในการเกิดเอธีลีนออกไซด์มากที่สุด (12.98 เปอร์เซ็นต์) คือ 12.5 เปอร์เซ็นต์โดยน้ำหนัก ณ สภาวะที่มีความต่างศักย์และความถี่เป็น 15 กิโลโวลต์ และ 500 เฮิรตซ์ ตามลำดับ สำหรับพลังงานที่ใช้ในสภาวะดังกล่าวเท่ากับ 12.6×10^{-16} วัตต์·วินาทีต่อโมเลกุลของเอธีลีนออกไซด์ที่เกิดขึ้น นอกจากนี้ ยังพบว่า เมื่ออัตราส่วนระหว่างออกซิเจนต่อเอธีลีนในก๊าซขาเข้าและอัตราการไหลขาเข้าของก๊าซลดลง จะส่งผลดีต่อกระบวนการอีพอกซิเดชันของเอธีลีน

ส่วนที่ 2: กระบวนการอีพอกซิเดชันของเอธีลีนไปเป็นเอธีลีนออกไซด์ยังถูกทำการทดลองในเครื่องปฏิกรณ์พลาสมาแบบไดอิเล็คทริคแบริเออร์ดีสชาร์จ เพื่อศึกษาสภาวะต่างๆที่เหมาะสมในการเกิดปฏิกิริยาอีกด้วย จากการทดลองพบว่า สำหรับระบบพลาสมาอุณหภูมิต่ำชนิดไดอิเล็คทริคแบริเออร์ดีสชาร์จ ผลได้ของเอธีลีนออกไซด์ลดลงเมื่อทำการเพิ่มอัตราส่วนของออกซิเจนต่อเอธีลีน อัตราการไหลของสารตั้งต้น ค่าความถี่ และระยะห่างระหว่างขั้วไฟฟ้า ในขณะที่ผลได้ของเอธีลีนออกไซด์เพิ่มขึ้นเมื่อทำการเพิ่มความต่างศักย์จนถึง 19 กิโลโวลต์ จากการทดลองยังพบว่าผลได้ของเอธีลีนออกไซด์มากที่สุดคือ 5.62 เปอร์เซ็นต์ ณ ภาวะความถี่และความต่างศักย์เป็น 500 เฮิรตซ์ และ 19 กิโลโวลต์ ตามลำดับ ด้วยอัตราส่วนของออกซิเจนต่อเอธีลีนเป็น 1/1 อัตราไหลของสารตั้งต้น

เป็น 50 ลูกบาศก์เซ็นติเมตรต่อนาที และระยะห่างระหว่างขั้วไฟฟ้าเป็น 10 มิลลิเมตร สำหรับพลังงานที่ใช้ในภาวะดังกล่าวเท่ากับ 6.07×10^{-16} วัตต์วินาทีต่อโมเลกุลของเอธีลีนออกไซด์ที่เกิดขึ้น

ส่วนที่ 3: ในงานวิจัยนี้ ได้ดำเนินการศึกษากระบวนการอีพอกซิเดชันของเอธีลีนในระบบประกายไฟฟ้าแบบอุณหภูมิต่ำกับตัวเร่งปฏิกิริยาต่างๆ ได้แก่ โลหะเงินบนอลูมินาเฟสแอลฟา ซีเลียม-โลหะเงินบนอลูมินาเฟสแอลฟา ทองแดง-โลหะเงินบนอลูมินาเฟสแอลฟา และ ทอง-โลหะเงินบนอลูมินาเฟสแอลฟา โดยพบว่า ตัวเร่งปฏิกิริยาที่ทำการทดลองทั้งหมดสามารถเพิ่มประสิทธิภาพการเปลี่ยนเอธีลีน และ ผลได้และการเลือกเกิดของเอธีลีนออกไซด์ ในระบบประกายไฟฟ้าแบบอุณหภูมิต่ำ โดยเฉพาะ 1% ซีเลียม-12.5%โลหะเงินบนอลูมินาเฟสแอลฟา และ 0.2% ทอง-12.5%โลหะเงินบนอลูมินาเฟสแอลฟา พลังงานที่ใช้ในการผลิตหนึ่งโมเลกุลของเอธีลีนออกไซด์ในระบบประกายไฟฟ้ากับตัวเร่งปฏิกิริยาโลหะสองชนิด มีค่าต่ำกว่าในระบบประกายไฟฟ้ากับตัวเร่งปฏิกิริยาโลหะเงินอย่างเดียว

Project Title	Ethylene Oxide Reaction over Ag Catalysts in Low-Temperature Corona Discharge
Name of the Investigators	Assoc. Prof. Sumaeth Chavadej, Asst. Prof. Thammanoon Sreethawong, Mr.Anothai Tansuwan, and Mr.Thanapoom Suwannabart
Year	October, 2009

Abstract

Part 1: The epoxidation of ethylene over different catalysts - namely Ag/(low-surface-area, LSA)α-Al_2O_3, Ag/(high-surface-area, HSA)γ-Al_2O_3, and Au-Ag/(HSA)γ-Al_2O_3 - in a low-temperature corona discharge system was investigated. In a comparison among the studied catalysts, the Ag/(LSA)α-Al_2O_3 catalyst was found to offer the highest selectivity for ethylene oxide, as well as the lowest selectivity for carbon dioxide and carbon monoxide. The selectivity for ethylene oxide increased with increasing applied voltage, while the selectivity for ethylene oxide remained unchanged when the frequency was varied in the range of 300-500 Hz. Nevertheless, the selectivity for ethylene oxide decreased with increasing frequency beyond 500 Hz. The optimum Ag loading on (LSA)α-Al_2O_3 was found to be 12.5 wt.%, at which a maximum ethylene oxide selectivity of 12.9% was obtained at the optimum applied voltage and input frequency of 15 kV and 500 Hz, respectively. Under these optimum conditions, the power consumption was found to be 12.6×10^{-16} W·s/molecule of ethylene oxide produced. In addition, a low oxygen-to-ethylene molar ratio and a low feed flow rate were also experimentally found to be beneficial for the ethylene epoxidation.

Part 2: The epoxidation of ethylene under a low-temperature dielectric barrier discharge (DBD) was also feasibly investigated to find the best operating conditions. It was experimentally found that the EO yield decreased with increasing O_2/C_2H_4 feed molar ratio, feed flow rate, input frequency, and electrode gap distance, while it increased with increasing applied voltage up to 19 kV. The highest EO yield of 5.6% was obtained when an input frequency of 500 Hz and an applied voltage of 19 kV were used, with an O_2/C_2H_4 feed molar ratio of 1:1, a feed flow rate of 50 cm^3/min, and an electrode gap distance of 10 mm. Under these best conditions, the power consumption was found to be as low as 6.07×10^{-16} Ws/molecule of EO produced.

Part 3: In this work, the epoxidation of ethylene using a low-temperature corona discharge system was investigated with various reported catalytically active catalysts: $Ag/\alpha\text{-}Al_2O_3$, $Cs\text{-}Ag/\alpha Al_2O_3$, $Cu\text{-}Ag/\alpha Al_2O_3$, and $Au\text{-}Ag/\alpha Al_2O_3$. It was experimentally found that the investigated catalysts could improve the ethylene conversion and the ethylene oxide (EO) yield and selectivity for the corona discharge system, particularly 1 wt.% Cs-12.5% $Ag/\alpha Al_2O_3$ and 0.2% Au-12.5% $Ag/\alpha Al_2O_3$. The power consumption per EO molecule produced in the corona discharge system, combined with the superior bimetallic catalysts, was much lower than that of the sole corona discharge system and that of the corona discharge system combined with the monometallic Ag catalyst.

Table of Contents

List of Tables

List of Figures

Part 1: Ethylene Epoxidation over Alumina-Supported Silver Catalysts in Low-Temperature AC Corona Discharge

1.1 Introduction and Survey of Related Literature

The selective oxidation of ethylene, especially ethylene epoxidation, is currently the largest hydrocarbon partial oxidation process in industry because the desired product, ethylene oxide (C_2H_4O, EO), is a valuable chemical feedstock or intermediate product for many important applications, such as solvents, antifreeze agents, textiles, detergents, adhesives, polyurethane foam, and pharmaceuticals [1]. Besides, this is in good accordance with the currently high global demand for ethylene oxide, which exceeds 40 billion pounds per annum [2], indicating high ethylene oxide consumption around the world.

Ordinarily, ethylene can be oxidized to ethylene oxide with a high selectivity over unique traditional silver catalysts supported on low-surface-area alpha-alumina ($Ag/(LSA)\alpha\text{-}Al_2O_3$). Commercially, the addition of a few ppms of chloride to gaseous reactants as a moderator in the form of chlorine-containing hydrocarbon species, such as dichloroethane ($C_2H_4Cl_2$) and vinyl chloride (C_2H_3Cl), was reported to significantly increase the selectivity for ethylene oxide by 15-20% [3-6]. Alkali and alkali earth, such as Cs and Re, were also reported to provide an improvement of the selectivity toward ethylene oxide by 10% [7,8]. In a recent work [9], a silver catalyst supported on high-surface-area gamma-alumina ($Ag/(HSA)\gamma\text{-}Al_2O_3$) was proved to exhibit a good selectivity toward ethylene oxide. Moreover, adding a small amount of Au to form Au-Ag bimetallic catalysts on the high-surface-area alpha-alumina support was found to favor the epoxidation reaction of ethylene to ethylene oxide. They reported that ethylene conversion obtained from these catalysts did not occur at temperatures below 220°C. Even though the reaction temperature was raised to 270°C, ethylene conversion was still low, around 1-4% [10]. Consequently, this limitation results in high energy consumption for the catalytic reaction at high temperatures, which becomes an obstruction in developing the process for industrial application. A non-traditional catalysis technique is, therefore, expected to overcome this constraint. One potential technique is to combine selective traditional catalysis and non-thermal plasma, which is believed to reduce the power consumption and/or increase the

selectivity and yield for ethylene oxide production.

Non-thermal plasma is one kind of electric gas discharge [11]. In non-thermal plasmas, the electrons in electrodes gain energy from an external applied voltage until they possess enough energy to overcome the potential barrier of metal surface electrodes. Then, they can move from one electrode to the other, and these high-energy electrons will chemically excite or dissociate the gaseous species by colliding with the gaseous components present in the plasma zone. Typically, these excited or dissociated atoms or molecules have a much higher reactivity than neutral species at the ground state, and consequently they can easily lead to the formation of new chemical species. Furthermore, the most important characteristic of non-thermal plasma is that the electrons in the plasma zone have a higher energy, but the temperature of the bulk gas is still much lower [12]. Examples of chemical synthesis using plasma are oxidations of olefins, aromatics, and so on [13,14]. The combined processes of catalysis and non-thermal plasma have been demonstrated to offer a number of advantages over conventional catalytic processes. One advantage is to require low operational temperatures close to room temperature and low pressure at near or slightly higher than atmospheric pressure, as described above. This implies comparatively that non-thermal plasma processes offer a lower energy consumption used for activating catalysts as compared with conventional catalytic processes. Hence, corona discharge was employed for this research because it is capable of operating at low temperature and atmospheric pressure [11].

A basic configuration of corona discharge is to use a pair of in-homogeneous metal electrode geometries, which can stabilize the discharge generated. There are many industrial applications involving the utilization of corona discharge, such as NO_x and SO_x reduction in flue gas, toxic compound destruction, and ozone production [15-17]. From literature review, the combination of corona discharge and heterogeneous catalysts has been used for many applications [18-30]. Recently in our previous works, it was also used with photocatalysts for the gaseous removal of benzene and ethylene [31,32].

The objective of this work was, for the first time, to investigate a combined catalytic and corona discharge system for the epoxidation of ethylene using different catalysts: Ag/(LSA)α-Al_2O_3, Ag/(HSA)γ-Al_2O_3, and Au-Ag/(HSA)γ-Al_2O_3. In this

study, the effects of various operating parameters, including applied voltage, input frequency, molar ratio of oxygen to ethylene, and feed flow rate, on the activity of ethylene epoxidation were examined systematically. Moreover, the optimum conditions for maximum ethylene oxide production and minimum power consumption were determined.

1.2 Procedure

1.2.1 Materials and reactant gases

The two types of supports used were (LSA)α-Al_2O_3, supplied by A.C.S. Xenon Limited Partnership, and (HSA)γ-Al_2O_3, supplied by Aerosil®. Silver nitrate ($AgNO_3$), supplied by Carlo Erba, and hydrogen tetrachloroaurate (III) trihydrate ($HAuCl_4 \cdot 3H_2O$), supplied by Alfa Aesar, were employed as silver and gold catalyst precursors, respectively. All chemicals were used as received without further purification. Distilled water was used for catalyst preparation in this study. For the reactant gases, 99.995% helium (high purity grade), 40% ethylene balanced with helium, and 97% oxygen balanced with helium were obtained from Thai Industrial Gas (Public) Co., Ltd.

1.2.2 Catalyst preparation procedures

The incipient wetness impregnation method was used to prepare all catalysts according to literature [9,10,33]. For silver supported on (LSA)α-Al_2O_3, the alumina support was impregnated with aqueous solutions of silver nitrate to achieve various nominal Ag loadings ranging from 0-15 wt.% and then dried in air at 110°C overnight. These mixtures were calcined in air at 400°C for 12 h. After that, each impregnated catalyst was sieved in order to obtain the desired grain size range of 221-425 μm for the activity studies. For silver supported on (HSA)γ-Al_2O_3, the alumina support was impregnated with an aqueous solution of silver nitrate to achieve a nominal Ag loading of 13.18 wt.%, exhibiting superior activity in previous works [9,10], and then dried in air at 110°C overnight. This mixture was calcined in air at 500°C for 5 h. After that, the impregnated catalyst was also sieved in order to obtain the desired grain size range of 221-425 μm for the reaction activity experiments, which will be described later. For bimetallic Au-Ag supported on (HSA)γ-Al_2O_3, a Ag

catalyst on the alumina support with an optimum Ag loading of 13.18 wt.% was initially prepared and dried at 110°C for 2 h. This catalyst was then sequentially impregnated with an appropriate amount of an aqueous solution of tetrachloroaurate (III) trihydrate to achieve an optimum Au loading of 0.63 wt.% [9,10]. This impregnated catalyst was then dried in air at 110°C overnight and calcined in air at 500°C for 5 h. After that, the catalyst was sieved in the same manner as explained above.

1.2.3 Catalyst characterizations

The specific surface areas of all prepared catalysts were determined by a surface area analyzer (Quantachrom, Autosorb-1) using nitrogen adsorption analysis. A catalyst sample was dried and outgassed in a sample cell under vacuum at 150°C for 10 h to remove the humidity and any volatile components adsorbed on the catalyst surface before the analysis. The specific surface area of each catalyst was calculated from the 5-point adsorption isotherm. The results were analyzed by Autosorb ANAGAS software, version 2.10.

The actual contents of silver and gold in the prepared catalysts were determined by an atomic absorption spectroscope (AAS) (Varian Spectr, AA-300).

The crystalline phases of the prepared catalysts were investigated by an X-ray diffractometer (XRD, Rigaku RINT-2200) equipped with a graphite monochromator, a Cu tube for generating CuKα radiation (λ = 1.5406 Å) at a generator voltage of 40 kV and a generator current of 30 mA, and a nickel filter used as the filter for Kβ removal. The goniometer parameters were; divergence slit = 1°(2θ), scattering slit = 1°(2θ), and receiving slit = 0.3 mm. The catalyst sample was held in the hollow of a glass slide holder and was examined in the 2θ range of 20 to 90° at a scanning speed of 5°(2θ)/min and a scan step of 0.02°(2θ). The digital output of the proportional X-ray diffractometer and the goniometer angle measurements were sent to an online microcomputer to record the data and to perform subsequent analyses.

Transmission electron microscopy (TEM) was employed for investigating the average particle size of Ag particles and identifying the microstructures of the prepared catalysts. The catalyst sample was ground into a fine powder and ultrasonically dispersed in ethanol. A small droplet of the suspension was deposited

on a copper grid, and the solvent was evaporated prior to loading the sample into the TEM. The TEM (JEOL, 2000 CX) was operated at an accelerating voltage of 200 kV in bright field mode.

Temperature-programmed oxidation (TPO) was employed to quantitatively investigate the coke formation on the spent catalysts. The TPO analysis was performed at a continuous flow of O_2/He (ratio 2:1) with a total flow rate of 40 ml/min. A spent catalyst was placed in the quartz tube, and it was secured with packing quartz wool. The sample temperature was linearly increased with a constant rate of 10°C/min to reach a maximum temperature of 850°C. The carbon fraction of the sample was completely oxidized to form carbon dioxide. After this reaction, the effluent gas was passed through a methanator containing a Ni/Al_2O_3 catalyst to convert the carbon dioxide to methane. Subsequently, the produced methane was detected with a flame ionization detector (FID). The area under the obtained curve was used to calculate carbon content in the spent catalyst sample. The amount of coke formed is reported based on the weight of spent catalyst.

1.2.4 Experimental setup and reaction activity experiments

The experimental study of ethylene epoxidation was conducted in an AC corona discharge reactor, which was operated at atmospheric pressure and ambient temperature, around 25-27°C (room temperature). A schematic of the corona discharge system is shown in Fig. 1.1(a). The reactor comprised an 11.25-inch-long quartz tube with an outer diameter of 10 mm and an inner diameter of 8 mm. Plasma was generated in the reactor via pin-and-plate electrodes, which were located at the center of the reactor. The power used to generate plasma was alternating current, 200 V and 50 Hz, which was transformed to a high voltage current via a power supply unit. The output voltage and frequency was adjusted by a function generator, whereas the sinusoidal wave signal generated was monitored by an oscilloscope. Since the plasma generated in the reactor was found to have a very high fluctuation, it was not possible to measure the voltage across the electrodes of the reactor (high-side voltage). Therefore, the low-side voltage and current were measured instead, and the high-side voltage and current were then calculated by multiplying and dividing by a factor of 130, respectively. To investigate the effect of catalyst in the plasma reactor on the ethylene epoxidation, 0.24 g of each of the three studied catalysts was

individually placed on the plate electrode and secured by a quartz wool layer, as shown in Fig. 1.1(b). In this study, the gap distance between the two electrodes was fixed at 1 cm.

Reactant gases (ethylene, oxygen, and helium) fed through the plasma reactor were controlled by a set of electronic mass flow controllers to obtain a feed gas mixture having different flow rates and molar ratios of oxygen to ethylene, while the ethylene concentration was fixed at 6%. All reactant lines had 0.7 μm in-line filters before being passed through the mass flow controllers in order to trap any foreign particles. When the composition of the feed remained constant, the power supply unit was turned on. After 60 min, the composition of the effluent gas was analyzed every 60 min until it was invariant, indicating the steady state condition. Reactor pressure was controlled by a needle valve, and the outlet of the reactor was either vented to the atmosphere via rubber tube exhaust or was connected to an on-line gas chromatograph for analysis of the product gases. Before being fed to the on-line gas chromatograph, the moisture in the effluent gas was removed by a water trap filter. The gas chromatograph used was a Perkin-Elmer AutoSystem GC equipped with both a thermal conductivity detector (TCD) and a flame ionization detector (FID). For the TCD channel, a packed column (Carboxen 1000) was used for separating the product gases - oxygen (O_2), carbon monoxide (CO), carbon dioxide (CO_2), and ethylene (C_2H_4). For the FID channel, a capillary column (OV-Plot U) was used for analysis of the ethylene oxide (C_2H_4O), methane (CH_4), ethane (C_2H_6), acetylene (C_2H_2), and propane (C_3H_8). Since the gas volume was changed after the reactions, the flow rate of the outlet gas was also measured. The experimental data taken under steady state conditions were averaged, and these averages were used to evaluate the performance of the plasma system.

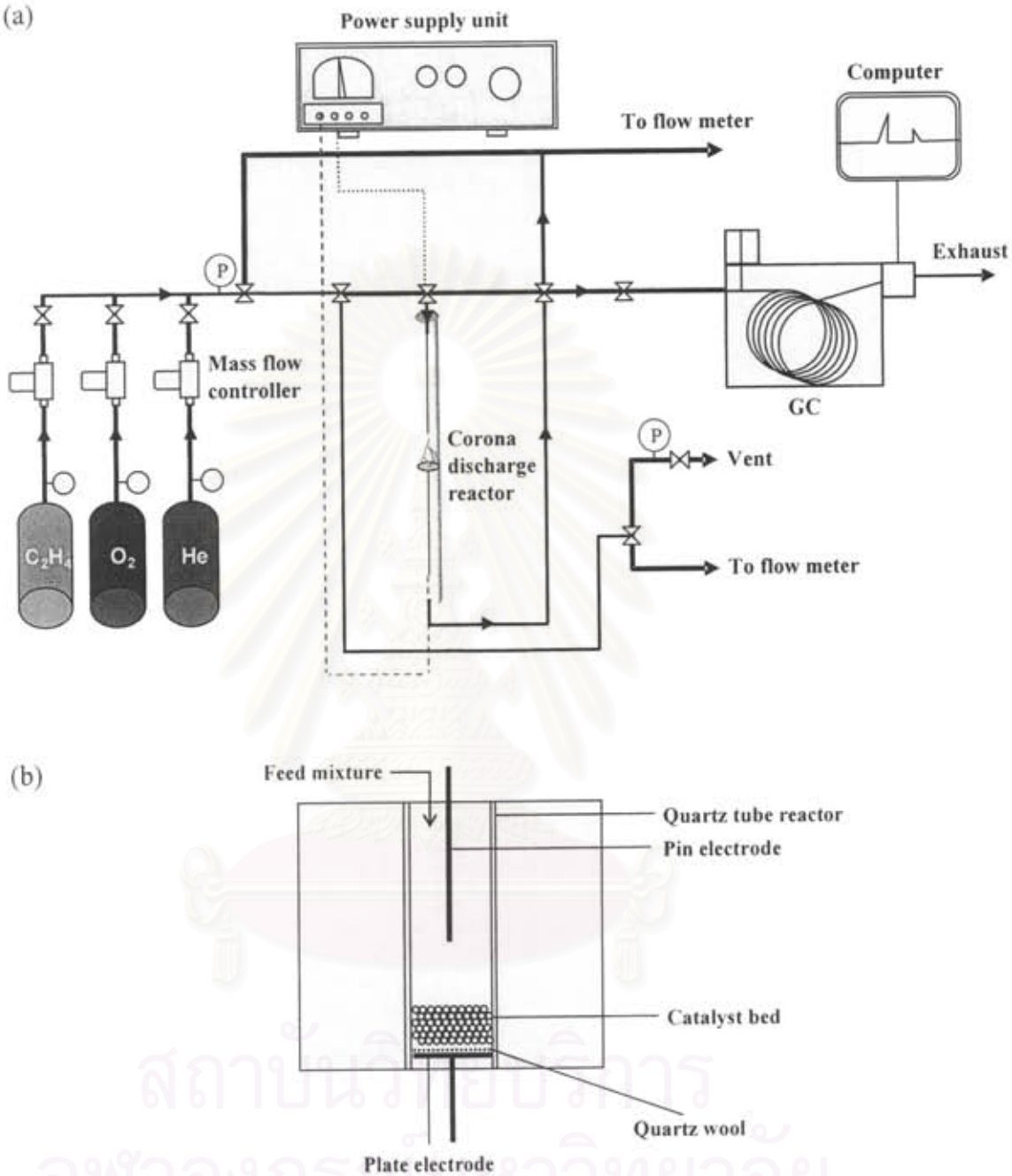

Fig.1.1. (a) Schematic of experimental setup for ethylene epoxidation reaction in corona discharge plasma system and (b) configuration of the corona discharge reactor.

To evaluate the process performance, the conversions of ethylene and oxygen and the selectivities for products, including CO, CO_2, C_2H_4O, CH_4, C_2H_6, C_2H_2, and traces of C_3, were considered. The conversion of either ethylene or oxygen is defined as:

$$\% \text{ Reactant conversion} = \frac{(\text{moles of reactant } \textit{in} - \text{moles of reactant } \textit{out}) \times 100}{(\text{moles of reactant } \textit{in})} \quad (1)$$

The product selectivity is calculated from the following equation:

$$\% \text{ Product selectivity} = \frac{(\text{number of carbon atom in product})(\text{moles of product produced}) \times 100}{(\text{number of carbon atom in ethylene})(\text{moles of ethylene converted})} \quad (2)$$

To determine the energy efficiency of the plasma system, the specific power consumption is calculated in a unit of W·s per molecule of converted ethylene or per molecule of produced ethylene oxide using the following equation:

$$\text{specific power consumption} = \frac{P \times 60}{\tilde{N} \times M} \quad (3)$$

where P = Power (W)

$\tilde{N}$ = Avogadro's number = 6.02×10^{23} molecules/mol

M = Rate of converted ethylene molecules in feed or rate of produced ethylene oxide molecules (mol/min).

1.3 Results and Discussion

1.3.1 Catalyst characterization results

The nominal metal loadings, actual metal loadings, and BET surface areas of all the studied catalysts are shown comparatively in Table 1.1. The actual metal loadings of these three catalysts obtained from AAS were not significantly different from the nominal metal loadings. This implies that the incipient wetness impregnation technique used for loading metals on supports is reliably effective to control any desired catalyst loading.

The BET surface areas of the Ag/(LSA)α-Al_2O_3 family slightly increased with increasing silver loading, indicating that the silver particles are well dispersed on the support without the sintering effect during the preparation step. For the other catalysts supported on (HSA)γ-Al_2O_3, their surface areas were similar to those of the unloaded support in the range of 97-101 m^2/g. These results also imply that both Ag and/or Au were highly dispersed on the surface of this high-surface-area support [10].

Table 1.1 Textural characteristics of all prepared catalysts

Catalyst	Nominal content (wt.%)		Actual content[a] (wt.%)		BET surface area[b] (m^2/g)
	Ag	Au	Ag	Au	
Ag/(LSA)α-Al_2O_3	0	0	0	0	0.44
	10	0	9.63	0	0.61
	12.5	0	12.54	0	0.74
	15	0	14.94	0	0.89
Ag/(HSA)γ-Al_2O_3	0	0	0	0	101
	13.18	0	12.98	0	98
Au-Ag/(HSA)γ-Al_2O_3	13.18	0.63	12.98	0.78	97

[a] Determined by AAS

[b] Determined by N_2 adsorption analysis

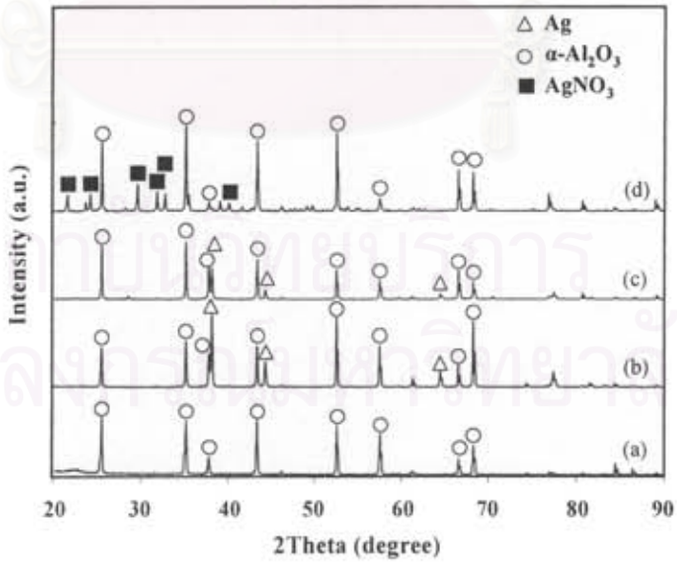

Fig. 1.2. XRD patterns of (a) (LSA)α-Al_2O_3, (b) 10 wt.% Ag/(LSA) α-Al_2O_3, (c) 12.5 wt.% Ag/(LSA) α-Al_2O_3, and (d) 15 wt.% Ag/(LSA) α-Al_2O_3.

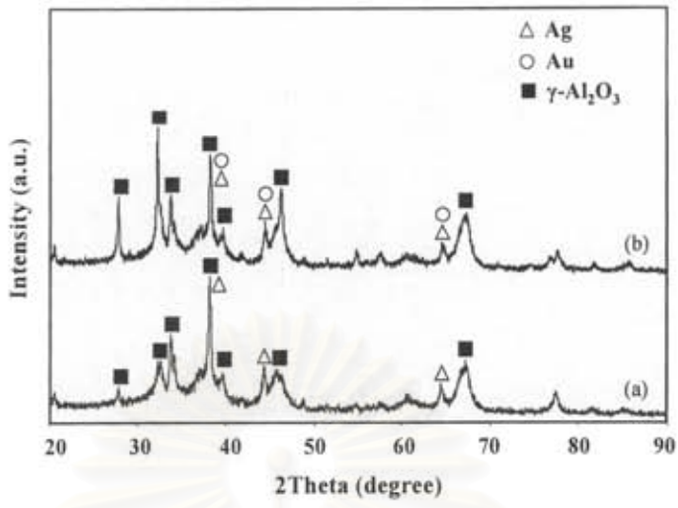

Fig. 1.3. XRD patterns of (a) 13.18 wt.% Ag/(HSA)γ-Al_2O_3 and (b) 0.63 wt.% Au-13.18 wt.% Ag/(HSA)γ-Al_2O_3.

Fig. 1.2 shows the XRD patterns of the Ag catalysts on (LSA)α-Al_2O_3 at different silver loadings. For the unloaded support, only the α-Al_2O_3 phase was observed as a major phase. The silver phase was found at the diffraction peaks of approximately 38, 44, and 64° when silver loading increased up to 12.5 wt.% Ag. At 15 wt.% Ag, a silver nitrate phase was additionally observed, probably due to overloading of the Ag precursor. As shown in Fig. 1.3, it can be observed from the XRD patterns that the γ-Al_2O_3 phase is a major phase of the (HSA)γ-Al_2O_3-supported catalysts. For the 13.18 wt.% Ag/(HSA)γ-Al_2O_3, the silver phase was found at the aforementioned diffraction peaks as well. When 0.63 wt.% Au was additionally loaded onto the 13.18 wt.% Ag/(HSA)γ-Al_2O_3, its XRD pattern was not significantly changed, without distinguishable diffraction peaks of gold phase due to their same positions as the diffraction peaks of silver phase.

Fig. 1.4 shows the morphology and mean particle size of Ag on the surface of the studied catalysts observed by using TEM. The TEM results show that Ag particles are highly dispersed on the alumina supports. The TEM micrographs of a representative 12.5 wt.% Ag/(LSA)α-Al_2O_3, which exhibited superior activity toward ethylene epoxidation as explained later, are depicted in Figs. 1.4(a) and (b) (low and high magnifications, respectively). From the TEM results, the mean Ag particle size was found to be approximately 9.5 nm.

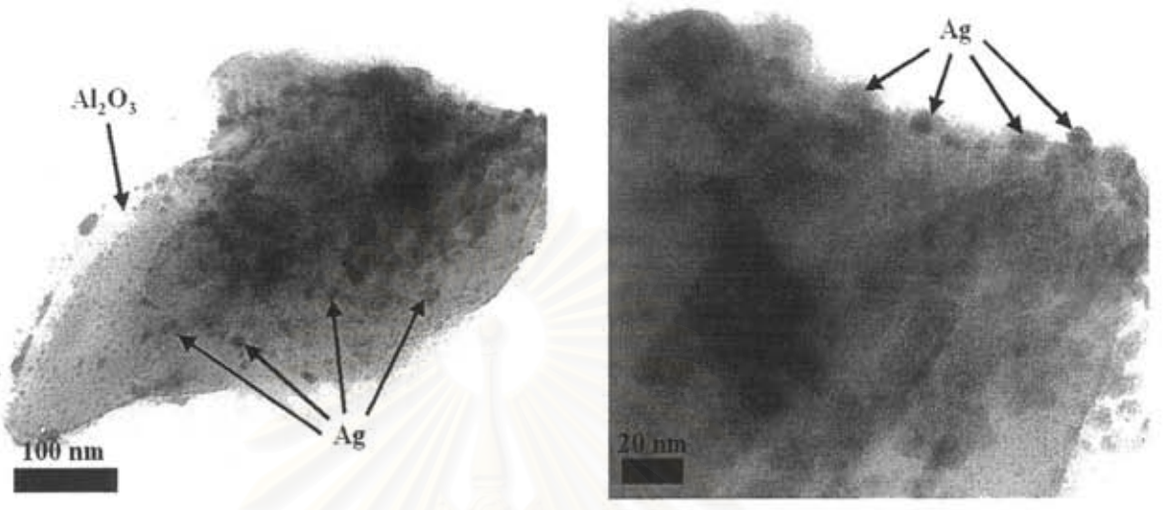

Fig. 1.4. TEM micrographs of 12.5 wt.% Ag/(LSA)α-Al_2O_3 at (a) low magnification and (b) high magnification.

1.3.2 Reaction activity performance

All experiments were carried out at ambient temperature and atmospheric pressure in order to determine the effects of type of catalyst, silver loading, applied voltage, input frequency, molar ratio of O_2/C_2H_4, and feed flow rate on the epoxidation activity of ethylene. Under the studied conditions, the product gas contained carbon monoxide, carbon dioxide, ethylene oxide, methane, ethane, acetylene, and traces of C_3. Interestingly, hydrocarbons containing a carbon number greater than C_3 were not detectable.

1.3.2.1 Effect of type of catalyst

In the corona discharge system without a catalyst, most of the discharge energy is used to produce and accelerate electrons, which then react with gas molecules to generate highly active species (metastable radicals and ions). Ethylene and oxygen are, therefore, chemically activated directly by electron collisions. For a combined catalytic-plasma system, a catalytic material in the plasma or discharge zone is used to enhance the selectivity and efficiency of the plasma process by surface reactions.

Fig. 1.5(a) shows the ethylene and oxygen conversions and ethylene oxide

yield over different catalysts. The ethylene conversion was always lower than the oxygen conversion in both the sole plasma and combined catalytic-plasma systems since the bond dissociation energy of ethylene (682 kJ/mol) is much higher than that of oxygen (498.38 kJ/mol). Under the studied oxygen-to-ethylene molar ratio of 1:1, both partial and complete oxidation to produce CO and CO_2 appear, as confirmed in Fig. 1.5(b). As a result, the oxygen conversion was higher than the ethylene conversion. The plasma system without a catalyst provided the highest oxygen conversion. The oxygen conversion on the Ag/(HSA)γ-Al_2O_3 was higher than that on the Ag/(LSA)α-Al_2O_3 since the high-surface-area alumina support can provide higher silver dispersion than the low-surface-area one, therefore improving oxygen adsorption for the oxidation reaction, to result in a higher oxygen conversion. Interestingly, the bimetallic Au-Ag/(HSA)γ-Al_2O_3 gave a lower oxygen conversion than both Ag/(HSA)γ-Al_2O_3 and Ag/(LSA)α-Al_2O_3. A possible explanation is that if chemisorption-induced surface enrichment is operative, it will tend to enhance the concentration of Ag on the surface. This is due to the fact that oxygen forms strong chemisorption bonds with silver, while it does not chemically adsorb, to any appreciable extent, on gold. It is well known that the component that forms the strongest chemisorption bonds tends to segregate at the surface of the alloy particles [34], resulting in less oxygen chemisorption and consequent lower oxygen conversion in the case of the Au-Ag/(HSA)γ-Al_2O_3. Interestingly, the oxygen conversion in the sole plasma system was higher than that in the case of the combined catalytic and plasma systems. This result indicates that the activity of the plasma can be slightly retarded in the presence of catalysts, since they simply reduce the volume of the plasma zone, as well as act as an electrically resistant material. However, the ethylene conversion on the Ag/(LSA)α-Al_2O_3 was found to be comparatively the same as that in the sole plasma system, but not in the case of Ag/(HSA)γ-Al_2O_3. Since the Ag catalysts have been found to be the hydrogenation sites for acetylene [35], this might be another important reason to explain how the lower conversion of ethylene was obtained on the Ag catalyst supported on (HSA)γ-Al_2O_3. This can imply that despite the presence of the Ag catalyst, C_2H_2 hydrogenation does not favorably occur on the (LSA)α-Al_2O_3 support. Interestingly, the Ag/(LSA)α-Al_2O_3 was also found to provide the highest ethylene oxide yield, plausibly due to the comparatively high ethylene

conversion and the highest ethylene oxide selectivity, as explained next.

By considering the product selectivities, as shown in Fig. 1.5(b), it can be seen that the type of catalyst significantly affects the selectivities for main products, i.e. C_2H_4O, CO, and CO_2. Even though the bimetallic Au-Ag/(HSA)γ-Al_2O_3 combined with plasma was shown to favor the total oxidation reaction as compared to the other two catalysts, it still provided a moderate ethylene oxide selectivity, even higher than the Ag/(HSA)γ-Al_2O_3. The reason is that gold could behave as a diluting agent on the silver surface, resulting in the destruction of multiple silver sites, which favor atomic oxygen adsorption. As a result, the addition of gold simply creates new adsorption sites for molecular oxygen, which is also responsible for the ethylene epoxidation reaction [10]. The reason why the Au-Ag/(HSA)γ-Al_2O_3 showed the highest selectivity for carbon dioxide is that the O^{2-} species are separated from each other, and the adsorbed ethylene complex can consequently react with atomic oxygen to form carbon dioxide and water [34]. Obviously, the Ag/(HSA)γ-Al_2O_3 catalyst was shown to be more active for the total oxidation reaction than the Ag/(LSA)α-Al_2O_3 and the sole plasma system. In the plasma system, it was found to show the highest selectivity for carbon monoxide and a low selectivity for carbon dioxide.

It is generally accepted that non-thermal plasma changes the status of reactant molecules. Instead of neutral ground state molecules, a mixture of electrons, excited molecules, ions, and radicals predominantly occupies the plasma zone. The energized electrons and excited active species are in a thermodynamically initial state for subsequent reactions. Besides, the interactions among the active species and catalyst lead to unusual plasma catalytic reactions [36]. In comparisons of these three catalysts combined with plasma and the sole plasma system, it is clear that the presence of a suitable catalyst in corona discharge can enhance the selectivity for the desired product, ethylene oxide. In this experiment, the Ag/(LSA)α-Al_2O_3 catalyst was found to offer the highest ethylene oxide selectivity, the lowest carbon dioxide selectivity, and the highest ethylene oxide yield. Interestingly, as shown in Fig. 1.5(c), the coke formed on the spent Ag/(LSA)α-Al_2O_3 was comparatively very low, as the amounts of coke formed on the spent Ag/(HSA)γ-Al_2O_3 and Au-Ag/(HSA)γ-Al_2O_3 were approximately 13 and 21 times higher than that on the Ag/(LSA)α-Al_2O_3. Hence, the Ag/(LSA)α-Al_2O_3 catalyst was selected for further studies.

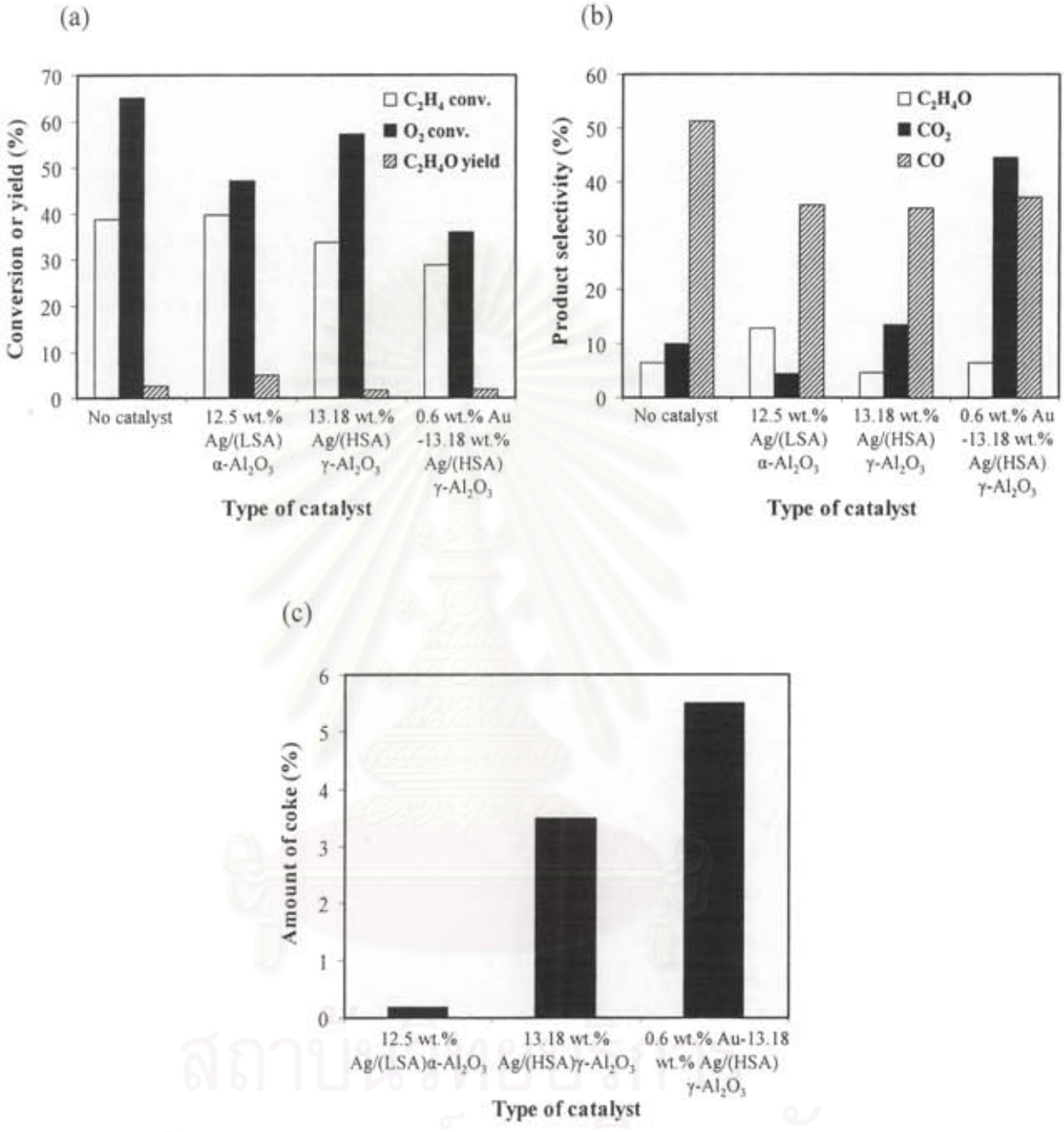

Fig. 1.5. (a) Ethylene and oxygen conversions and ethylene oxide yield, (b) product selectivities, and (c) amount of coke formed as a function of different catalysts (molar ratio of O_2/C_2H_4 = 1/1; feed flow rate = 50 ml/min; gap distance = 1 cm; frequency = 500 Hz; and, voltage = 15 kV).

1.3.2.2 Effect of silver loading

Fig. 1.6(a) illustrates the conversions of C_2H_4 and O_2 and the C_2H_4O yield over the Ag/(LSA)α-Al_2O_3 as a function of silver loading. The catalyst having a Ag loading greater than 15 wt.% was found to produce a large amount of coke on the surface of the pin electrode and on the surface of the catalyst. The lowest ethylene and oxygen conversions were observed for the blank support, as compared to the Ag-loaded ones. This result indicates that the presence of silver on this support is necessary to enhance both C_2H_4 and O_2 conversions. The conversion of C_2H_4 increased with increasing Ag loading up to 10 wt.% and remained almost constant beyond 10 wt.% Ag, while the conversion of O_2 also increased with increasing the Ag loading up to 10 wt.%, but substantially decreased with further increasing the Ag loading. Interestingly, a Ag loading of 12.5 wt.% was found to give the highest ethylene oxide yield. Besides, as shown in Fig. 1.6(b), it is worth noting that at high Ag loadings, especially higher than 12.5 wt.%, the amount of coke formed was observed to be relatively high, resulting in significant decreases in the O_2 conversion and the C_2H_4O yield.

The influence of silver loading on the selectivities for C_2H_4O, CO, CO_2, CH_4, C_2H_2, C_2H_6, and C_3H_8 is depicted in Fig. 1.6(c). It is apparent that an increase in silver loading resulted in increases in both CO and CO_2 selectivities, especially with a Ag loading higher than 12.5 wt.%; however, the selectivities for C_2H_4O increased with increasing Ag loading up to 12.5 wt.% and substantially declined with further increasing Ag loading. The results also show that the selectivities for C_2H_2 and C_3H_8 tended to decrease as the Ag loading increased. The selectivities for CH_4 and C_2H_6 first increased and then decreased with increasing Ag loading. By comparing the activity of the catalysts with various Ag loadings, 12.5 wt.% Ag was considered to be the optimum value because it provided the highest C_2H_4O selectivity and yield with relatively low CO and CO_2 selectivities.

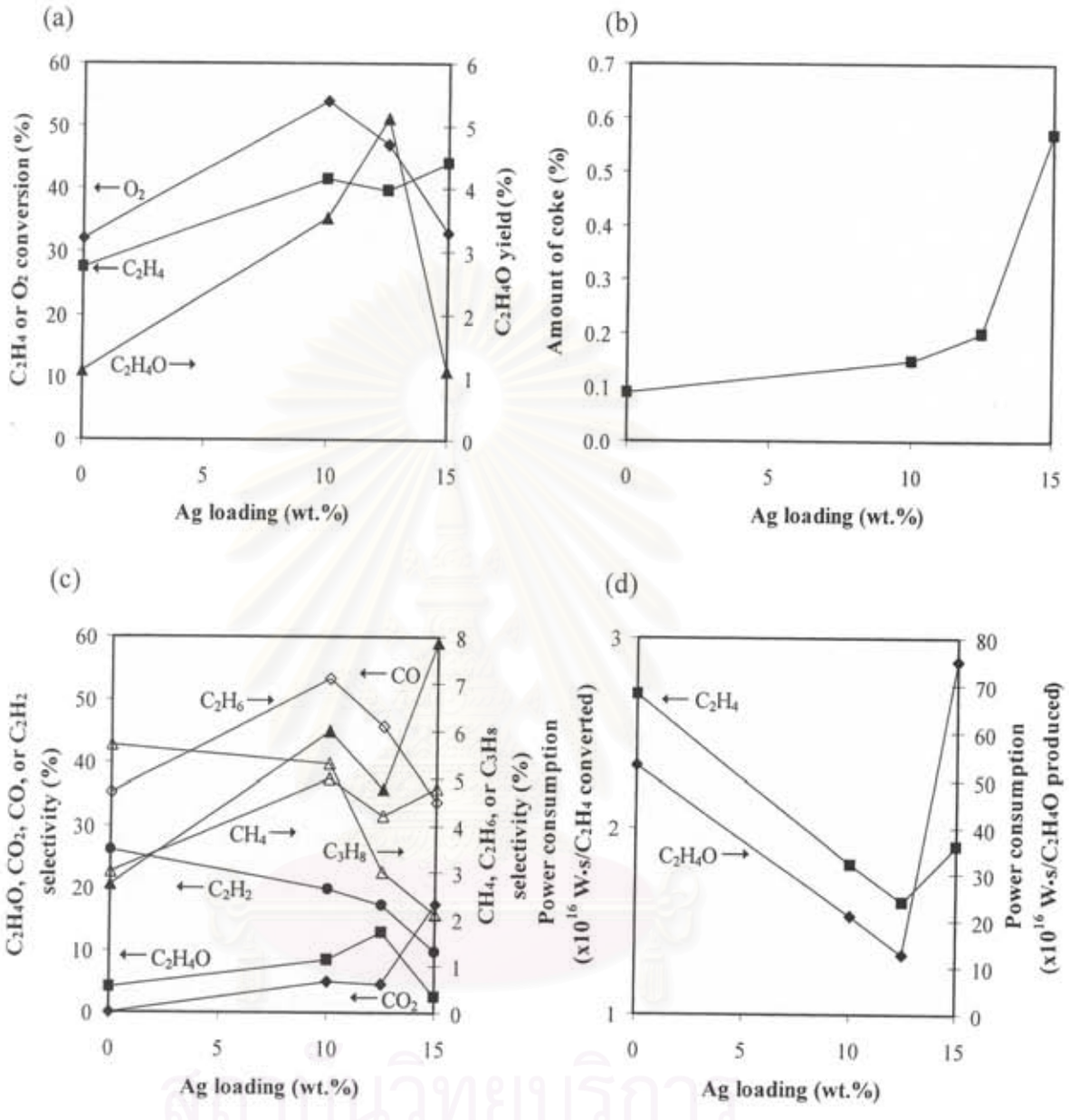

Fig. 1.6. (a) Ethylene and oxygen conversions and ethylene oxide yield, (b) amount of coke formed, (c) product selectivities, and (d) power consumptions as a function of Ag loading on (LSA)α-Al_2O_3 (molar ratio of O_2/C_2H_4 = 1/1; feed flow rate = 50 ml/min; gap distance = 1 cm; frequency = 500 Hz; and, voltage = 15 kV).

Fig. 1.6(d) shows the effect of silver loading on the power consumption for ethylene conversion and ethylene oxide production. The results show that the power consumption per molecule of C_2H_4 converted was much lower than the power consumption per molecule of C_2H_4O produced. With increasing the silver loading, the

power consumption per molecule of C_2H_4 converted or per molecule of C_2H_4O produced substantially decreased and reached the minimum at a Ag loading of 12.5 wt.%. Beyond this optimum Ag loading, the power consumption dramatically increased with further increasing the Ag loading. The increase in the power consumption at above the 15 wt.% Ag loading resulted from the increase in coke formation. The optimum Ag loading of 12.5 wt.% on (LSA)α-Al_2O_3 was selected for further investigation since it gave the highest ethylene oxide selectivity, the highest ethylene oxide yield, and the lowest power consumption. This optimum Ag loading was in good agreement with our previous study [10].

1.3.2.3 Effect of applied voltage

Based on the preliminary tests on the voltage range that could be applied to the studied system, the break-down voltage, or the lowest voltage (onset voltage), to generate plasma was found to be about 7 kV, and at an applied voltage higher than 15 kV, the plasma system became unstable due to a large amount of coke formation. Therefore, the reaction experiments were conducted in the voltage range of 7-15 kV in order to determine the effect of applied voltage. The effect of applied voltage on the C_2H_4 and O_2 conversions and the C_2H_4O yield is illustrated in Fig. 1.7(a). The oxygen conversion and ethylene oxide yield tended to increase with increasing applied voltage in the range of 7-15 kV, whereas the ethylene conversion remained almost unchanged. One plausible explanation for the converted oxygen increase is that a higher voltage results in a higher generated current, as shown in Fig. 1.7(b), leading to more available electrons that, in turn, increase an opportunity for collision with reactant molecules. Moreover, an increase in the O active species generated in the plasma zone results in their more opportunities to adsorb on the surface of the catalyst for further subsequent reactions, especially to yield the desired ethylene oxide product. In contrast, it was unexpected that C_2H_4 conversion remained nearly constant with increasing applied voltage. This indicates that the converted C_2H_4 species in the plasma zone may be recombined to form C_2H_4 as a secondary reaction in the catalytic zone. More discussion will be given in the next paragraph.

The effect of applied voltage on the selectivities for C_2H_4O, CO, CO_2, CH_4, C_2H_2, C_2H_6, and C_3H_8 is shown in Fig. 1.7(c). The selectivity for C_2H_4O obviously increased, but only slightly for the CO_2 selectivity, with increasing applied voltage, in

contrast to the selectivity for C_2H_2, whereas the selectivities for CH_4 and C_2H_6 first increased and then decreased. The selectivity for C_3H_8 remained almost unchanged in the studied range of voltage. When the applied voltage increased, corresponding to the increasing O active species as mentioned above, active hydrocarbon species are further oxidized to form CO and C_2H_4O on the surface of the catalyst, but CO is not further oxidized to CO_2, as confirmed by a sharp drop with increasing applied voltage from 13 to 15 kV. These results suggest that a higher number of O active species at a higher applied voltage is more favorable for C_2H_4O production than complete combustion. Interestingly, the amount of C_2H_2, a product from the C_2H_4 dehydrogenation in the plasma zone, tended to decrease with increasing applied voltage due to the simultaneous hydrogenation reaction of C_2H_2 on the Ag catalyst [35], which may compensate for the amount of C_2H_4 converted in the plasma zone, consequently resulting in almost unchanged C_2H_4 conversion.

Fig. 1.7(d) shows the effect of applied voltage on the power consumption. With increasing applied voltage, the power consumption per molecule of converted C_2H_4 increased, whereas the power consumption per molecule of produced C_2H_4O substantially decreased. As shown above concerning the almost unchanged ethylene conversion, the rising average electron energy and the increasing number of electrons in the plasma zone could not enhance the conversion of ethylene, probably due to the C_2H_2 hydrogenation to reform C_2H_4 on the surface of the silver catalyst in the catalytic zone, resulting in an insignificant increase in energy consumption per molecule of C_2H_4 converted when increasing the applied voltage. In contrast, an increase in the selectivity for C_2H_4O was comparatively much higher when increasing the applied voltage, resulting in lower power consumption per molecule of produced C_2H_4O. From the results, the optimum voltage of 15 kV, which produced reasonably high C_2H_4 and O_2 conversions, the highest ethylene oxide selectivity, and the highest ethylene oxide yield with the lowest power consumption per C_2H_4O molecule produced, was selected for further experiments.

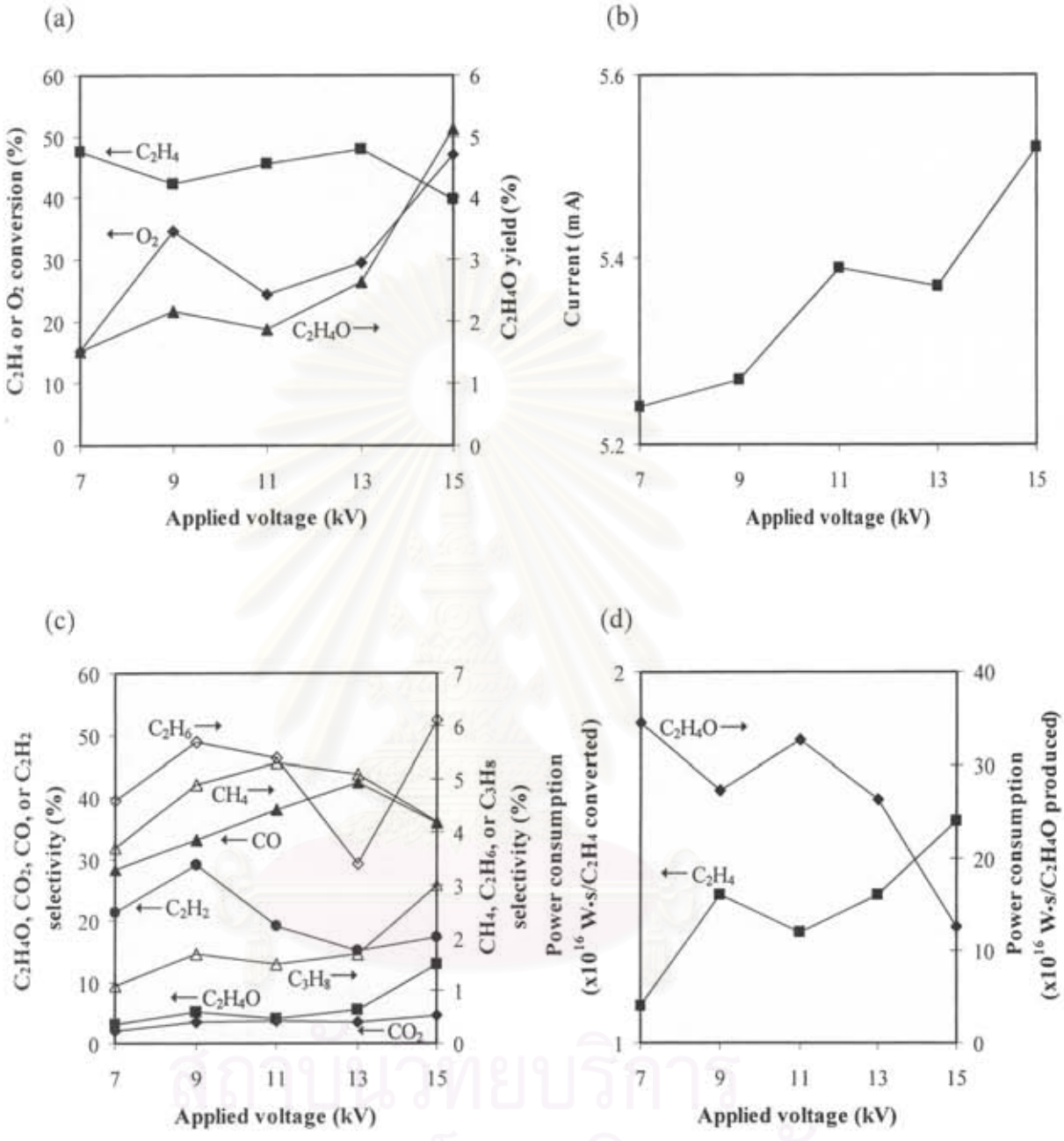

Fig. 1.7. (a) Ethylene and oxygen conversions and ethylene oxide yield, (b) generated current, (c) product selectivities, and (d) power consumptions as a function of applied voltage in the presence of 12.5 wt.% Ag on (LSA)α-Al_2O_3 (molar ratio of O_2/C_2H_4 = 1/1; feed flow rate = 50 ml/min; gap distance = 1 cm; and, frequency = 500 Hz).

1.3.2.4 Effect of input frequency

Input frequency is another important parameter greatly affecting the plasma characteristics in terms of stability and efficiency performance. In order to investigate the effect of input frequency, the studied plasma system was operated in the 300-800 Hz frequency range since a large amount of coke was found to deposit on the electrode surface at a frequency lower than 300 Hz, and the plasma could not exist at a frequency higher than 800 Hz. The effect of input frequency on the C_2H_4 and O_2 conversions and the C_2H_4O yield is illustrated in Fig. 1.8(a). When the input frequency increased, the O_2 conversion decreased, whereas the C_2H_4 conversion remained almost constant. The explanation is that, as shown in Fig. 1.8(b), a higher frequency results in lower current, which corresponds to the reduction of the number of electrons generated. Consequently, the opportunity for collision between electrons and O_2 or C_2H_4 molecules declines with decreasing current. Therefore, it was expected that the conversions of both C_2H_4 and O_2, and the C_2H_4O yield, should decrease with increasing input frequency; however, the conversion of C_2H_4 did not follow this expectation, which is similar to the case of increasing applied voltage. As mentioned earlier, the invariant conversion of C_2H_4 is the trade off between the C_2H_4 dehydrogenation in the plasma zone and the C_2H_2 hydrogenation on the surface of the silver catalyst in the catalytic zone. Moreover, in the frequency range of 300-500 Hz, the C_2H_4O yield was found to remain almost unchanged, but beyond 500 Hz, it significantly decreased, probably due to the dramatic decrease in O_2 conversion.

The effect of input frequency on the product selectivities is shown in Fig. 1.8(c). The selectivity for C_2H_4O remained nearly unchanged when the frequency was varied in the range of 300-500 Hz. Beyond 500 Hz, the selectivity decreased substantially with increasing frequency. Since the decrease in the input frequency from 800 to 500 Hz results in increased current, there are accordingly more O active species available to adsorb on the surface of the silver catalyst for the epoxidation reaction, leading to the higher selectivities for all products, including C_2H_4O. At a frequency lower than 500 Hz, the selectivity for C_2H_4O did not further increase with decreasing frequency, despite a higher amount of generated electrons, because of the coke formation. The selectivities for CO and CO_2 also tended to increase with decreasing input frequency. This is because more O active species at lower input

frequency could lead to the increase in the selectivities for CO and CO_2. Therefore, an input frequency of 500 Hz was considered to be a potentially optimum condition, exhibiting reasonably high C_2H_4O selectivity with relatively low CO and CO_2 concentrations.

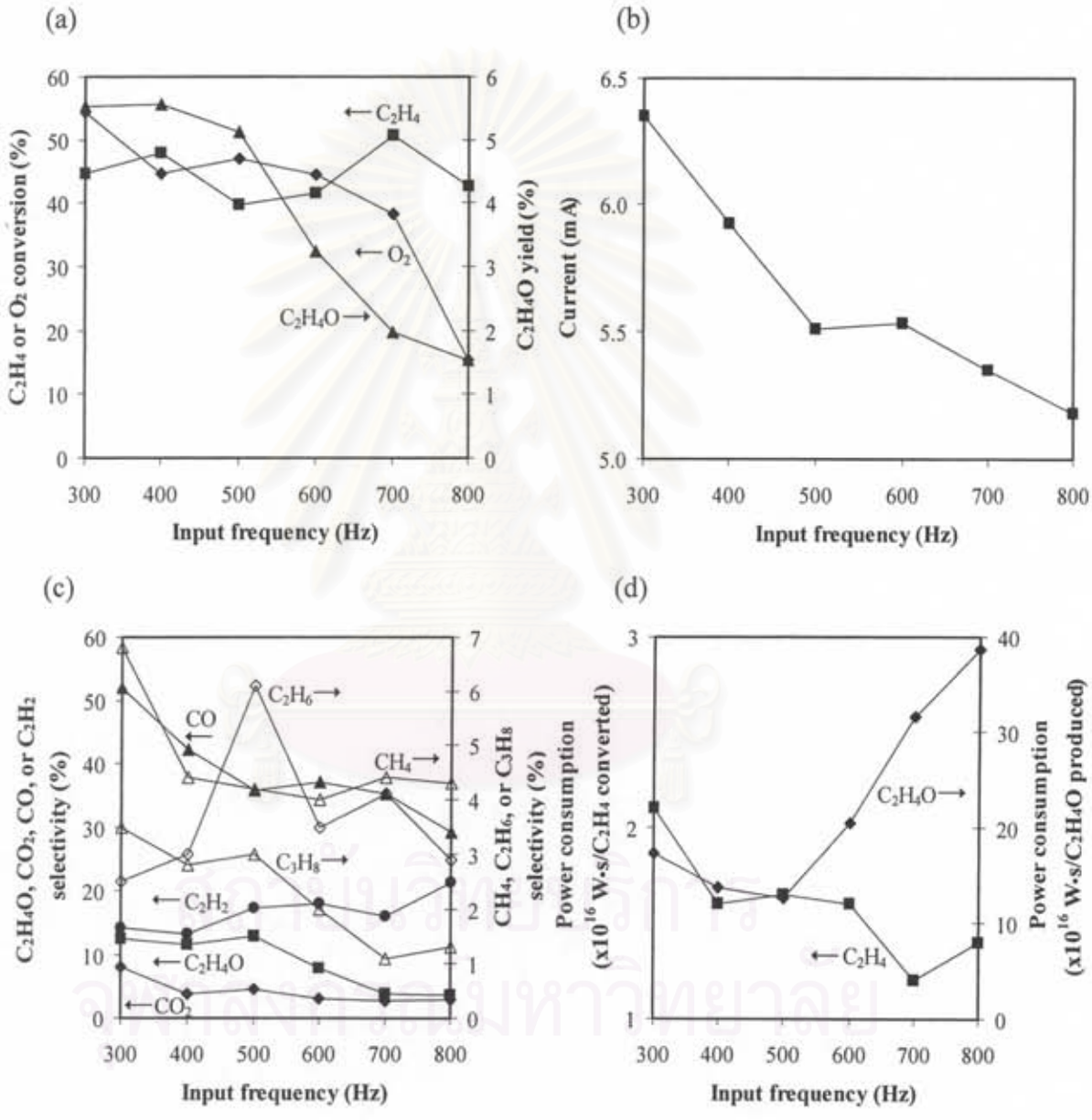

Fig. 1.8. (a) Ethylene and oxygen conversions and ethylene oxide yield, (b) generated current, (c) product selectivities, and (d) power consumptions as a function of input frequency in the presence of 12.5 wt.% Ag on (LSA)α-Al_2O_3 (molar ratio of O_2/C_2H_4 = 1/1; feed flow rate = 50 ml/min; gap distance = 1 cm; and, applied voltage = 15 kV).

The effect of frequency on the power consumption to break down each C_2H_4 molecule or to create each C_2H_4O molecule is shown in Fig. 1.8(d). The result shows that the power consumption per C_2H_4 molecule converted tended to gradually decline with increasing input frequency. Interestingly, the power consumption to create each C_2H_4O molecule decreased with increasing the input frequency up to 500 Hz; beyond this frequency, the power consumption dramatically increased. This is because a higher frequency gives a lower current, resulting in lowering the number of electrons to initiate the plasma reactions. At a frequency lower than 500 Hz, both power consumptions increased considerably with decreasing frequency. This is because the coke formation simply decreases the power efficiency. Based upon a relatively high ethylene oxide selectivity and ethylene oxide yield, as well as the lowest power consumption per molecule of ethylene oxide produced, an optimum input frequency of 500 Hz was selected for further experiments.

1.3.2.5 Effect of molar ratio of O_2/C_2H_4

To determine the influence of the feed gas composition on the ethylene epoxidation reaction under a corona discharge environment, the feed O_2/C_2H_4 molar ratio was varied in the range of 1/1 to 5/1, while the applied voltage and input frequency were kept constant at 15 kV and 500 Hz, respectively. An increase in the O_2/C_2H_4 molar ratio significantly enhanced only the C_2H_4 conversion, while the O_2 conversion increased and then decreased with further increasing the molar ratio higher than 3/1, as shown in Fig. 1.9(a). The explanation is that an increase in the molar ratio of O_2/C_2H_4 results in having more O_2 available to react with ethylene molecules, leading to higher C_2H_4 conversion. Interestingly, the maximum conversion of O_2 was found to approximately be at the molar ratio of 3/1, which is the theoretical ratio for the C_2H_4 complete combustion. When considering the C_2H_4O yield, as also shown in Fig. 1.9(a), it was interestingly found to drastically decrease with increasing the molar ratio from 1/1 to 2/1; and beyond the molar ratio of 2/1, the yield tended to slightly decrease to almost zero at the molar ratio of 5/1.

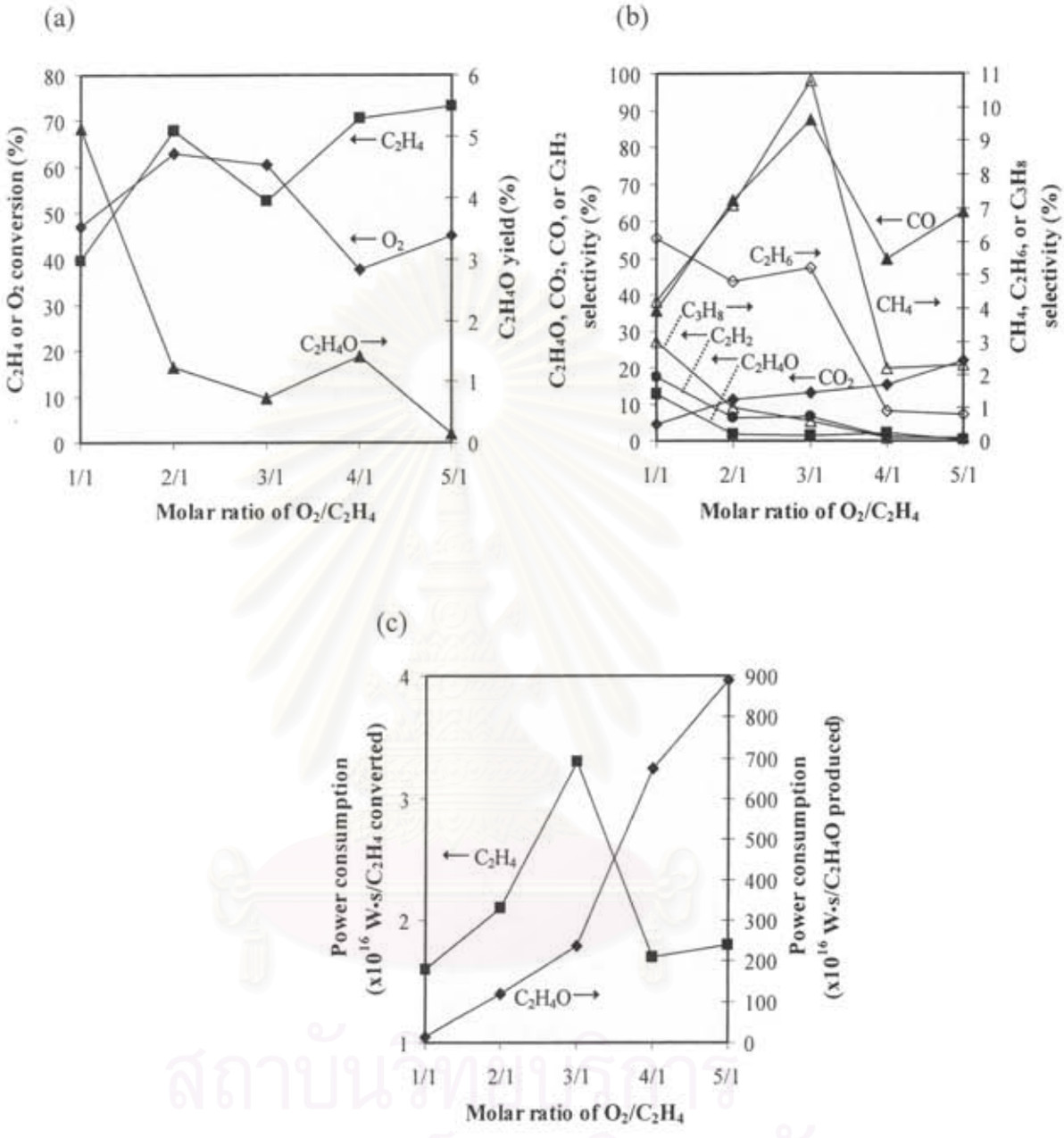

Fig. 1.9. (a) Ethylene and oxygen conversions and ethylene oxide yield, (b) product selectivities, and (c) power consumptions as a function of molar ratio of O_2/C_2H_4 in the presence of 12.5 wt.% Ag on (LSA)α-Al_2O_3 (feed flow rate = 50 ml/min; gap distance = 1 cm; applied voltage = 15 kV; and, input frequency = 500 Hz).

The effect of O_2/C_2H_4 molar ratio on the product selectivities is shown in Fig. 1.9(b). In this corona discharge system, the selectivities for C_2H_4O, C_2H_2, C_2H_6, and C_3H_8 decreased, but, in contrast, the selectivity for CO_2 increased with increasing

O_2/C_2H_4 molar ratio. Interestingly, the selectivities for CO and CH_4 increased up to the O_2/C_2H_4 molar ratio of 3/1; however, beyond this ratio, their selectivities rapidly declined. At the O_2/C_2H_4 molar ratio of 3/1, O_2 was contributed to form the highest amount of CO. At a molar ratio higher than 3/1, known as an excess O_2 condition, CO is further oxidized to form CO_2, as confirmed by an increase in the CO_2 selectivity. Moreover, at an O_2/C_2H_4 molar ratio of 5/1, the selectivity for C_2H_4O reached zero, suggesting that C_2H_4O can be formed under a deficient O_2 condition. The highest C_2H_4O selectivity was found at an O_2/C_2H_4 molar ratio of 1/1, which is in good agreement with our previous study [10].

Fig. 1.9(c) shows the power consumption needed to convert ethylene and to produce ethylene oxide at different O_2/C_2H_4 molar ratios. The power consumption per molecule of converted ethylene reached a maximum at an O_2/C_2H_4 molar ratio of 3/1. At an O_2/C_2H_4 molar ratio higher than 3/1, the power consumption rapidly decreased. However, there was an extremely significant increase in the power consumption per molecule of produced ethylene oxide with increasing the O_2/C_2H_4 molar ratio, especially at a molar ratio of 5/1. An O_2/C_2H_4 molar ratio of 1/1 was selected for further experiments because it provided the highest ethylene oxide selectivity, the highest ethylene oxide yield, and the lowest power consumption, in spite of having the lowest ethylene conversion.

1.3.2.6 Effect of feed flow rate

The feed flow rate has a significant effect on the residence time of gas molecules within both the plasma and catalytic zones, affecting the performance of the plasma system. The experiments were performed by varying the feed flow rates from 50 to 150 ml/min at an O_2/C_2H_4 molar ratio of 1/1. The optimum applied voltage of 15 kV and the input frequency of 500 Hz were still applied to control the plasma system. Fig. 1.10(a) illustrates the influence of the feed flow rate on the C_2H_4 and O_2 conversions and the C_2H_4O yield. The conversions of C_2H_4 and O_2 and the C_2H_4O yield decreased almost linearly with increasing feed flow rate from 50 to 150 ml/min, corresponding to decreasing the residence time from 0.6 to 0.2 s. An increase in the feed flow rate reduces the gas residence time in the reaction zone, resulting in a shorter contact time for ethylene and oxygen molecules to collide with electrons. As a result, a reduction in the feed flow rate enhanced the conversions of both C_2H_4 and O_2.

The feed flow rate dependence for product selectivities is depicted in Fig. 1.10(b). It is apparent that the selectivities for C_2H_4O, CO, CO_2, and other by-products tended to decrease with increasing feed flow rate. As explained above, this is because a higher feed flow rate reduces the opportunity for collision between electrons and reactant/intermediate molecules, as well as subsequent secondary reactions.

Fig. 1.10(c) shows the effect of feed flow rate on the power consumption. Even though the power consumption per molecule of converted ethylene and per molecule of produced ethylene oxide slightly decreased when increasing feed flow rate, a lower feed flow rate could provide much higher reactant conversions and desired ethylene oxide selectivity. This is possibly because the power consumption per molecule of produced ethylene oxide at different feed flow rates is not varied much in the studied range, and its change is relatively small compared to those for all previous operating parameters.

From all experimental results obtained above, it was found that the ethylene epoxidation preferably occurred in the combined catalytic and corona discharge plasma system using Ag/(LSA)α-Al_2O_3 as a catalyst under a deficient O_2 condition with an O_2/C_2H_4 molar ratio of 1/1, as compared with the sole plasma system. The chemistry of the combined catalytic and plasma system is considerably complicated, and further investigation is needed to obtain a better understanding of the interaction between plasma and catalysts on simultaneously occurring chemical reactions including ethylene epoxidation. Based on the current knowledge, for the corona discharge system without the catalyst, various oxygen and hydrocarbon active species can be mostly generated by electron collision. The oxygen active species can mainly react with ethylene molecules/radicals in the bulk gas phase to form ethylene oxide. When the combined catalytic and corona discharge is used, the ethylene oxide can be additionally produced by the partial oxidation of ethylene molecule with oxygen molecularly adsorbed at the catalyst surface [10]. Therefore, the ethylene oxide formed in the combined system can be plausibly produced via the combination of gaseous discharge mechanism and catalytic surface chemistry.

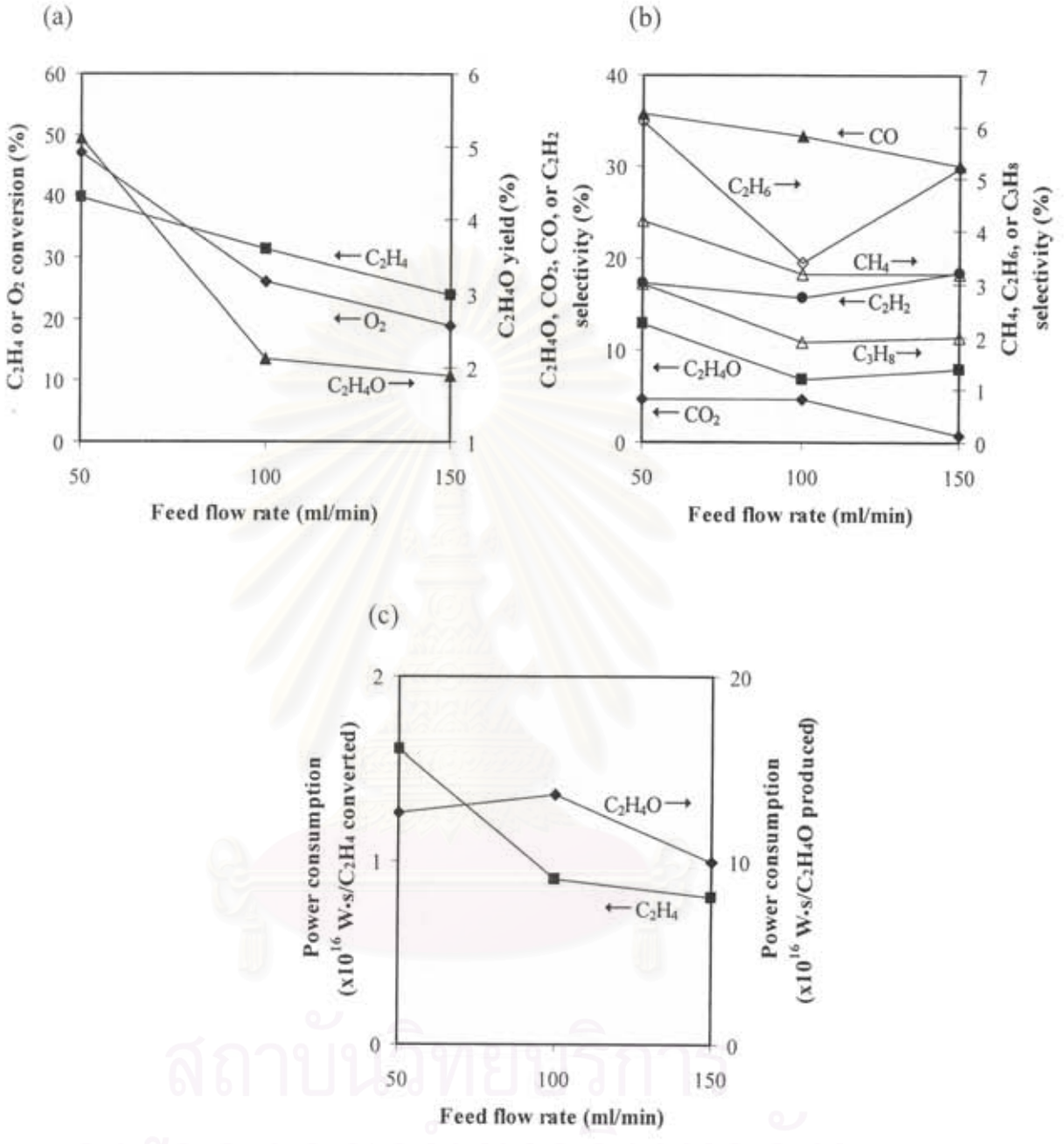

Fig. 1.10. (a) Ethylene and oxygen conversions and ethylene oxide yield, (b) product selectivities, and (c) power consumptions as a function of feed flow rate in the presence of 12.5 wt.% Ag on (LSA)α-Al_2O_3 (molar ratio of O_2/C_2H_4 = 1/1; gap distance = 1 cm, applied voltage = 15 kV; and, input frequency = 500 Hz).

1.3.2.7 Durability of catalyst

To study the durability of the 12.5 wt.% Ag/(LSA)α-Al_2O_3 catalyst, the activity test was performed in two consecutive runs without any intermediate treatment. The studied plasma reactor packed with the catalyst was operated about 3 h for each run to reach the steady state. Fig. 1.11 shows the comparison of the process performance of the two consecutive runs under the optimum conditions. The results show that the process performance of the second run was lower than that of the first run in terms of the oxygen conversion and all product selectivities except the ethylene conversion. This lower activity could possibly be due to the coke formation on the spent catalyst, observed by TPO, as mentioned previously, as well as the Ag agglomeration verified by the TEM micrographs, as shown in Fig. 1.12. When comparing the TEM micrographs of the fresh catalyst (Fig. 1.4) and of the spent catalyst (Fig. 1.12), the mean particle size of Ag increased from 9.5 to 15 nm after the activity experiment. The Ag agglomeration on the catalyst surface is believed to result from the high energy intensity of the corona discharge used in this study. For non-thermal AC plasma, the bulk gas temperature is comparatively low; however, the energetic electrons may have energy ranging from 1 to 10 eV, which corresponds to extremely high temperatures of about 10,000 to 100,000 K [12]. Therefore, the catalyst surface has high probability to be collided intermittently with these high-temperature electrons, causing the increase in temperature on scattering micro-sized spots in a very short period throughout the catalyst surface and subsequently resulting in the Ag agglomeration. The measured temperature of the bulk gas was low in the range of 100-200°C, whereas the temperature of these aforementioned spots was expected to be significantly higher. In our future study, a dielectric barrier discharge (DBD), which can produce microdischarge with much lower energy intensity, will also be tested for the ethylene epoxidation reaction without causing the sintering effect of Ag nanoparticles.

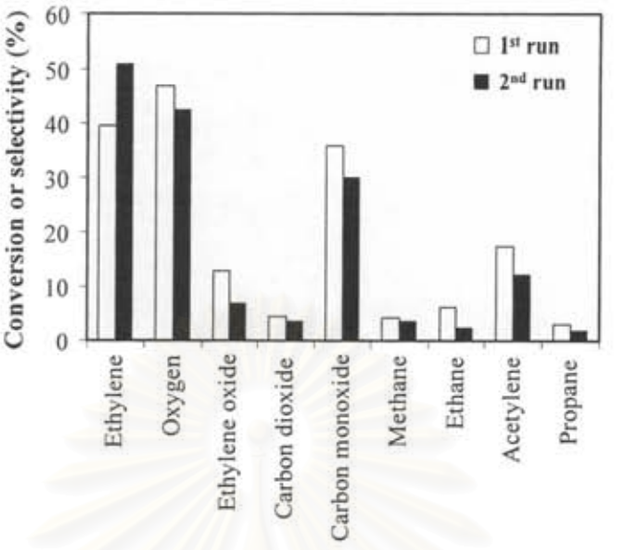

Fig. 1.11. Reactant conversions and product selectivities obtained by catalytic-plasma system at the optimum conditions for two consecutive runs (molar ratio of O_2/C_2H_4 = 1/1; feed flow rate = 50 ml/min; gap distance = 1 cm; frequency = 500 Hz; and, voltage = 15 kV).

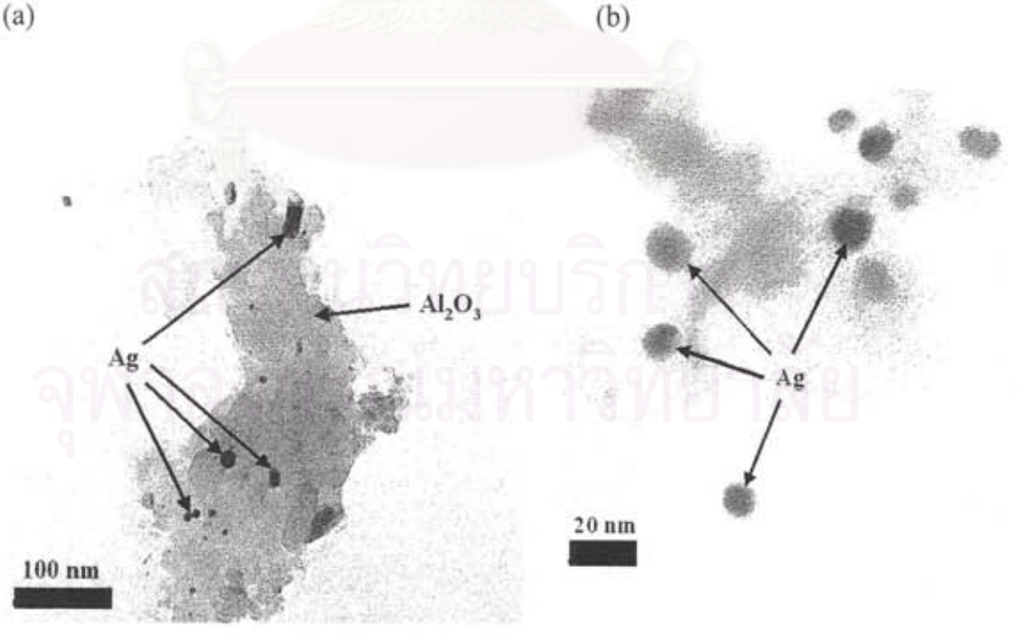

Fig. 1.12. TEM micrographs of spent 12.5 wt.% Ag/(LSA)α-Al_2O_3 at (a) low magnification and (b) high magnification.

1.4 Conclusions

In this work, the epoxidation reaction of ethylene under AC low-temperature corona discharge was investigated in the presence of catalysts; Ag/(LSA)α-Al_2O_3, Ag/(HSA)γ-Al_2O_3, and Au-Ag/(HSA)γ-Al_2O_3. In comparisons among the studied catalysts, Ag/(LSA)α-Al_2O_3 was experimentally found to be the best catalyst to provide the highest ethylene oxide selectivity. The optimum Ag loading on the (LSA)α-Al_2O_3 was found to be 12.5 wt.%, at which a maximum ethylene oxide selectivity of 12.9% was obtained at the optimum applied voltage and input frequency of 15 kV and 500 Hz, respectively. Under these optimum conditions, the power consumption was found to be 12.6×10^{-16} W·s/molecule of ethylene oxide produced. In addition, decreases in the oxygen-to-ethylene molar ratio and feed flow rate were also experimentally found to provide better ethylene epoxidation activity.

References

1. http://www.osha.gov/OshDoc/data_General_Facts/ethylene-oxide-factsheet.pdf
2. http://www.dow.com/ethyleneoxide/news/20050405b.htm
3. G.H. Law, H.C. Chitwood, Catalyst Composition for Oxidation of Ethylene to Ethylene Oxide, US Patent No. 2,279,470, 1942.
4. C.T. Campbell, M.T. Paffett, Appl. Surf. Sci. 19 (1984) 28-42.
5. S.A. Tan, R.B. Grant, R.M. Lambert, J. Catal. 100 (1986) 383-391.
6. K.L. Yeung, A. Gavriilidis, A. Varma, M.M. Bhasin, J. Catal. 174 (1998) 1-12.
7. G. Iwakura, A Novel Silver Catalyst Prepared by Using Superheated-Steam as a Heating Medium for Ethylene Oxide Production, Japan Patent No. 63-126552, 1985.
8. M.M. Bhasin, Catalyst Composition for Oxidation of Ethylene to Ethylene Oxide, US Patent No. 4,908,343, 1988.
9. S. Rojluechai, S. Chavadej, J.W. Schwank, V. Meeyoo, Catal. Commun. 8 (2007) 57-64.
10. S. Rojluechai, S. Chavadej, J.W. Schwank, V. Meeyoo, J. Chem. Eng. Jpn. 39 (2006) 321-326.
11. B. Eliasson, U. Kogelschatz, IEEE Trans. Plasma Sci. 19 (1991) 1063-1077.
12. L.A. Rosacha, G.K. Anderson, L.A. Bechtold, J.J. Coogan, H.G. Heck, M. Kang, W.H. McCulla, R.A. Tennant, P.J. Wantuck, NATO ASI Series Part B (1993) 34.
13. H. Suhr, Plasma Chem. Plasma Process. 3 (1983) 1-61.
14. P. Patiño, M. Ropero, D. Iacocca, Plasma Chem. Plasma Process. 16 (1995) 563-575.
15. J.S. Chang, P.A. Lawless, T. Yamamoto, IEEE Trans. Plasma Sci. 19 (1991) 1152-1166.
16. K. Yan, H. Hui, M. Cui, J. Miao, X. Wu, C. Bao, R. Li, J. Electrostat. 44 (1998) 17-39.
17. S. Bröer, T. Hammer, Appl. Catal. B: Environ. 28 (2000) 101-111.
18. A. Marafee, C. Liu, G. Xu, R. Mallinson, L. Lobban, Ind. Eng. Chem. Res. 36 (1997) 632-637.

19. C. Liu, A. Marafee, R. Mallinson, L. Lobban, Appl. Catal. A: Gen. 164 (1997) 21-33.
20. C. Liu, R. Mallinson, L. Lobban, J. Catal. 179 (1998) 326-334.
21. C. Liu, R. Mallinson, L. Lobban, Appl. Catal. A: Gen. 178 (1999) 17-27.
22. K.P. Francke, H. Miessner, R. Rudolph, Plasma Chem. Plasma Process. 20 (2000) 393-403.
23. Y. Wen, X. Jiang, Plasma Chem. Plasma Process. 21 (2001) 665-678.
24. D. Li, D. Yakushiji, S. Kanazawa, T. Ohkubo, Y. Nomoto, J. Electrostat. 55 (2002) 311-319.
25. M.G. Sobacchi, A.V. Saveliev, A.A. Fridman, L.A. Kennedy, S. Ahmed, T. Krause, Int. J. Hydrogen Energ. 27 (2002) 635-642.
26. C.L. Gordon, L.L. Lobban, R.G. Mallinson, Catal. Today 84 (2003) 51-57.
27. M. Dors, J. Mizeraczyk, Catal. Today 89 (2004) 127-133.
28. H. Kušić, N. Koprivanac, B.R. Locke, J. Hazard. Mater. 125 (2005) 190-200.
29. M.W.Li, C.P. Liu, Y.L. Tian, G.H. Xu, F.C. Zhang, Y.Q. Wang, Energ. Fuel. 20 (2006) 1033-1038.
30. J. Van Durme, J. Dewulf, W. Sysmans, C. Leys, H. Van Langenhove, Appl. Catal. B: Environ. 74 (2007) 161-169.
31. S. Chavadej, W. Kiatubolpaiboon, P. Rangsunvigit, T. Sreethawong, J. Mol. Catal. A: Chem. 263 (2007) 128-136.
32. S. Chavadej, K. Saktrakool, P. Rangsunvigit, L.L. Lobban, T. Sreethawong, Chem. Eng. J. 132 (2007) 345-353.
33. S. Linic, J.T. Jankowiak, M.A. Barteau, J. Catal. 224 (2004) 489-493.
34. P.V. Geenen, H.J. Boss, G.T. Pott, J. Catal. 77 (1982) 499-510.
35. A. Sárkány, Zs. Révay, Appl. Catal. A: Gen. 243 (2003) 347-355.
36. M.A. Malik, S.A. Malik, Platinum Metals Rev. 43 (1999) 109-113.

Part 2: Ethylene Epoxidation in Low-Temperature AC Dielectric Barrier Discharge: Effects of Oxygen-to-Ethylene Feed Molar Ratio and Operating Parameters

2.1 Introduction and Survey of Related Literature

Ethylene oxide (C_2H_4O, EO) is an important industrial chemical, which is primarily used as an intermediate in the production of various useful chemicals. Its major use is in the production of ethylene glycol. It is also used for the manufacture of surfactants and detergents by a process called ethoxylation, solvents, antifreezes, adhesives, polyurethane foam, fumigants for agricultural products, and sterilants for medical equipment and supplies, spices, and cosmetics [1,2]. Since EO is a valuable chemical feedstock for many applications, the selective partial oxidation of ethylene to EO, so-called ethylene epoxidation, has been of great interest in global research works.

As discovered by Lefort in 1931 [3], the gas phase epoxidation of ethylene to EO using molecular oxygen and silver catalysts is one of the greatest findings in heterogeneous catalysis, being the most widely used method for ethylene epoxidation. Since 1940, almost all EO produced industrially has been made using this method [4]. To date, silver catalysts supported on alpha-alumina ($Ag/\alpha\text{-}Al_2O_3$) with alkali and transition metal promoters [5-15], such as Cs, Cu, Re, and Au, or with addition of chlorine-containing moderators into gaseous reactants [16-20], such as dichloroethane ($C_2H_4Cl_2$) and vinyl chloride (C_2H_3Cl), provide high selectivity for EO. However, the conventional catalytic process normally requires high temperatures, i.e. implying high energy consumption, to sufficiently activate the catalyst for the ethylene epoxidation, basically higher than 200°C. Moreover, the catalytic problems at high temperature operation, i.e. catalyst deactivation, catalyst regeneration, and catalyst replacement, greatly reduces the working efficiency of the process, as well as directly leads to a high production cost. These turn out to become necessary for developing a new approach to overcome the mentioned problems.

Non-thermal plasmas, such as dielectric barrier discharge (DBD), corona discharge, and glow discharge, are a highly potential alternative for chemical reaction

investigation under non-equilibrium conditions operated at low temperatures and atmospheric pressure. The main characteristic of the non-equilibrium plasma is its high electron temperatures (10^4-10^5 K), whereas the bulk gas temperature remains as low as room temperature [21,22]. This implies comparatively lower energy consumption used for operating the reaction system as compared with conventional catalytic processes. The non-equilibrium plasma with the highly energetic electrons and low temperature in the bulk gas can initiate several chemical reactions, which are normally not possible to occur at low temperatures [23].

DBD is the most commonly used technique for atmospheric pressure plasma operation. The basic principle of this technique is to utilize non-equilibrium plasma, in which the major part of electrical energy is transferred to energetic electrons and active radical species generated from subsequent reactions [24]. A major advantage of DBD is that the entire electrode area is effectively employed for discharge generation, resulting in the comparatively high discharge volume with a very low temperature typically close to room temperature. The uses of DBD for chemical syntheses and conversions have become increasingly important for several applications, such as the partial oxidation of methane to methanol [24], the ozone production from molecular oxygen [25], the removal of gaseous H_2S and NH_3 [26], the oxidation of propene [27], the decomposition of trichloroethylene [28], the reforming of hydrocarbons and alcohols for hydrogen production [29], and the methane conversion to C_2 hydrocarbons [30]. However, up to now, the use of DBD for gas phase epoxidation reaction has been rarely investigated. To our knowledge, only one recent published work described about gas phase epoxidation of propylene [31]; however, there has been no any literature reporting the epoxidation of ethylene using DBD yet.

In this work, a low-temperature dielectric barrier discharge (DBD) system was employed for the first time for non-catalytic ethylene epoxidation at atmospheric pressure. The effects of various operating parameters, including O_2/C_2H_4 feed molar ratio, feed flow rate, input frequency, applied voltage, and electrode gap distance, on the activity of ethylene epoxidation and the system performance were extensively examined.

2.2 Procedure

2.2.1 Reactant gases

All gases used in this work, i.e. 99.995% helium (high purity grade), 40% ethylene balanced with helium, and 97% oxygen balanced with helium, were supplied by Thai Industrial Gas (Public) Co., Ltd.

2.2.2 Dielectric barrier discharge system

The experimental study of ethylene epoxidation was conducted in a low-temperature dielectric barrier discharge (DBD) system, which was operated at atmospheric pressure and ambient temperature, around 25-27°C (room temperature). The schematic of the dielectric barrier discharge system is shown in Fig. 2.1(a). The acrylic plate-made DBD reactor sizes were 2 cm height x 3 cm width x 15 cm length for the inner dimensions, and 3 cm height x 7 cm width x 19 cm length for the outer dimensions. As shown in Fig. 2.1(b), it consisted of a 5-mm-thick dielectric glass plate placed between two parallel stainless steel electrodes, on the lower electrode. The gap distance between the electrodes was varied from 10 to 14 mm. The input power used to generate microdischarge plasma between the electrode gap was domestic alternating current (AC), 200 V and 50 Hz, which was transmitted to a high voltage current via a power supply unit. The power supply unit consisted of three steps. For the first step, the domestic AC input of 220 V and 50 Hz was converted to a DC output of 70 V by a DC power supply converter. For the second step, a 500 W power amplifier with a function generator was used to transform the DC into AC current with a sinusoidal waveform and different frequencies. For the third step, the outlet voltage was stepped up by using a high voltage transformer. The description of the power supply unit was given elsewhere [32]. The output voltage and frequency were controlled by the function generator. The voltage and current at the low voltage side were measured instead of those at the high voltage side across the electrodes since the plasma generated is non-equilibrium in nature. The high side voltage and current were thereby calculated by multiplying and dividing by a factor of 130, respectively [32-35]. A power analyzer was used to measure power, current, frequency, and voltage at the low voltage side of the power supply unit.

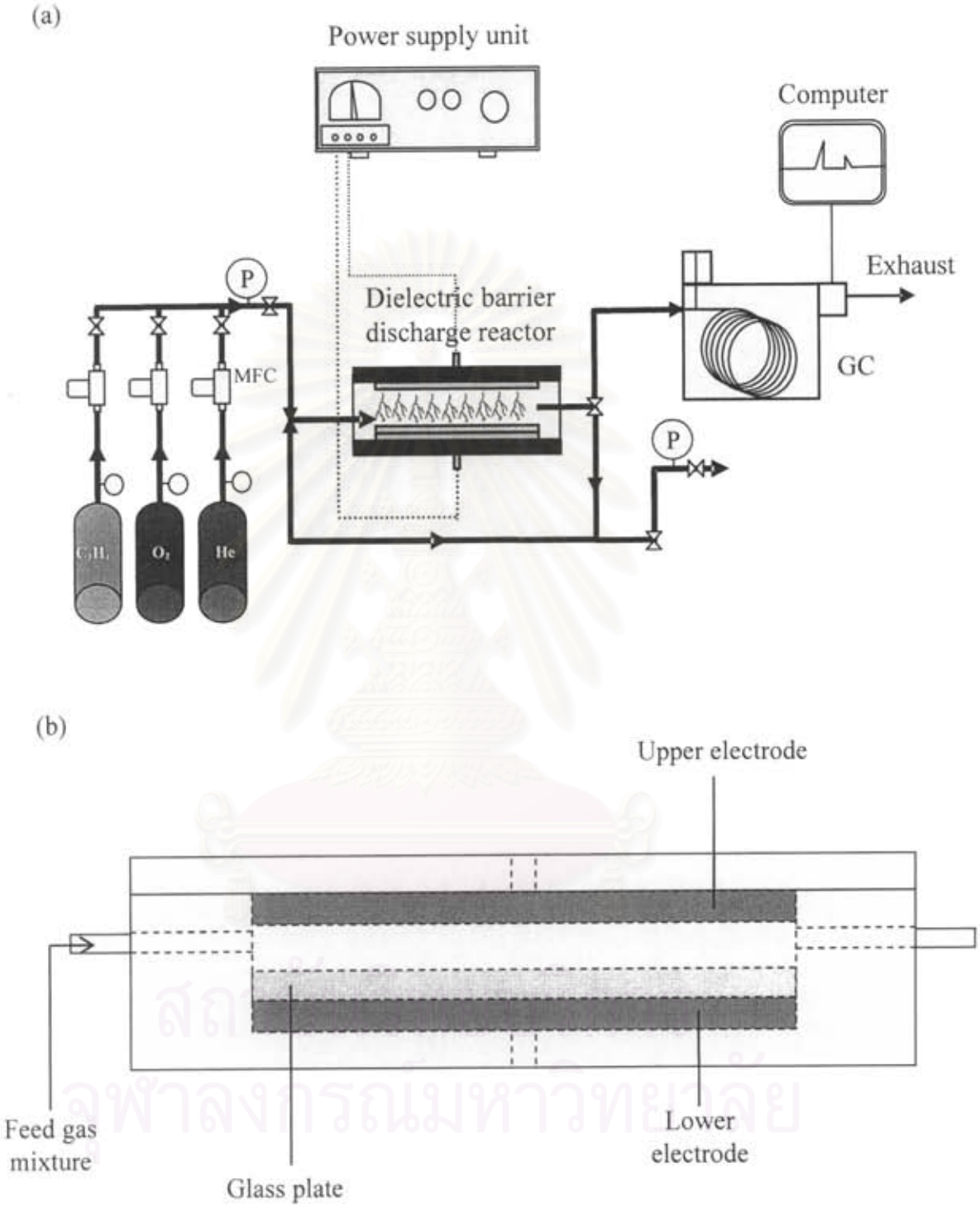

Fig. 2.1 (a) Schematic of experimental setup for ethylene epoxidation reaction in dielectric barrier discharge plasma system and (b) configuration of the dielectric barrier discharge reactor.

2.2.3 Reaction testing procedure

Reactant gases (ethylene, oxygen, and helium) fed through the plasma reactor were controlled by a set of electronic mass flow controllers and transducers, supplied by SIERRA® Instrument Inc., to obtain a feed gas mixture having different flow rates and oxygen-to-ethylene molar ratios. A 7-μm in-line filter was placed upstream of each mass flow controller in order to trap any solid particles. A check valve was placed downstream of each mass flow controller to prevent any back flow of the reactant gases. All of the reactant gases were mixed inside a single line before being introduced into the DBD reactor. For any studied conditions, the feed gas mixture was first introduced into the DBD system without turning on the power supply unit. After the composition of outlet gas was invariant with time, it was turned on. The outlet of the reactor was either vented to the atmosphere via rubber tube exhaust or was connected to an on-line gas chromatograph (Perkin-Elmer, AutoSystem GC) for analysis of the product gases. The moisture in the product gas stream was trapped by a water trap filter before entering a heated stainless steel line to the on-line gas chromatograph. The gas chromatograph was equipped with both a thermal conductivity detector (TCD) and a flame ionization detector (FID). For the TCD channel, the packed column (Carboxen 1000) was used for separating the product gases, which were hydrogen (H_2), oxygen (O_2), carbon monoxide (CO), carbon dioxide (CO_2), and ethylene (C_2H_4). For the FID channel, the capillary column (OV-Plot U) was used for analysis of EO and other by-product gases, i.e. CH_4, C_2H_2, C_2H_6, and C_3H_8. The composition of product gas stream was analyzed by the on-line gas chromatograph every 20 min. After the system reached steady state, an analysis of outlet gas composition was taken at least a few times. The experimental data taken under steady state conditions were averaged, and these averages were used to evaluate the performance of the plasma system. It is also worth noting that during the reaction, the temperature at the reactor wall was found to be lower than the melting temperature of acrylic plate (130°C), which was used to construct the DBD reactor.

2.2.4 Reaction performance assessment

To evaluate the process performance, the conversions of ethylene and oxygen and the selectivities for products, including EO, CO, CO_2, H_2, CH_4, C_2H_2, C_2H_6, and traces of C_3, were considered. The conversion of either ethylene or oxygen is defined as:

$$\% \text{ Reactant conversion} = \frac{(\text{moles of reactant } in - \text{moles of reactant } out)\,(100)}{(\text{moles of reactant } in)}$$

The product selectivity is calculated from the following equation:

$$\% \text{ Product selectivity} = \frac{[(\text{number of carbon or hydrogen atom in product})\,(\text{moles of product produced})]\,(100)}{[(\text{number of carbon or hydrogen atom in ethylene})\,(\text{moles of ethylene converted})]}$$

The EO yield is calculated from the following equation:

$$\% \text{ EO yield} = (\% \text{ ethylene conversion})\,(\% \text{ EO selectivity}) / (100)$$

To determine the energy efficiency of the plasma system, the specific power consumption is calculated in a unit of Ws per molecule of converted ethylene or per molecule of produced EO using the following equation:

$$\text{Specific power consumption} = \frac{(P)\,(60)}{(N)\,(M)}$$

where P = Power (W)

N = Avogadro's number = 6.02×10^{23} molecules/mol

M = Rate of converted ethylene molecules in feed or rate of produced EO molecules (mol/min).

2.3 Results and Discussion

2.3.1 Effect of feed molar ratio of O_2/C_2H_4

The effect of O_2/C_2H_4 feed molar ratio was initially studied in order to obtain the most suitable feed gas composition for ethylene epoxidation reaction under the low-temperature DBD system. In this study, the O_2/C_2H_4 feed molar ratio was investigated in the range of 1:1 to 4:1, while an applied voltage of 17 kV, an input frequency of 550 Hz, and a residence time of 0.45 min were used as base conditions to operate the DBD system. The residence time is calculated by the inside volume of the DBD reactor divided by a feed flow rate. The effect of O_2/C_2H_4 feed molar ratio on the C_2H_4 and O_2 conversions and the EO yield is shown in Fig. 2.2(a), and that on the selectivities for EO, CO, CO_2, H_2, CH_4, C_2H_2, C_2H_6, and C_3H_8 is shown in Fig. 2.2(b). The increase in the O_2/C_2H_4 feed molar ratio slightly affected the reactant conversions, but it mainly affected the EO and CO_2 selectivities, especially in the O_2/C_2H_4 feed molar ratio range between 1:1 and 3:1. This can be explained in that a higher O_2/C_2H_4 feed molar ratio leads to more O_2 content available to react with various hydrocarbon molecules, as well as EO and CO, to convert to CO_2. However, the conversion of O_2 reached a maximum in the O_2/C_2H_4 feed molar ratio range between 2:1 and 3:1, which is about the theoretical ratio for C_2H_4 complete combustion, as shown in the following equation. At a feed molar ratio higher than 3:1 or excess O_2 condition, the conversion of O_2 tended to decrease since O_2 is probably consumed at the same level.

$$C_2H_4 + 3O_2 \rightarrow 2CO_2 + 2H_2O$$

For the DBD system operated under the studied conditions, the yield of EO and the selectivities for EO, H_2, C_2H_2, and C_2H_6 tended to decrease, but in contrast, the selectivity for CO_2 increased with increasing O_2/C_2H_4 feed molar ratio, as aforementioned. Interestingly, the selectivity for CH_4 remained almost constant in the studied range of O_2/C_2H_4 feed molar ratio. The CO selectivity increased when the O_2/C_2H_4 feed molar ratio increased, and it reached a maximum at the O_2/C_2H_4 feed molar ratio of 2:1. Beyond the O_2/C_2H_4 feed molar ratio of 2:1, the CO selectivity decreased and reached a plateau at the theoretical O_2/C_2H_4 feed molar ratio for complete combustion of 3:1. Under the studied conditions, the main products were CO and CO_2 with significant amounts of EO, H_2, CH_4, and C_2 products (C_2H_2 and

C_2H_6). The highest hydrocarbon, i.e. C_3H_8, was found in a very small fraction. The results can be explained by the fact that under the presence of oxygen, both complete and partial oxidation reactions are dominant. The decrease in the selectivities for these hydrocarbons and H_2 and the increase in the selectivity for CO_2 with increasing oxygen fraction in feed clearly reveal that the oxidative dehydrogenation and coupling reactions unfavorably occurred under O_2-rich conditions, as expected. The EO selectivity was found to be the highest at the O_2/C_2H_4 feed molar ratio of 1:1 and decreased with increasing O_2/C_2H_4 feed molar ratio. Furthermore, at a very high O_2/C_2H_4 feed molar ratio of 4:1, the selectivity for EO dropped to zero level since this high O_2/C_2H_4 feed molar ratio induced the complete combustion to occur more favorably than the partial oxidation, as well as the epoxidation, indicating that the epoxidation reaction to produce EO is more likely to occur under O_2-lean conditions.

Fig. 2.2(c) shows the power consumptions used to convert an ethylene molecule and to produce an EO molecule at different O_2/C_2H_4 feed molar ratios. The power consumption per molecule of converted ethylene reached a maximum when the O_2/C_2H_4 feed molar ratio increased up to 2:1 and slightly decreased with further increasing feed molar ratio. However, there was a significant increase in the power consumption per molecule of produced EO with increasing O_2/C_2H_4 feed molar ratio, especially at the feed molar ratio higher than 3:1. It is also worth noting that the power consumption per molecule of EO produced was approximately two orders of magnitude higher than that per molecule of ethylene converted. Hence, an O_2/C_2H_4 feed molar ratio of 1:1 was therefore selected for further investigation because it provided the highest selectivity and yield for EO and the lowest power consumption per molecule of EO produced.

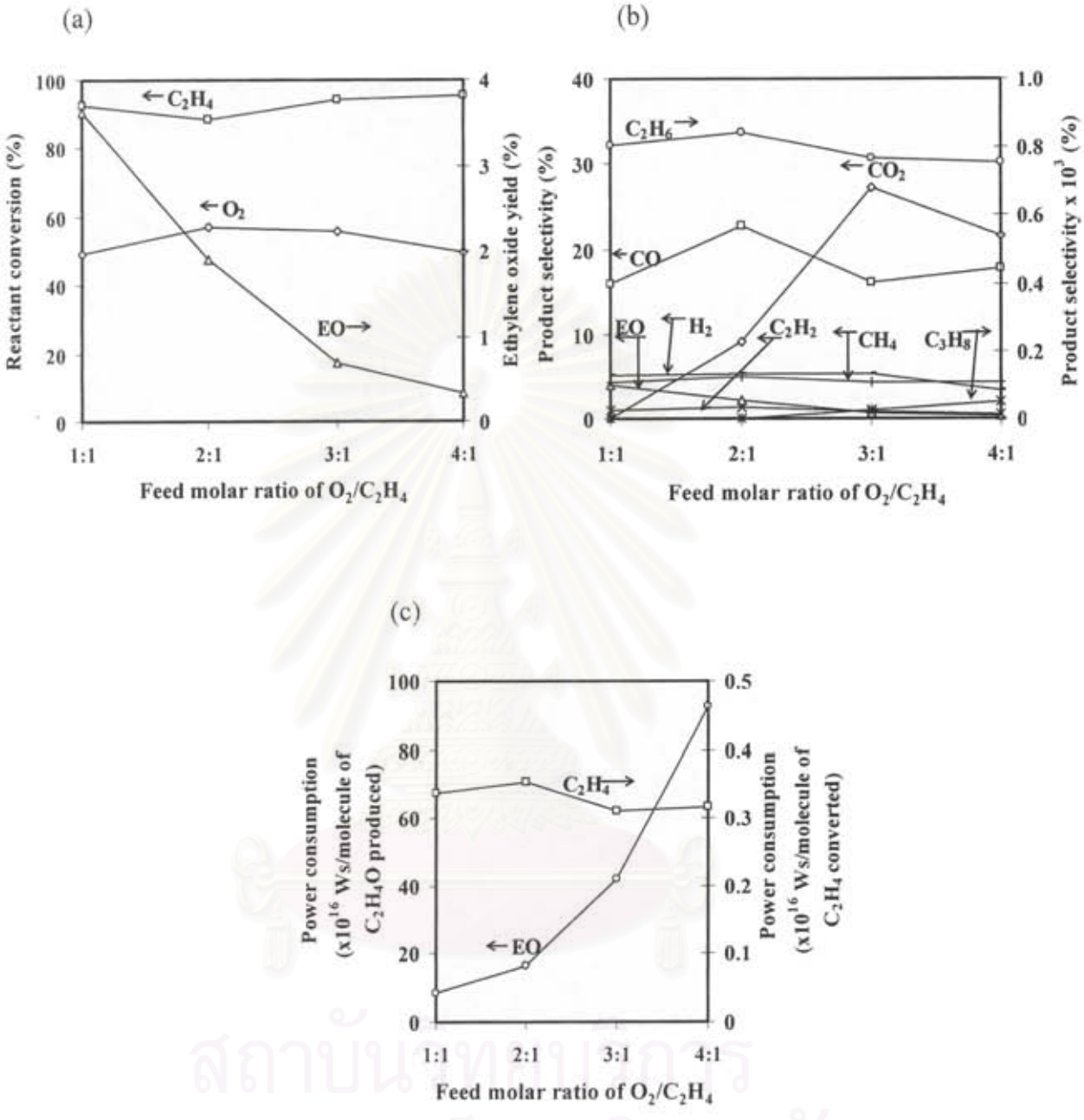

Fig. 2.2 (a) Conversions of ethylene and oxygen and yield of EO, (b) product selectivities, and (c) power consumptions as a function of O_2/C_2H_4 feed molar ratio (feed flow rate = 50 cm^3/min; electrode gap distance = 10 mm; applied voltage = 17 kV; input frequency = 550 Hz; and residence time = 0.45 min).

2.3.2 Effect of feed flow rate

The feed flow rate plays a significant role on the residence time of gas molecules within the plasma zone, affecting the performance of the plasma system. The experiments were performed by varying feed flow rate from 50 to 75, 100, and 125 cm^3/min, corresponding to the residence time of 0.45, 0.3, 0.225, and 0.18 min, respectively. At a feed flow rate lower than 50 cm^3/min, the O_2 flow rate cannot be adjusted due to the limitation of a mass flow controller. The studied plasma system was operated at an O_2/C_2H_4 feed molar ratio of 1:1, an applied voltage of 17 kV, and an input frequency of 550 Hz. Fig. 2.3(a) illustrates the influences of the feed flow rate on the C_2H_4 and O_2 conversions. The conversion of O_2 gradually decreased with increasing the feed flow rate from 50 to 125 cm^3/min while the conversion of C_2H_4 more sharply decreased. An increase in the feed flow rate generally reduces the gas residence time in the reaction system, resulting in having a shorter contact time of ethylene and oxygen molecules to collide with electrons. As a result, a reduction in the feed flow rate enhances the conversions of both C_2H_4 and O_2, which leads to an increase in the yield of EO, as also shown in Fig. 2.3(a).

The feed flow rate dependence of product selectivities is depicted in Fig. 2.3(b). It is apparent that increasing feed flow rate predominantly resulted in decreases in the selectivities for EO and CO. This is because a higher feed flow rate reduces the opportunity of collision between electrons/oxygen active species and reactant/intermediate molecules to render the partial oxidation and epoxidation reactions. But for other products, especially C_2H_2 and C_3H_8, their selectivities tended to increase at shorter residence times due to higher feed flow rates, suggesting that the oxidative dehydrogenation and coupling reaction are more favorable to occur than the partial oxidation when the residence time is decreased.

Fig. 2.3(c) shows the effect of feed flow rate on the power consumptions. The power consumption per molecule of converted ethylene slightly decreased, but the power consumption per molecule of produced EO tended to greatly increase with increasing feed flow rate. The lower feed flow rate gave comparatively low power consumption per molecule of produced EO, as well as much higher reactant conversions and desired product selectivity. Therefore, the feed flow rate of 50 cm^3/min was selected as a best condition and used for further investigation.

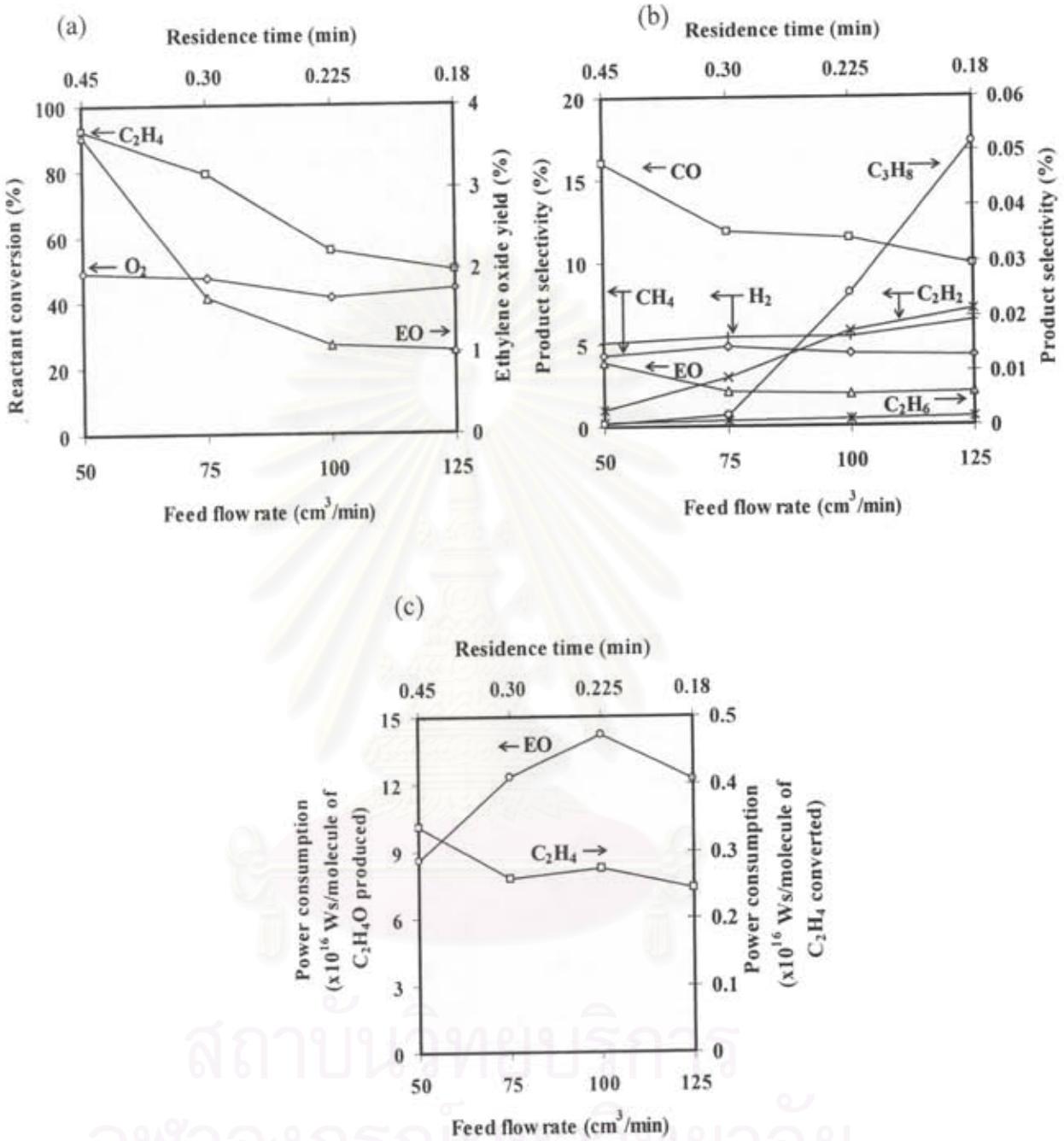

Fig. 2.3 (a) Conversions of ethylene and oxygen and yield of EO, (b) product selectivities, and (c) power consumptions as a function of feed flow rate (feed molar ratio of O_2/C_2H_4 = 1:1; electrode gap distance = 10 mm, applied voltage = 17 kV, and input frequency = 550 Hz).

2.3.3 Effect of input frequency

Input frequency is one of the most important parameters in plasma reactor operation, significantly affecting the field strength in the plasma zone. The studied DBD system was operated in the frequency range of 500-800 Hz. At a frequency lower than 500 Hz, the plasma distribution was not fairly uniform over the whole electrode surface, and it tended to appear as a single strong stream of plasma discharge, whereas the plasma could not exist at a frequency higher than 800 Hz. The effect of input frequency on the C_2H_4 and O_2 conversions and the yield of EO is illustrated in Fig. 2.4(a). When the input frequency was increased in the range of 500-650 Hz, the O_2 and C_2H_4 conversions and EO yield decreased dramatically, and they turned to slightly decrease with further increasing input frequency from 650 up to 800 Hz. The explanation is that a higher frequency results in a lower current that corresponds to the reduction of the number of electrons generated (weaker field strength), as shown in Fig. 2.4(b). It therefore causes the decrease in amount of active species for further reactions, resulting in the decrease in the C_2H_4 and O_2 conversions and subsequently leading to the lower yield of EO.

The effect of input frequency on the product selectivities is shown in Fig. 2.4(c). The selectivities for EO and CO tended to slightly decrease with increasing input frequency up to 650 Hz. At a higher frequency than 650 Hz, the partial oxidation, oxidative dehydrogenation, and coupling reactions to form various products increasingly occurred. Beyond 650 Hz, the selectivity for EO also gradually increased with increasing frequency and reached a maximum of 7.3% at 800 Hz, as compared with 5.0% at 500 Hz for the low frequency range between 500-650 Hz. However, the input frequency of 500 Hz was considered as a potentially best value, exhibiting the highest EO yield with a reasonably high EO selectivity and a relatively low CO selectivity.

The effect of input frequency on the power consumptions to break down each C_2H_4 molecule and to create each EO molecule is shown in Fig. 2.4(d). The results showed that both the power consumptions per C_2H_4 molecule converted and per EO molecule produced tended to increase with increasing input frequency, especially at an input frequency higher than 600 Hz. Based upon the relatively high EO yield and

the lowest power consumption per molecule of EO produced, the best input frequency of 500 Hz was selected for further investigation.

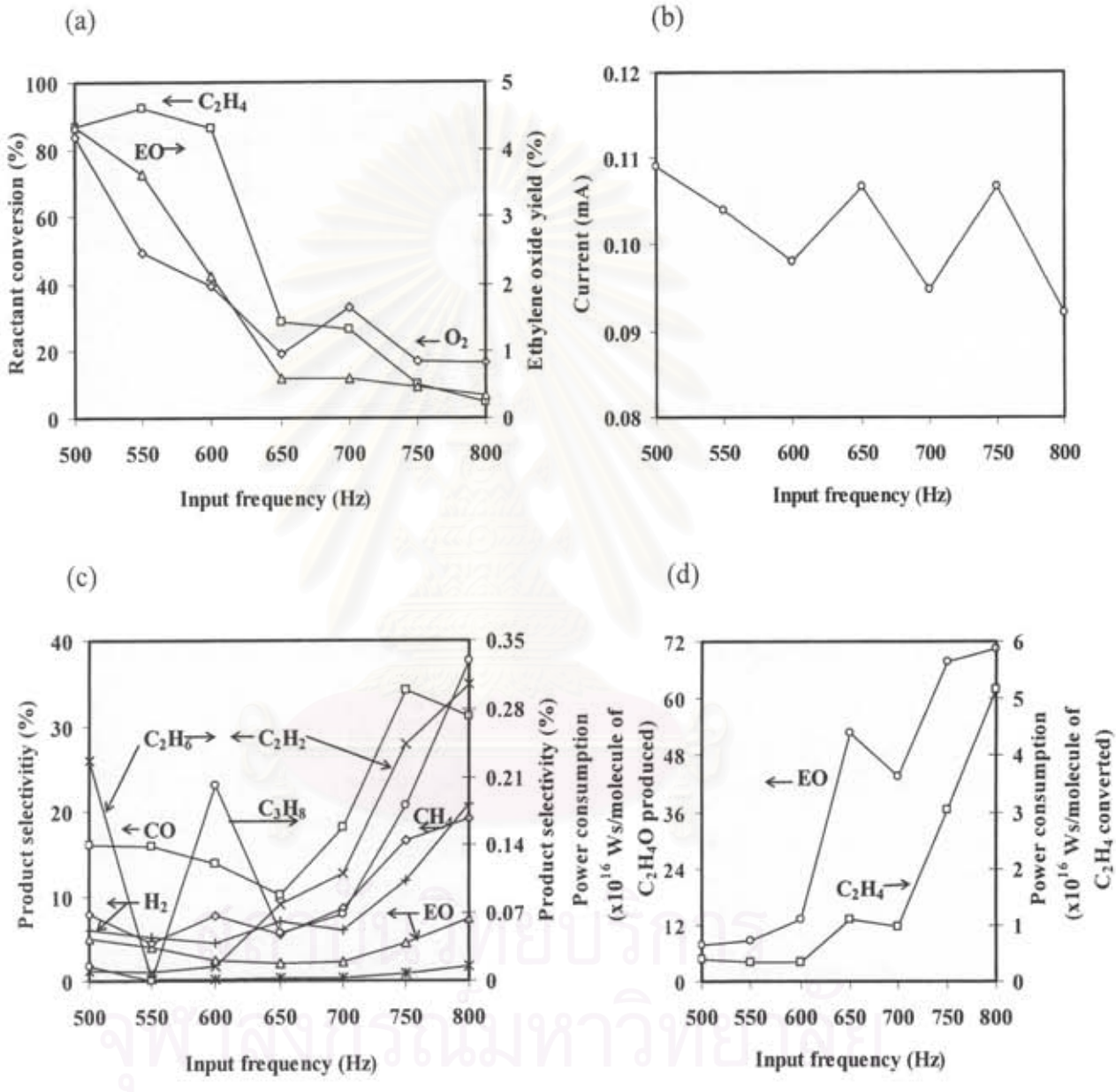

Fig. 2.4 (a) Conversions of ethylene and oxygen and yield of EO, (b) generated current, (c) product selectivities, and (d) power consumptions as a function of input frequency (feed molar ratio of O_2/C_2H_4 = 1:1; feed flow rate = 50 cm^3/min; electrode gap distance = 10 mm; applied voltage = 17 kV; and residence time = 0.45 min).

2.3.4 Effect of applied voltage

Under the studied conditions, the break-down voltage or the lowest voltage to generate plasma (onset voltage) was found to be about 13 kV, and the DBD system could not be operated at the applied voltage higher than 21 kV since the generated plasma was found to have the non-uniform distribution characteristic. Therefore, the reaction experiments were conducted in the voltage range of 13-21 kV in order to determine the effect of the applied voltage. The effect of applied voltage on the C_2H_4 and O_2 conversions and EO yield is illustrated in Fig. 2.5(a). The oxygen conversion and EO yield tended to considerably increase with increasing applied voltage in the range of 13-19 kV, whereas the ethylene conversion slightly increased. With further increasing applied voltage higher than 19 kV, the reactant conversions and the EO yield did not significantly change. The explanation for the rapid increment in the O_2 conversion with increasing applied voltage is that a higher voltage results in a higher current (stronger field strength), as shown in Fig. 2.5(b), leading to more available electrons to increase an opportunity for collision with oxygen. The results correspond well with the previous works [32-37]. In contrast, it is unexpected that the C_2H_4 conversion only slightly increased with increasing applied voltage. This can be explained in that the bond dissociation energy of C_2H_4 (16.7 eV) is much higher than that of O_2 (12.2 eV), particularly causing O_2 molecules to be converted more easily than C_2H_4.

The effect of applied voltage on the selectivities for EO, CO, H_2, CH_4, C_2H_2, C_2H_6, and C_3H_8 is shown in Fig. 2.5(c). The selectivities for EO, CO, H_2, and other hydrocarbon products, except C_2H_2 selectivity, increased with increasing applied voltage. When the applied voltage increased, corresponding to increasing O active species as mentioned above, C_2H_4 and other hydrocarbons are easily oxidized to form more CO and EO. Interestingly, no CO_2 was detected under the studied conditions since the system was operated under the O_2-lean condition (the O_2/C_2H_4 feed molar ratio of 1:1). The results therefore suggest that a higher applied voltage is more favorable for EO production under the O_2-lean condition. Only the selectivity for C_2H_2 was observed to decrease with increasing applied voltage. This might be because the formed C_2H_2 further reacts with largely available O active species to form other

products more easily. Interestingly, the further increase in applied voltage higher than 19 kV did not help enhance the EO production.

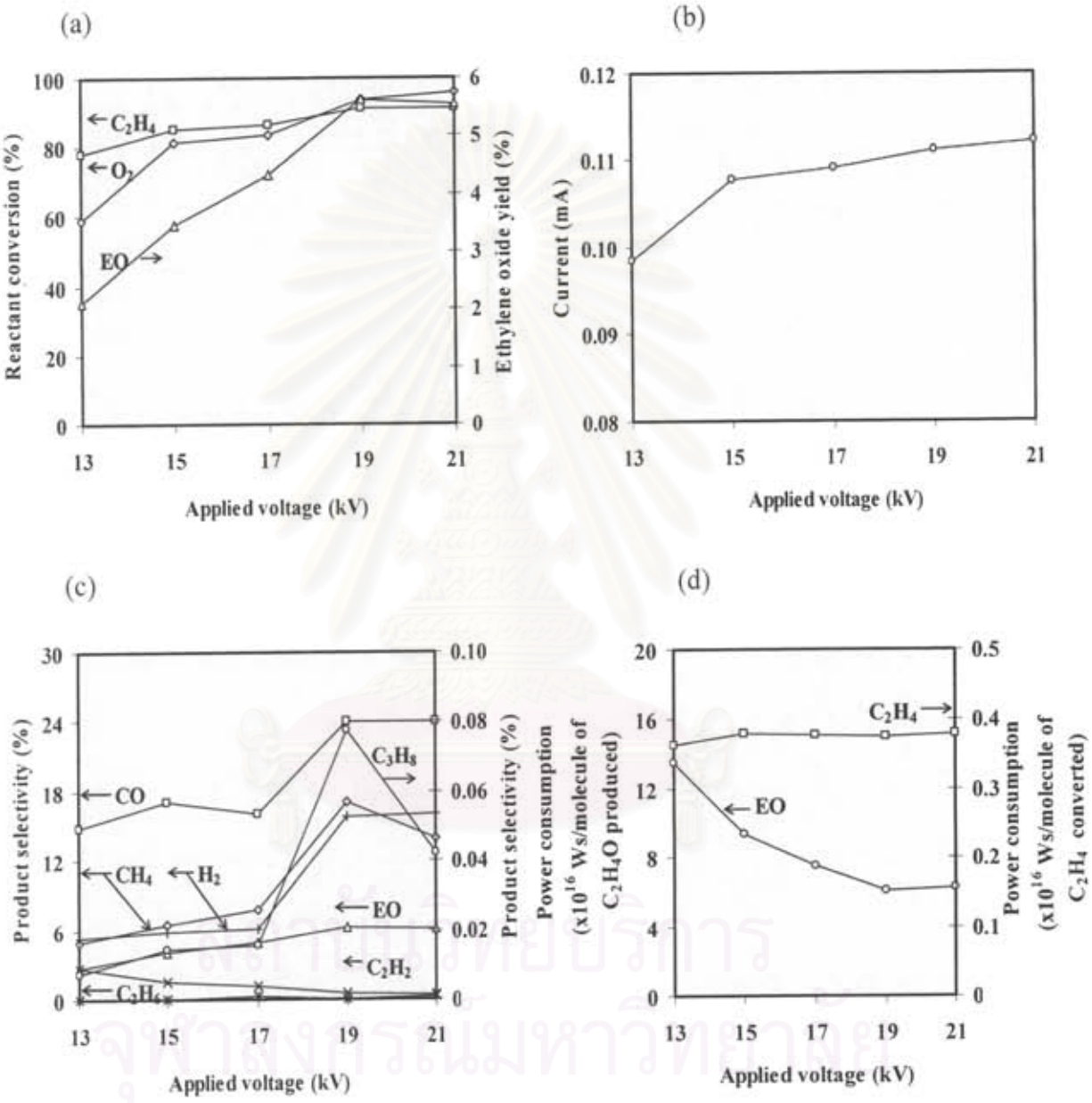

Fig. 2.5 (a) Conversions of ethylene and oxygen and yield of EO, (b) generated current, (c) product selectivities, and (d) power consumptions as a function of applied voltage (feed molar ratio of O_2/C_2H_4 = 1:1; feed flow rate = 50 cm^3/min; electrode gap distance = 10 mm; input frequency = 500 Hz; and residence time = 0.45 min).

Fig. 2.5(d) shows the effect of applied voltage on the power consumptions. With increasing applied voltage, the power consumption per molecule of converted C_2H_4 remained almost unchanged, whereas the power consumption per molecule of produced EO substantially decreased. As mentioned earlier, the slight increase in ethylene conversion with increasing applied voltage caused insignificant change in the power consumption per molecule of ethylene converted. In contrast, an increase in the selectivity for EO was comparatively high as increasing applied voltage, resulting in lower power consumption per molecule of produced EO.

From the results, the applied voltage of 19 kV was selected to be the best value because this voltage provided the reasonably high conversions of C_2H_4 and O_2, and the highest selectivity and yield for EO. At a higher voltage, it did not affect any of reactant conversion, EO selectivity, and EO yield. Moreover, at the applied voltage of 19 kV, the lowest power consumption per EO molecule produced was obtained.

2.3.5 Effect of electrode gap distance

The effects of electrode gap distance and corresponding residence time have been shown to be very important in plasma operation [35,37-39]. The effect of electrode gap distance was studied under the best conditions achieved above; an O_2/C_2H_4 feed molar ratio of 1:1, a feed flow rate of 50 cm^3/min, an input frequency of 500 Hz, and an applied voltage of 19 kV. The electrode gap distance was varied from 10 to 11, 12, 13, and 14 nm, corresponding to the residence time of 0.45, 0.54, 0.63, 0.72, and 0.81 min, respectively. The lowest electrode gap distance for the studied DBD system was limited at 10 mm due to its configuration. At an electrode gap distance higher than 14 mm, the generated plasma became unfavorably non-uniform. Therefore, the reaction experiments were conducted in the range of electrode gap distance between 10 and 14 mm in order to determine the effect of the electrode gap distance.

The effect of electrode gap distance on the C_2H_4 and O_2 conversions and EO yield is illustrated in Fig. 2.6(a). The ethylene conversion and EO yield tended to decrease with increasing the electrode gap distance, whereas the oxygen conversion tended to be almost unchanged. The explanation for slight ethylene conversion decrement is that a wider electrode gap distance results in a higher residence time for several hydrocarbon species to recombine via coupling reactions, including backward reaction to form ethylene, causing lower conversion of ethylene. The unexpected

nearly constant O_2 conversion with increasing electrode gap distance can be explained in that the current slightly increases with increasing electrode gap distance, as shown in Fig. 2.6(b), while the residence time is also increased. The results suggest that for the O_2 conversion, the higher probability in converting O_2 molecules due to higher electron density might trade off the higher probability in oxygen active species recombination due to a longer residence time of gas flow. The expected increase in current, i.e. electron density, might be contributed to the special characteristic of the DBD system containing the dielectric plate, as well as the various compositions of gaseous species inside the plasma zone. At a higher electrode gap distance, the dielectric plate might sustain the discharge a little bit more effectively due to less loss of electrons via various reactions, under the identical input frequency and applied voltage.

The effect of electrode gap distance on the selectivities for EO, CO, H_2, CH_4, C_2H_2, C_2H_6, and C_3H_8 is shown in Fig. 2.6(c). The selectivities for EO, CO, H_2, and CH_4 decreased with increasing gap distance while the opposite trend was observed for C_2H_2, C_2H_6, and C_3H_8. These may be implied that when increasing electrode gap distance, the opportunity of coupling reactions more favorably occur as secondary reactions than the partial oxidation, as above explained.

Fig. 2.6(d) shows the effect of electrode gap distance on the power consumptions. It is clearly seen that both the power consumptions per molecule of converted C_2H_4 conversion and per molecule of produced EO substantially increased with increasing electrode gap distance. A higher electrode gap distance causes a higher probability of secondary reactions, which unavoidably uses up some power. From the results, the electrode gap distance of 10 mm was considered as a best value because at 10 mm gap distance, the highest EO selectivity and EO yield with the lowest power consumption per EO molecule produced were achieved.

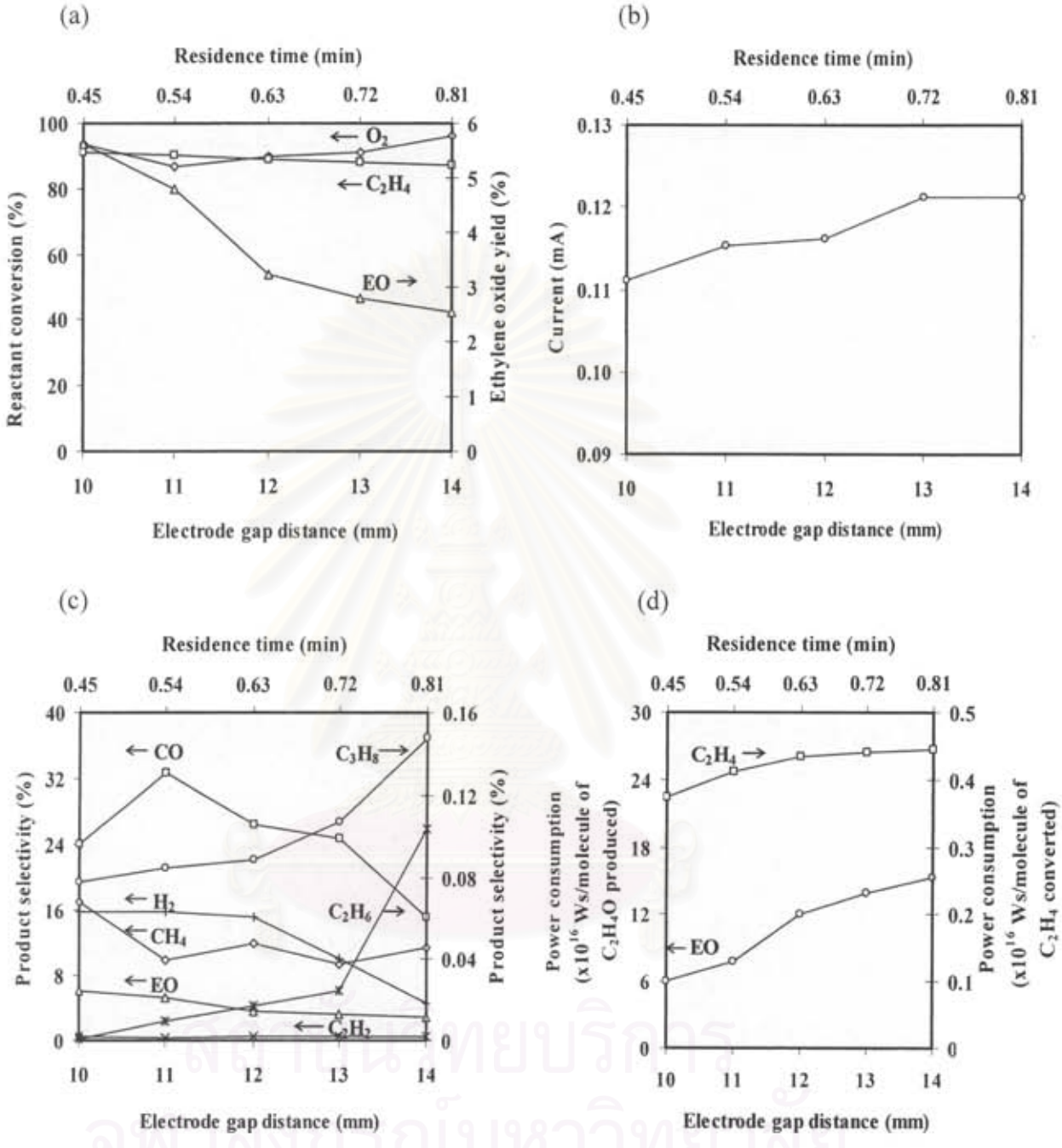

Fig. 2.6 (a) Conversions of ethylene and oxygen and yield of EO, (b) generated current, (c) product selectivities, and (d) power consumptions as a function of electrode gap distance (feed molar ratio of O_2/C_2H_4 = 1:1; feed flow rate = 50 cm^3/min; applied voltage = 19 kV; and input frequency = 500 Hz).

In comparisons, although the maximum EO yield of 5.6% obtained under the aforementioned best conditions (an O_2/C_2H_4 feed molar ratio of 1:1, a feed flow rate

of 50 cm^3/min, an input frequency of 500 Hz, an applied voltage of 19 kV, and an electrode gap distance of 10 mm) using the studied DBD system was lower than the EO yields of 30 and 10% obtained from the catalytic epoxidation process using 15 wt.% Ag/Al_2O_3 at reaction temperatures of 280 and 350°C, respectively [15], the DBD system is still considered to exhibit a high potential to be employed for EO production under much lower operating temperatures. Again, the present work is the first time to demonstrate the use of the sole DBD system to synthesize EO without the presence of catalysts. As shown in the aforementioned results, there were several reactions occurring in the plasma reaction zone so it is not possible to easily carry out the kinetic consideration of the ethylene epoxidation reaction. Future works will then be focused on the combination of the low-temperature DBD system with various reported catalytically active catalysts used in the conventional catalytic process, especially Ag/Al_2O_3-based catalysts [5-15,20], aiming to enhance the EO yield. The comparative study of ethylene epoxidation under different kinds of low-temperature plasma discharges, such as corona discharge system with pin and plate electrodes, is also of our strong interest. Moreover, the kinetic studies of the ethylene epoxidation reaction will be conducted in order to optimize the DBD process. The experimental results will be presented in the next contribution.

2.4 Conclusions

In this work, the epoxidation reaction of ethylene was investigated in the low-temperature dielectric barrier discharge (DBD) plasma system. The effects of various operating parameters, including feed molar ratio of O_2/C_2H_4, feed flow rate, input frequency, applied voltage, and electrode gap distance, on the ethylene epoxidation reaction was studied in order to achieve the best conditions. In order to obtain the highest EO yield of 5.6% and the highest selectivity of 6.2%, the DBD system must be operated at an O_2/C_2H_4 feed molar ratio of 1:1, a feed flow rate of 50 cm^3/min, an input frequency of 500 Hz, an applied voltage of 19 kV, and an electrode gap distance of 10 mm. At these best conditions, the power consumptions to break down each C_2H_4 molecule and to create EO molecule were found to be 0.37×10^{-16} Ws/molecule of C_2H_4 converted and 6.07×10^{-16} Ws/molecule of EO produced.

References

1. http://www.osha.gov/OshDoc/data_General_Facts/ethylene-oxide-factsheet.pdf
2. http://en.wikipedia.org/wiki/Ethylene_oxide#cite_note-1
3. T.E. Lefort, French Patent 729 (1931) 952.
4. P.P. McClellan, Ind. Eng. Chem. 42 (1950) 2402-2407.
5. P.A. Kilty, N.C. Rol, W.M.H. Sachtler, Catal. Lett. 99 (1973) 45-53.
6. P.V. Geenen, H.J. Boss, G.T. Pott, J. Catal. 77 (1982) 499-510.
7. G. Iwakura, Japan Patent 63-126552 (1985).
8. N. Tories, X.E. Verikios, J. Catal. 108 (1987) 161-174.
9. M.M. Bhasin, US Patent 4,908,343 (1988).
10. S. Matar, M.J. Mirbach, H.A. Tayim, Catalysis in Petrochemical Processes, Kluwer Academic Publishers, Dordrecht: The Netherlands, (1989).
11. S.N. Goncharova, E.A. Paukshtis, B.S. Bal'zhinimaev, Appl. Catal. A: Gen. 126 (1995) 67-84.
12. D.I. Kondaries, X.E. Verykios, J. Catal. 158 (1996) 363-377.
13. W.S. Epling, G.B. Hoflund, D.M. Minahan, J. Catal. 171 (1997) 490-497.
14. J.T. Jankowiak, M.A. Barteau, J. Catal. 236 (2005) 366-378.
15. M.C.N. Amorim de Carvalho, F.B. Passos, M. Schmal, J. Catal. 248 (2007) 124-129.
16. G.H. Law, H.C. Chitwood, US Patent 2,279,470 (1942).
17. C.T. Campbell, M.T. Paffett, Appl. Surf. Sci. 19 (1984) 28-42.
18. S.A. Tan, R.B. Grant, R.M. Lambert, J. Catal. 100 (1986) 383-391.
19. K.L. Yeung, A. Gavriilidis, A. Varma, M.M. Bhasin, J. Catal. 174 (1998) 1-12.
20. J.T. Jankowiak, M.A. Barteau, J. Catal. 236 (2005) 379-386.
21. H. Suhr, H. Pfreundschuh, Plasma Chem. Plasma Process. 8 (1988) 67-74.
22. P. Patiño, F.E. Hernández, S. Rondón, Plasma Chem. Plasma Process. 15 (1995) 159-171.
23. H. Suhr, Plasma Chem. Plasma Process. 3 (1983) 1-61.
24. L.M. Zhou, B. Xue, U. Kogelschatz, B. Eliasson, Plasma Chem. Plasma Process. 18 (1998) 375-393.
25. B. Eliasson, M. Hirth, U. Kogeischatz, J. Appl. Phys. 20 (1987) 1421-1437.

26. M.B. Chang, T.D. Tseng, J. Environ. Eng. (1996) 41-46.
27. I. Orlandini, U. Riedel, Catal. Today 89 (2004) 83-88.
28. M. Magureanu, N.B. Mandache, V.I. Parvulescu, Ch. Subrahmanyam, A. Renken, L. Kiwi-Minsker, Appl. Catal. B: Environ. 74 (2007) 270-277.
29. B. Sarmiento, J.J. Brey, I.G. Viera, A.R. González-Elipe, J. Cotrino, V.J. Rico, J. Power Sources 169 (2007) 140-143.
30. N.S. Matin, H.A. Savadkoohi, S.Y. Feizabadi, Plasma Chem. Plasma Process. 28 (2008) 189-202.
31. M.X. Guo, H.C. Guo, X.S. Wang, W.M. Gong, Chin. J. Chem. 23 (2005) 471-473.
32. S. Chavadej, W. Kiattubolpaiboon, P. Rangsunvigit, T. Sreethawong, J. Mol. Catal. A: Chem. 263 (2007) 128-136.
33. S. Chavadej, K. Saktrakool, P. Rangsunvigit, L.L. Lobban, T. Sreethawong, Chem. Eng. J. 132 (2007) 345-353.
34. N. Rueangjitt, T. Sreethawong, S. Chavadej, Plasma Chem. Plasma Ptrocess. 28 (2008) 49-67.
35. T. Sreethawong, P. Thakonpatthanakun, S. Chavadej, Int. J. Hydrogen Energ. 32 (2007) 1067-1079.
36. K. Morinaga, M. Suzuki, Bull. Chem. Soc. Jpn. 35 (1962) 204-217.
37. K. Supat, S. Chavadej, L.L. Lobban, R.G. Mallinson, Ind. Eng. Chem. Res. 42 (2003) 1654-1661.
38. K. Supat, A. Kruapong, S. Chavadej, L.L. Lobban, R.G. Mallinson, Energ. Fuel 17 (2003) 474-481.
39. T.A. Caldwell, H. Le, L.L. Lobban, R.G. Mallinson, Surface Science and Catalysis, Volume 136, Elsevier: New York, 2001.

List of Publication papers

1. Sreethawong, T., Suwannabart, T., and Chavadej, S. (2008), Ethylene Epoxidation in Low-Temperature AC Dielectric Barrier Discharge: Effects of Oxygen-to-Ethylene Feed Molar Ratio and Operating Parameters, *Plasma Chemistry and Plasma Processing*, 28, 629-642
2. Chavadej, S., Tansuwan, A. and Sreethawong, T. (2008), Ethylene Epoxidation over Alumina-Supported Silver Catalysts in Low-Temperature AC Corona Discharge, *Plasma Chemistry and Plasma Processing*, 28, 643-662
3. Sreethawong, T., Suwannabart, T., and Chavadej, S. (2010), Ethylene Epoxidation in low-Temperature AC Corona Discharge over Ag Catalysts: Effect of Promoter, *Chemical Engineering Journal* (in press)

Plasma Chem Plasma Process (2008) 28:629–642
DOI 10.1007/s11090-008-9149-8

ORIGINAL PAPER

Ethylene Epoxidation in Low-Temperature AC Dielectric Barrier Discharge: Effects of Oxygen-to-Ethylene Feed Molar Ratio and Operating Parameters

Thammanoon Sreethawong · Thanapoom Suwannabart · Sumaeth Chavadej

Received: 28 June 2008 / Accepted: 31 July 2008 / Published online: 14 August 2008

Abstract Ethylene oxide (EO), a valuable chemical feedstock in producing many industrial chemicals, which is industrially produced by the partial oxidation of ethylene, so-called ethylene epoxidation, has been of great interest in many global research studies. In this work, the epoxidation of ethylene under a low-temperature dielectric barrier discharge (DBD) was feasibly investigated to find the best operating conditions. It was experimentally found that the EO yield decreased with increasing O_2/C_2H_4 feed molar ratio, feed flow rate, input frequency, and electrode gap distance, while it increased with increasing applied voltage up to 19 kV. The highest EO yield of 5.6% was obtained when an input frequency of 500 Hz and an applied voltage of 19 kV were used, with an O_2/C_2H_4 feed molar ratio of 1:1, a feed flow rate of 50 cm^3/min, and an electrode gap distance of 10 mm. Under these best conditions, the power consumption was found to be as low as 6.07×10^{-16} Ws/molecule of EO produced.

Keywords Epoxidation · Ethylene oxide · Dielectric barrier discharge

Introduction

Ethylene oxide (C_2H_4O, EO) is an important industrial chemical, which is primarily used as an intermediate in the production of various useful chemicals. Its major use is in the production of ethylene glycol. It is also used for the manufacture of surfactants and detergents by a process called ethoxylation, solvents, antifreezes, adhesives, polyurethane foam, fumigants for agricultural products, and sterilants for medical equipment and supplies, spices, and cosmetics [1, 2]. Since EO is a valuable chemical feedstock for many

T. Sreethawong · T. Suwannabart · S. Chavadej (✉)
The Petroleum and Petrochemical College, Chulalongkorn University, Soi Chula 12, Phyathai Road, Pathumwan, Bangkok 10330, Thailand
e-mail: sumaeth.c@chula.ac.th

applications, the selective partial oxidation of ethylene to EO, so-called ethylene epoxidation, has been of great interest in global research works.

As discovered by Lefort in 1931 [3], the gas phase epoxidation of ethylene to EO using molecular oxygen and silver catalysts is one of the greatest findings in heterogeneous catalysis, being the most widely used method for ethylene epoxidation. Since 1940, almost all EO produced industrially has been made using this method [4]. To date, silver catalysts supported on alpha-alumina (Ag/α-Al_2O_3) with alkali and transition metal promoters [5–15], such as Cs, Cu, Re, and Au, or with addition of chlorine-containing moderators into gaseous reactants [16–20], such as dichloroethane ($C_2H_4Cl_2$) and vinyl chloride (C_2H_3Cl), provide high selectivity for EO. However, the conventional catalytic process normally requires high temperatures, i.e. implying high energy consumption, to sufficiently activate the catalyst for the ethylene epoxidation, basically higher than 200°C. Moreover, the catalytic problems at high temperature operation, i.e. catalyst deactivation, catalyst regeneration, and catalyst replacement, greatly reduces the working efficiency of the process, as well as directly leads to a high production cost. These turn out to become necessary for developing a new approach to overcome the mentioned problems.

Non-thermal plasmas, such as dielectric barrier discharge (DBD), corona discharge, and glow discharge, are a highly potential alternative for chemical reaction investigation under non-equilibrium conditions operated at low temperatures and atmospheric pressure. The main characteristic of the non-equilibrium plasma is its high electron temperatures (10^4–10^5 K), whereas the bulk gas temperature remains as low as room temperature [21, 22]. This implies comparatively lower energy consumption used for operating the reaction system as compared with conventional catalytic processes. The non-equilibrium plasma with the highly energetic electrons and low temperature in the bulk gas can initiate several chemical reactions, which are normally not possible to occur at low temperatures [23].

DBD is the most commonly used technique for atmospheric pressure plasma operation. The basic principle of this technique is to utilize non-equilibrium plasma, in which the major part of electrical energy is transferred to energetic electrons and active radical species generated from subsequent reactions [24]. A major advantage of DBD is that the entire electrode area is effectively employed for discharge generation, resulting in the comparatively high discharge volume with a very low temperature typically close to room temperature. The uses of DBD for chemical syntheses and conversions have become increasingly important for several applications, such as the partial oxidation of methane to methanol [24], the ozone production from molecular oxygen [25], the removal of gaseous H_2S and NH_3 [26], the oxidation of propene [27], the decomposition of trichloroethylene [28], the reforming of hydrocarbons and alcohols for hydrogen production [29], and the methane conversion to C_2 hydrocarbons [30]. However, up to now, the use of DBD for gas phase epoxidation reaction has been rarely investigated. To our knowledge, only one recent published work described about gas phase epoxidation of propylene [31]; however, there has been no any literature reporting the epoxidation of ethylene using DBD yet.

In this work, a low-temperature DBD system was employed for the first time for non-catalytic ethylene epoxidation at atmospheric pressure. The effects of various operating parameters, including O_2/C_2H_4 feed molar ratio, feed flow rate, input frequency, applied voltage, and electrode gap distance, on the activity of ethylene epoxidation and the system performance were extensively examined.

Experimental

Reactant Gases

All gases used in this work, i.e. 99.995% helium (high purity grade), 40% ethylene balanced with helium, and 97% oxygen balanced with helium, were supplied by Thai Industrial Gas (Public) Co., Ltd.

Dielectric Barrier Discharge System

The experimental study of ethylene epoxidation was conducted in a low-temperature DBD system, which was operated at atmospheric pressure and ambient temperature, around 25–27°C (room temperature). The schematic of the DBD system is shown in Fig. 1a. The acrylic plate-made DBD reactor sizes were 2 cm height × 3 cm width × 15 cm length for the inner dimensions, and 3 cm height × 7 cm width × 19 cm length for the outer dimensions. As shown in Fig. 1b, it consists of a 5-mm-thick dielectric glass plate placed between two parallel stainless steel electrodes, on the lower electrode. The gap distance between the electrodes was varied from 10 to 14 mm. The input power used to generate

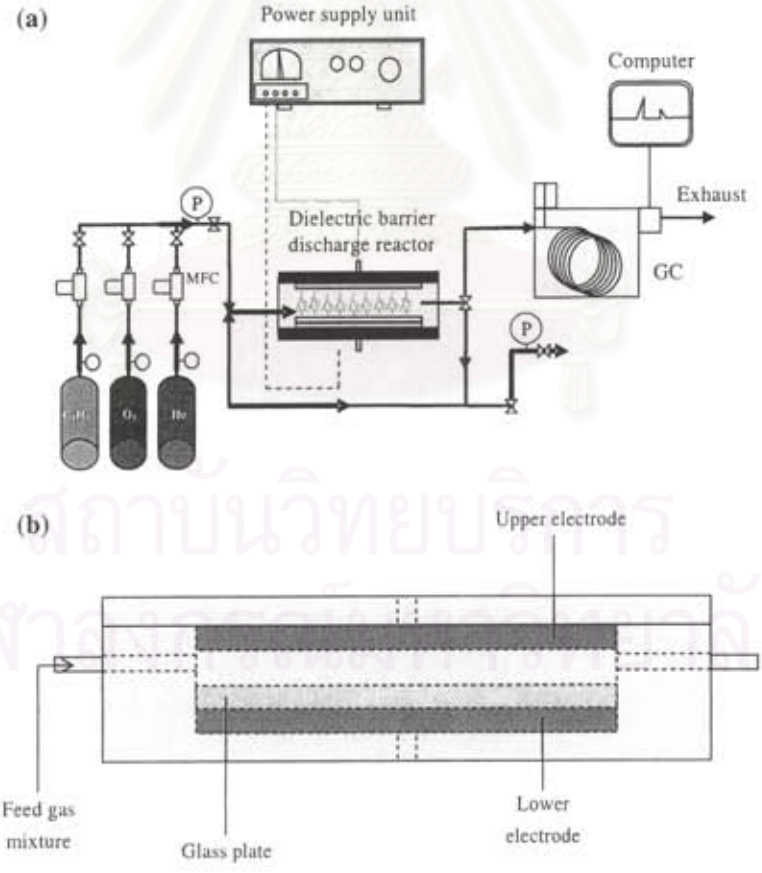

Fig. 1 (**a**) Schematic of experimental setup for ethylene epoxidation reaction in dielectric barrier discharge plasma system and (**b**) configuration of the dielectric barrier discharge reactor

microdischarge plasma between the electrode gap was domestic alternating current (AC), 200 V and 50 Hz, which was transmitted to a high voltage current via a power supply unit. The power supply unit consisted of three steps. For the first step, the domestic AC input of 220 V and 50 Hz was converted to a DC output of 70 V by a DC power supply converter. For the second step, a 500 W power amplifier with a function generator was used to transform the DC into AC current with a sinusoidal waveform and different frequencies. For the third step, the outlet voltage was stepped up by using a high voltage transformer. The description of the power supply unit was given elsewhere [32]. The output voltage and frequency were controlled by the function generator. The voltage and current at the low voltage side were measured instead of those at the high voltage side across the electrodes since the plasma generated is non-equilibrium in nature. The high side voltage and current were thereby calculated by multiplying and dividing by a factor of 130, respectively [32–35]. A power analyzer was used to measure power, current, frequency, and voltage at the low voltage side of the power supply unit.

Reaction Testing Procedure

Reactant gases (ethylene, oxygen, and helium) fed through the plasma reactor were controlled by a set of electronic mass flow controllers and transducers, supplied by SIERRA® Instrument Inc., to obtain a feed gas mixture having different flow rates and oxygen-to-ethylene molar ratios. A 7-μm in-line filter was placed upstream of each mass flow controller in order to trap any solid particles. A check valve was placed downstream of each mass flow controller to prevent any back flow of the reactant gases. All of the reactant gases were mixed inside a single line before being introduced into the DBD reactor. For any studied conditions, the feed gas mixture was first introduced into the DBD system without turning on the power supply unit. After the composition of outlet gas was invariant with time, it was turned on. The outlet of the reactor was either vented to the atmosphere via rubber tube exhaust or was connected to an on-line gas chromatograph (Perkin–Elmer, AutoSystem GC) for analysis of the product gases. The moisture in the product gas stream was trapped by a water trap filter before entering a heated stainless steel line to the on-line gas chromatograph. The gas chromatograph was equipped with both a thermal conductivity detector (TCD) and a flame ionization detector (FID). For the TCD channel, the packed column (Carboxen 1000) was used for separating the product gases, which were hydrogen (H_2), oxygen (O_2), carbon monoxide (CO), carbon dioxide (CO_2), and ethylene (C_2H_4). For the FID channel, the capillary column (OV-Plot U) was used for analysis of EO and other by-product gases, i.e. CH_4, C_2H_2, C_2H_6, and C_3H_8. The composition of product gas stream was analyzed by the on-line gas chromatograph every 20 min. After the system reached steady state, an analysis of outlet gas composition was taken at least a few times. The experimental data taken under steady state conditions were averaged, and these averages were used to evaluate the performance of the plasma system. It is also worth noting that during the reaction, the temperature at the reactor wall was found to be lower than the melting temperature of acrylic plate (130°C), which was used to construct the DBD reactor.

Reaction Performance Assessment

To evaluate the process performance, the conversions of ethylene and oxygen and the selectivities for products, including EO, CO, CO_2, H_2, CH_4, C_2H_2, C_2H_6, and traces of C_3, were considered. The conversion of either ethylene or oxygen is defined as:

$$\%\,\text{Reactant conversion} = \frac{(\text{moles of reactant } in - \text{moles of reactant } out)(100)}{(\text{moles of reactant } in)}$$

The product selectivity is calculated from the following equation:

$$\%\ \text{Product selectivity} = \frac{[(\text{number of carbon or hydrogen atom in product})\ (\text{moles of product produced})](100)}{[(\text{number of carbon or hydrogen atom in ethylene})(\text{moles of ethylene converted})]}$$

The EO yield is calculated from the following equation:

$$\%\ \text{EO yield} = (\%\ \text{ethylene conversion})\ (\%\ \text{EOselectivity})\ (100)$$

To determine the energy efficiency of the plasma system, the specific power consumption is calculated in a unit of Ws per molecule of converted ethylene or per molecule of produced EO using the following equation:

$$\text{Specific power consumption} = \frac{(\text{P})(60)}{(\text{N})(\text{M})}$$

where P = Power (W), N = Avogadro's number = 6.02×10^{23} molecules/mol, M = Rate of converted ethylene molecules in feed or rate of produced EO molecules (mol/min).

Results and Discussion

Effect of Feed Molar Ratio of O_2/C_2H_4

The effect of O_2/C_2H_4 feed molar ratio was initially studied in order to obtain the most suitable feed gas composition for ethylene epoxidation reaction under the low-temperature DBD system. In this study, the O_2/C_2H_4 feed molar ratio was investigated in the range of 1:1–4:1, while an applied voltage of 17 kV, an input frequency of 550 Hz, and a residence time of 0.45 min were used as base conditions to operate the DBD system. The residence time is calculated by the inside volume of the DBD reactor divided by a feed flow rate. The effect of O_2/C_2H_4 feed molar ratio on the C_2H_4 and O_2 conversions and the EO yield is shown in Fig. 2a, and that on the selectivities for EO, CO, CO_2, H_2, CH_4, C_2H_2, C_2H_6, and C_3H_8 is shown in Fig. 2b. The increase in the O_2/C_2H_4 feed molar ratio slightly affected the reactant conversions, but it mainly affected the EO and CO_2 selectivities, especially in the O_2/C_2H_4 feed molar ratio range between 1:1 and 3:1. This can be explained in that a higher O_2/C_2H_4 feed molar ratio leads to more O_2 content available to react with various hydrocarbon molecules, as well as EO and CO, to convert to CO_2. However, the conversion of O_2 reached a maximum in the O_2/C_2H_4 feed molar ratio range between 2:1 and 3:1, which is about the theoretical ratio for C_2H_4 complete combustion, as shown in the following equation. At a feed molar ratio higher than 3:1 or excess O_2 condition, the conversion of O_2 tended to decrease since O_2 is probably consumed at the same level.

$$C_2H_4 + 3O_2 \rightarrow 2CO_2 + 2H_2O$$

For the DBD system operated under the studied conditions, the yield of EO and the selectivities for EO, H_2, C_2H_2, and C_2H_6 tended to decrease, but in contrast, the selectivity for CO_2 increased with increasing O_2/C_2H_4 feed molar ratio, as aforementioned.

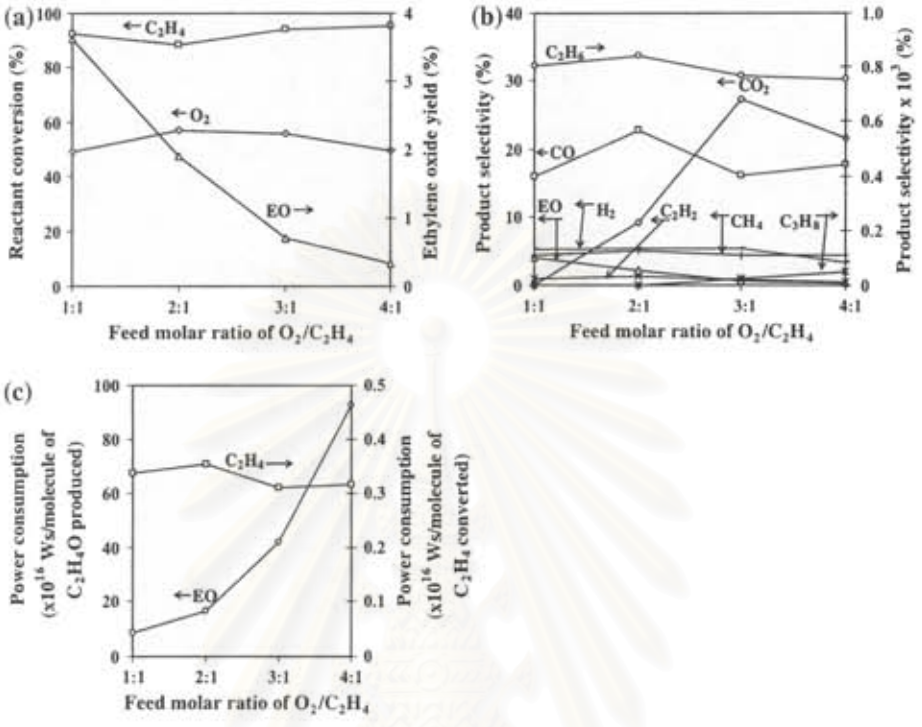

Fig. 2 (**a**) Conversions of ethylene and oxygen and yield of EO, (**b**) product selectivities, and (**c**) power consumptions as a function of O_2/C_2H_4 feed molar ratio (feed flow rate = 50 cm^3/min; electrode gap distance = 10 mm; applied voltage = 17 kV; input frequency = 550 Hz; and residence time = 0.45 min)

Interestingly, the selectivity for CH_4 remained almost constant in the studied range of O_2/C_2H_4 feed molar ratio. The CO selectivity increased when the O_2/C_2H_4 feed molar ratio increased, and it reached a maximum at the O_2/C_2H_4 feed molar ratio of 2:1. Beyond the O_2/C_2H_4 feed molar ratio of 2:1, the CO selectivity decreased and reached a plateau at the theoretical O_2/C_2H_4 feed molar ratio for complete combustion of 3:1. Under the studied conditions, the main products were CO and CO_2 with significant amounts of EO, H_2, CH_4, and C_2 products (C_2H_2 and C_2H_6). The highest hydrocarbon, i.e. C_3H_8, was found in a very small fraction. The results can be explained by the fact that under the presence of oxygen, both complete and partial oxidation reactions are dominant. The decrease in the selectivities for these hydrocarbons and H_2 and the increase in the selectivity for CO_2 with increasing oxygen fraction in feed clearly reveal that the oxidative dehydrogenation and coupling reactions unfavorably occurred under O_2-rich conditions, as expected. The EO selectivity was found to be the highest at the O_2/C_2H_4 feed molar ratio of 1:1 and decreased with increasing O_2/C_2H_4 feed molar ratio. Furthermore, at a very high O_2/C_2H_4 feed molar ratio of 4:1, the selectivity for EO dropped to zero level since this high O_2/C_2H_4 feed molar ratio induced the complete combustion to occur more favorably than the partial oxidation, as well as the epoxidation, indicating that the epoxidation reaction to produce EO is more likely to occur under O_2-lean conditions.

Figure 2c shows the power consumptions used to convert an ethylene molecule and to produce an EO molecule at different O_2/C_2H_4 feed molar ratios. The power consumption per molecule of converted ethylene reached a maximum when the O_2/C_2H_4 feed molar

ratio increased up to 2:1 and slightly decreased with further increasing feed molar ratio. However, there was a significant increase in the power consumption per molecule of produced EO with increasing O_2/C_2H_4 feed molar ratio, especially at the feed molar ratio higher than 3:1. It is also worth noting that the power consumption per molecule of EO produced was approximately two orders of magnitude higher than that per molecule of ethylene converted. Hence, an O_2/C_2H_4 feed molar ratio of 1:1 was therefore selected for further investigation because it provided the highest selectivity and yield for EO and the lowest power consumption per molecule of EO produced.

Effect of Feed Flow Rate

The feed flow rate plays a significant role on the residence time of gas molecules within the plasma zone, affecting the performance of the plasma system. The experiments were performed by varying feed flow rate from 50 to 75, 100, and 125 cm^3/min, corresponding to the residence time of 0.45, 0.3, 0.225, and 0.18 min, respectively. At a feed flow rate lower than 50 cm^3/min, the O_2 flow rate cannot be adjusted due to the limitation of a mass flow controller. The studied plasma system was operated at an O_2/C_2H_4 feed molar ratio of 1:1, an applied voltage of 17 kV, and an input frequency of 550 Hz. Figure 3a illustrates the influences of the feed flow rate on the C_2H_4 and O_2 conversions. The conversion of O_2 gradually decreased with increasing the feed flow rate from 50 to 125 cm^3/min while the conversion of C_2H_4 more sharply decreased. An increase in the feed flow rate generally reduces the gas residence time in the reaction system, resulting in having a shorter contact time of ethylene and oxygen molecules to collide with electrons. As a result, a reduction in the feed flow rate enhances the conversions of both C_2H_4 and O_2, which leads to an increase in the yield of EO, as also shown in Fig. 3a.

The feed flow rate dependence of product selectivities is depicted in Fig. 3b. It is apparent that increasing feed flow rate predominantly resulted in decreases in the selectivities for EO and CO. This is because a higher feed flow rate reduces the opportunity of collision between electrons/oxygen active species and reactant/intermediate molecules to render the partial oxidation and epoxidation reactions. But for other products, especially C_2H_2 and C_3H_8, their selectivities tended to increase at shorter residence times due to higher feed flow rates, suggesting that the oxidative dehydrogenation and coupling reaction are more favorable to occur than the partial oxidation when the residence time is decreased.

Figure 3c shows the effect of feed flow rate on the power consumptions. The power consumption per molecule of converted ethylene slightly decreased, but the power consumption per molecule of produced EO tended to greatly increase with increasing feed flow rate. The lower feed flow rate gave comparatively low power consumption per molecule of produced EO, as well as much higher reactant conversions and desired product selectivity. Therefore, the feed flow rate of 50 cm^3/min was selected as a best condition and used for further investigation.

Effect of Input Frequency

Input frequency is one of the most important parameters in plasma reactor operation, significantly affecting the field strength in the plasma zone. The studied DBD system was operated in the frequency range of 500–800 Hz. At a frequency lower than 500 Hz, the plasma distribution was not fairly uniform over the whole electrode surface, and it tended to appear as a single strong stream of plasma discharge, whereas the plasma could not exist

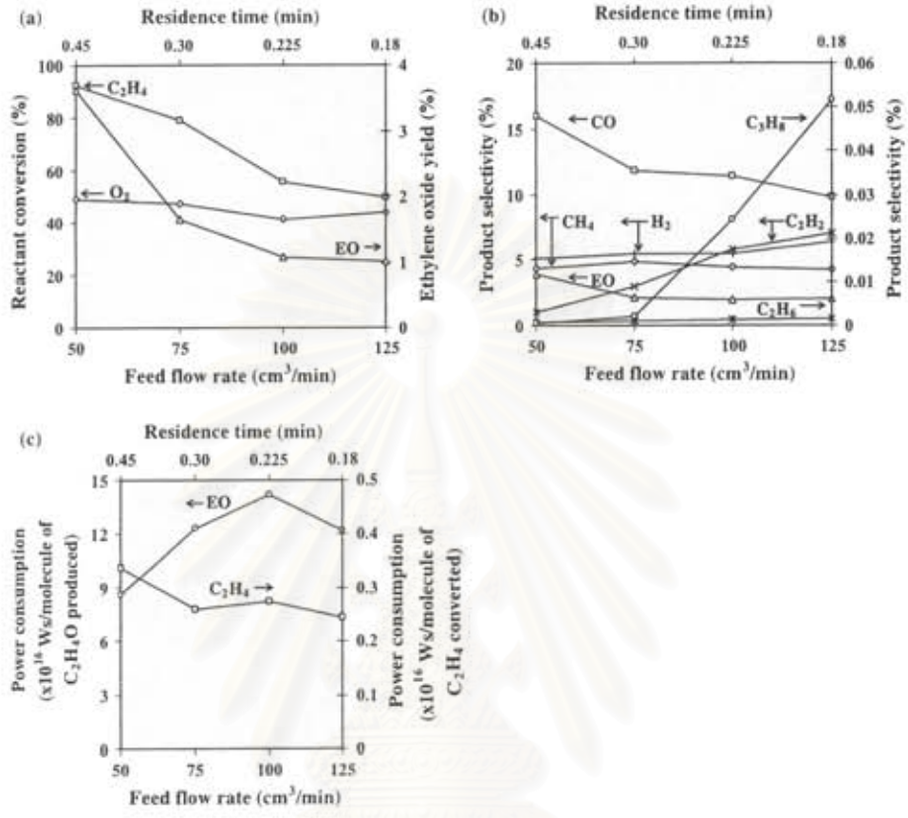

Fig. 3 (**a**) Conversions of ethylene and oxygen and yield of EO, (**b**) product selectivities, and (**c**) power consumptions as a function of feed flow rate (feed molar ratio of O_2/C_2H_4 = 1:1; electrode gap distance = 10 mm, applied voltage = 17 kV, and input frequency = 550 Hz)

at a frequency higher than 800 Hz. The effect of input frequency on the C_2H_4 and O_2 conversions and the yield of EO is illustrated in Fig. 4a. When the input frequency was increased in the range of 500–650 Hz, the O_2 and C_2H_4 conversions and EO yield decreased dramatically, and they turned to slightly decrease with further increasing input frequency from 650 up to 800 Hz. The explanation is that a higher frequency results in a lower current that corresponds to the reduction of the number of electrons generated (weaker field strength), as shown in Fig. 4b. It therefore causes the decrease in amount of active species for further reactions, resulting in the decrease in the C_2H_4 and O_2 conversions and subsequently leading to the lower yield of EO.

The effect of input frequency on the product selectivities is shown in Fig. 4c. The selectivities for EO and CO tended to slightly decrease with increasing input frequency up to 650 Hz. At a higher frequency than 650 Hz, the partial oxidation, oxidative dehydrogenation, and coupling reactions to form various products increasingly occurred. Beyond 650 Hz, the selectivity for EO also gradually increased with increasing frequency and reached a maximum of 7.3% at 800 Hz, as compared with 5.0% at 500 Hz for the low frequency range between 500 and 650 Hz. However, the input frequency of 500 Hz was considered as a potentially best value, exhibiting the highest EO yield with a reasonably high EO selectivity and a relatively low CO selectivity.

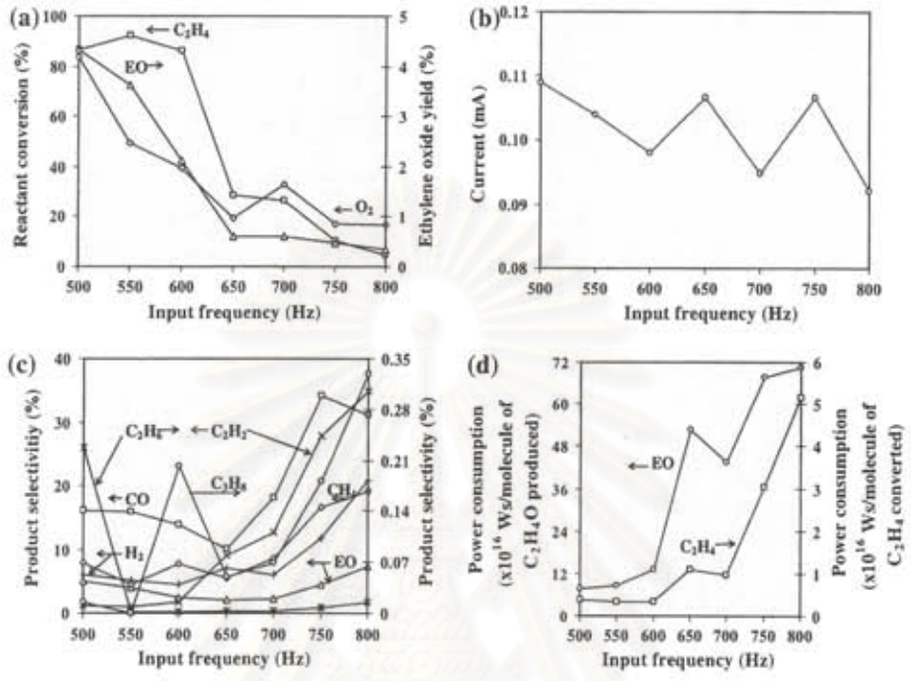

Fig. 4 (**a**) Conversions of ethylene and oxygen and yield of EO, (**b**) generated current, (**c**) product selectivities, and (**d**) power consumptions as a function of input frequency (feed molar ratio of O_2/C_2H_4 = 1:1; feed flow rate = 50 cm^3/min; electrode gap distance = 10 mm; applied voltage = 17 kV; and residence time = 0.45 min)

The effect of input frequency on the power consumptions to break down each C_2H_4 molecule and to create each EO molecule is shown in Fig. 4d. The results showed that both the power consumptions per C_2H_4 molecule converted and per EO molecule produced tended to increase with increasing input frequency, especially at an input frequency higher than 600 Hz. Based upon the relatively high EO yield and the lowest power consumption per molecule of EO produced, the best input frequency of 500 Hz was selected for further investigation.

Effect of Applied Voltage

Under the studied conditions, the break-down voltage or the lowest voltage to generate plasma (onset voltage) was found to be about 13 kV, and the DBD system could not be operated at the applied voltage higher than 21 kV since the generated plasma was found to have the non-uniform distribution characteristic. Therefore, the reaction experiments were conducted in the voltage range of 13–21 kV in order to determine the effect of the applied voltage. The effect of applied voltage on the C_2H_4 and O_2 conversions and EO yield is illustrated in Fig. 5a. The oxygen conversion and EO yield tended to considerably increase with increasing applied voltage in the range of 13–19 kV, whereas the ethylene conversion slightly increased. With further increasing applied voltage higher than 19 kV, the reactant conversions and the EO yield did not significantly change. The explanation for the rapid increment in the O_2 conversion with increasing applied voltage is that a higher voltage results in a higher current (stronger field strength), as shown in Fig. 5b, leading to more

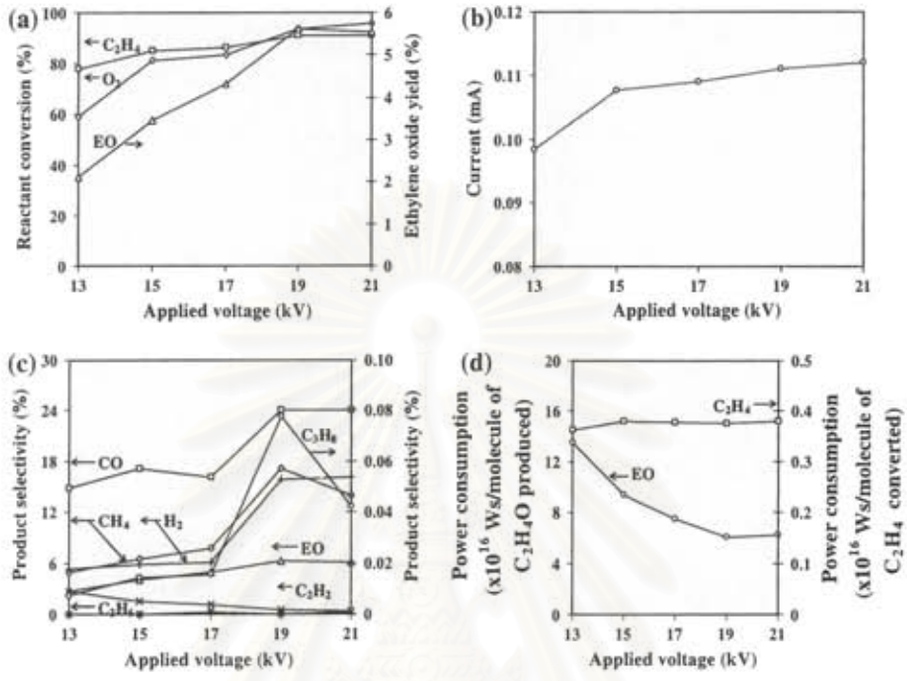

Fig. 5 (**a**) Conversions of ethylene and oxygen and yield of EO, (**b**) generated current, (**c**) product selectivities, and (**d**) power consumptions as a function of applied voltage (feed molar ratio of O_2/C_2H_4 = 1:1; feed flow rate = 50 cm^3/min; electrode gap distance = 10 mm; input frequency = 500 Hz; and residence time = 0.45 min)

available electrons to increase an opportunity for collision with oxygen. The results correspond well with the previous works [32–37]. In contrast, it is unexpected that the C_2H_4 conversion only slightly increased with increasing applied voltage. This can be explained in that the bond dissociation energy of C_2H_4 (16.7 eV) is much higher than that of O_2 (12.2 eV), particularly causing O_2 molecules to be converted more easily than C_2H_4.

The effect of applied voltage on the selectivities for EO, CO, H_2, CH_4, C_2H_2, C_2H_6, and C_3H_8 is shown in Fig. 5c. The selectivities for EO, CO, H_2, and other hydrocarbon products, except C_2H_2 selectivity, increased with increasing applied voltage. When the applied voltage increased, corresponding to increasing O active species as mentioned above, C_2H_4 and other hydrocarbons are easily oxidized to form more CO and EO. Interestingly, no CO_2 was detected under the studied conditions since the system was operated under the O_2-lean condition (the O_2/C_2H_4 feed molar ratio of 1:1). The results therefore suggest that a higher applied voltage is more favorable for EO production under the O_2-lean condition. Only the selectivity for C_2H_2 was observed to decrease with increasing applied voltage. This might be because the formed C_2H_2 further reacts with largely available O active species to form other products more easily. Interestingly, the further increase in applied voltage higher than 19 kV did not help enhance the EO production.

Figure 5d shows the effect of applied voltage on the power consumptions. With increasing applied voltage, the power consumption per molecule of converted C_2H_4 remained almost unchanged, whereas the power consumption per molecule of produced EO substantially decreased. As mentioned earlier, the slight increase in ethylene

conversion with increasing applied voltage caused insignificant change in the power consumption per molecule of ethylene converted. In contrast, an increase in the selectivity for EO was comparatively high as increasing applied voltage, resulting in lower power consumption per molecule of produced EO.

From the results, the applied voltage of 19 kV was selected to be the best value because this voltage provided the reasonably high conversions of C_2H_4 and O_2, and the highest selectivity and yield for EO. At a higher voltage, it did not affect any of reactant conversion, EO selectivity, and EO yield. Moreover, at the applied voltage of 19 kV, the lowest power consumption per EO molecule produced was obtained.

Effect of Electrode Gap Distance

The effects of electrode gap distance and corresponding residence time have been shown to be very important in plasma system operation [35, 37–39]. The effect of electrode gap distance was studied under the best conditions achieved above; an O_2/C_2H_4 feed molar ratio of 1:1, a feed flow rate of 50 cm^3/min, an input frequency of 500 Hz, and an applied voltage of 19 kV. The electrode gap distance was varied from 10 to 11, 12, 13, and 14 nm, corresponding to the residence time of 0.45, 0.54, 0.63, 0.72, and 0.81 min, respectively. The lowest electrode gap distance for the studied DBD system was limited at 10 mm due to its configuration. At an electrode gap distance higher than 14 mm, the generated plasma became unfavorably non-uniform. Therefore, the reaction experiments were conducted in the range of electrode gap distance between 10 and 14 mm in order to determine the effect of the electrode gap distance.

The effect of electrode gap distance on the C_2H_4 and O_2 conversions and EO yield is illustrated in Fig. 6a. The ethylene conversion and EO yield tended to decrease with increasing the electrode gap distance, whereas the oxygen conversion tended to be almost unchanged. The explanation for slight ethylene conversion decrement is that a wider electrode gap distance results in a higher residence time for several hydrocarbon species to recombine via coupling reactions, including backward reaction to form ethylene, causing lower conversion of ethylene. The unexpected nearly constant O_2 conversion with increasing electrode gap distance can be explained in that the current slightly increases with increasing electrode gap distance, as shown in Fig. 6b, while the residence time is also increased. The results suggest that for the O_2 conversion, the higher probability in converting O_2 molecules due to higher electron density might trade off the higher probability in oxygen active species recombination due to a longer residence time of gas flow. The expected increase in current, i.e. electron density, might be contributed to the special characteristic of the DBD system containing the dielectric plate, as well as the various compositions of gaseous species inside the plasma zone. At a higher electrode gap distance, the dielectric plate might sustain the discharge a little bit more effectively due to less loss of electrons via various reactions, under the identical input frequency and applied voltage.

The effect of electrode gap distance on the selectivities for EO, CO, H_2, CH_4, C_2H_2, C_2H_6, and C_3H_8 is shown in Fig. 6c. The selectivities for EO, CO, H_2, and CH_4 decreased with increasing gap distance while the opposite trend was observed for C_2H_2, C_2H_6, and C_3H_8. These may be implied that when increasing electrode gap distance, the opportunity of coupling reactions more favorably occur as secondary reactions than the partial oxidation, as above explained.

Figure 6d shows the effect of electrode gap distance on the power consumptions. It is clearly seen that both the power consumptions per molecule of converted C_2H_4 conversion

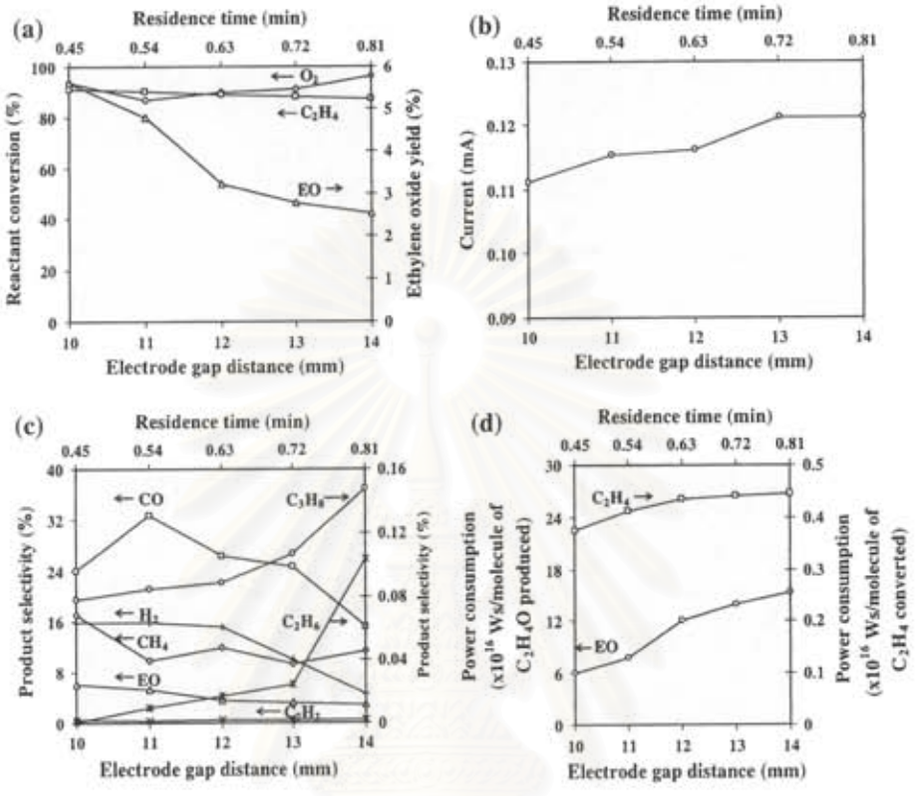

Fig. 6 (**a**) Conversions of ethylene and oxygen and yield of EO, (**b**) generated current, (**c**) product selectivities, and (**d**) power consumptions as a function of electrode gap distance (feed molar ratio of O_2/C_2H_4 = 1:1; feed flow rate = 50 cm^3/min; applied voltage = 19 kV; and input frequency = 500 Hz)

and per molecule of produced EO substantially increased with increasing electrode gap distance. A higher electrode gap distance causes a higher probability of secondary reactions, which unavoidably uses up some power. From the results, the electrode gap distance of 10 mm was considered as a best value because at 10 mm gap distance, the highest EO selectivity and EO yield with the lowest power consumption per EO molecule produced were achieved.

In comparisons, although the maximum EO yield of 5.6% obtained under the aforementioned best conditions (an O_2/C_2H_4 feed molar ratio of 1:1, a feed flow rate of 50 cm^3/min, an input frequency of 500 Hz, an applied voltage of 19 kV, and an electrode gap distance of 10 mm) using the studied DBD system was lower than the EO yields of 30 and 10% obtained from the catalytic epoxidation process using 15 wt.% Ag/Al_2O_3 at reaction temperatures of 280 and 350°C, respectively [15], the DBD system is still considered to exhibit a high potential to be employed for EO production under much lower operating temperatures. Again, the present work is the first time to demonstrate the use of the sole DBD system to synthesize EO without the presence of catalysts. As shown in the aforementioned results, there were several reactions occurring in the plasma reaction zone so it is not possible to easily carry out the kinetic consideration of the ethylene epoxidation reaction. Future works will then be focused on the combination of the low-temperature DBD system with various reported catalytically active catalysts used in the conventional catalytic process, especially Ag/Al_2O_3-based catalysts [5–15, 20], aiming to enhance the

EO yield. The comparative study of ethylene epoxidation under different kinds of low-temperature plasma discharges, such as corona discharge system with pin and plate electrodes, is also of our strong interest. Moreover, the kinetic studies of the ethylene epoxidation reaction will be conducted in order to optimize the DBD process. The experimental results will be presented in the next contribution.

Conclusions

In this work, the epoxidation reaction of ethylene was investigated in the low-temperature DBD plasma system. The effects of various operating parameters, including feed molar ratio of O_2/C_2H_4, feed flow rate, input frequency, applied voltage, and electrode gap distance, on the ethylene epoxidation reaction was studied in order to achieve the best conditions. In order to obtain the highest EO yield of 5.6% and the highest selectivity of 6.2%, the DBD system must be operated at an O_2/C_2H_4 feed molar ratio of 1:1, a feed flow rate of 50 cm^3/min, an input frequency of 500 Hz, an applied voltage of 19 kV, and an electrode gap distance of 10 mm. At these best conditions, the power consumptions to break down each C_2H_4 molecule and to create EO molecule were found to be 0.37×10^{-16} Ws/molecule of C_2H_4 converted and 6.07×10^{-16} Ws/molecule of EO produced.

Acknowledgements The authors would like to gratefully acknowledge the Ratchadapisek Somphot Endowment Fund, Chulalongkorn University, Thailand; the National Excellence Center for Petroleum, Petrochemicals, and Advanced Materials under the Ministry of Education, Thailand; and the Research Unit of Petrochemical and Environmental Catalysis under the Ratchadapisek Somphot Endowment Fund, Chulalongkorn University, Thailand.

References

1. http://www.osha.gov/OshDoc/data_General_Facts/ethylene-oxide-factsheet.pdf
2. http://en.wikipedia.org/wiki/Ethylene_oxide#cite_note-1
3. Lefort TE (1931) French Patent 729952
4. McClellan PP (1950) Ind Eng Chem 42:2402–2407
5. Kilty PA, Rol NC, Sachtler WMH (1973) Catal Lett 99:45–53
6. Geenen PV, Boss HJ, Pott GT (1982) J Catal 77:499–510
7. Iwakura G (1985) Japan Patent 63-126552
8. Tories N, Verikios XE (1987) J Catal 108:161–174
9. Bhasin MM (1988) US Patent 4,908,343
10. Matar S, Mirbach MJ, Tayim HA (1989) Catalysis in petrochemical processes. Kluwer Academic Publishers, Dordrecht, The Netherlands
11. Goncharova SN, Paukshtis EA, Bal'zhinimaev BS (1995) Appl Catal A: Gen 126:67–84
12. Kondaries DI, Verykios XE (1996) J Catal 158:363–377
13. Epling WS, Hoflund GB, Minahan DM (1997) J Catal 171:490–497
14. Jankowiak JT, Barteau MA (2005) J Catal 236:366–378
15. Amorim de Carvalho MCN, Passos FB, Schmal M (2007) J Catal 248:124–129
16. Law GH, Chitwood HC (1942) US Patent 2,279,470
17. Campbell CT, Paffett MT (1984) Appl Surf Sci 19:28–42
18. Tan SA, Grant RB, Lambert RM (1986) J Catal 100:383–391
19. Yeung KL, Gavriilidis A, Varma A, Bhasin MM (1998) J Catal 174:1–12
20. Jankowiak JT, Barteau MA (2005) J Catal 236:379–386
21. Suhr H, Pfreundschuh H (1988) Plasma Chem Plasma Process 8:67–74
22. Patiño P, Hernández FE, Rondón S (1995) Plasma Chem Plasma Process 15:159–171
23. Suhr H (1983) Plasma Chem Plasma Process 3:1–61
24. Zhou LM, Xue B, Kogelschatz U, Eliasson B (1998) Plasma Chem Plasma Process 18:375–393
25. Eliasson B, Hirth M, Kogelschatz U (1987) J Appl Phys 20:1421–1437

26. Chang MB, Tseng TD (1996) J Environ Eng 41–46
27. Orlandini I, Riedel U (2004) Catal Today 89:83–88
28. Magureanu M, Mandache NB, Parvulescu VI, Subrahmanyam Ch, Renken A, Kiwi-Minsker L (2007) Appl Catal B: Environ 74:270–277
29. Sarmiento B, Brey JJ, Viera IG, González-Elipe AR, Cotrino J, Rico VJ (2007) J Power Sources 169:140–143
30. Matin NS, Savadkoohi HA, Feizabadi SY (2008) Plasma Chem Plasma Process 28:189–202
31. Guo MX, Guo HC, Wang XS, Gong WM (2005) Chin J Chem 23:471–473
32. Chavadej S, Kiattubolpaiboon W, Rangsunvigit P, Sreethawong T (2007) J Mol Catal A: Chem 263:128–136
33. Chavadej S, Saktrakool K, Rangsunvigit P, Lobban LL, Sreethawong T (2007) Chem Eng J 132:345–353
34. Rueangjitt N, Sreethawong T, Chavadej S (2008) Plasma Chem Plasma Ptrocess 28:49–67
35. Sreethawong T, Thakonpatthanakun P, Chavadej S (2007) Int J Hydrogen Energ 32:1067–1079
36. Morinaga K, Suzuki M (1962) Bull Chem Soc Jpn 35:204–217
37. Supat K, Chavadej S, Lobban LL, Mallinson RG (2003) Ind Eng Chem Res 42:1654–1661
38. Supat K, Kruapong A, Chavadej S, Lobban LL, Mallinson RG (2003) Energ Fuel 17:474–481
39. Caldwell TA, Le H, Lobban LL, Mallinson RG (2001) Surface science and catalysis, vol 136. Elsevier, New York

Plasma Chem Plasma Process (2008) 28:643–662
DOI 10.1007/s11090-008-9150-2

ORIGINAL PAPER

Ethylene Epoxidation over Alumina-Supported Silver Catalysts in Low-Temperature AC Corona Discharge

Sumaeth Chavadej · Anothai Tansuwan · Thammanoon Sreethawong

Received: 6 May 2008 / Accepted: 11 August 2008 / Published online: 3 September 2008

Abstract In this paper, the epoxidation of ethylene over different catalysts—namely Ag/(low-surface-area, LSA)α-Al_2O_3, Ag/(high-surface-area, HSA)γ-Al_2O_3, and Au–Ag/(HSA)γ-Al_2O_3—in a low-temperature corona discharge system was investigated. In a comparison among the studied catalysts, the Ag/(LSA)α-Al_2O_3 catalyst was found to offer the highest selectivity for ethylene oxide, as well as the lowest selectivity for carbon dioxide and carbon monoxide. The selectivity for ethylene oxide increased with increasing applied voltage, while the selectivity for ethylene oxide remained unchanged when the frequency was varied in the range of 300–500 Hz. Nevertheless, the selectivity for ethylene oxide decreased with increasing frequency beyond 500 Hz. The optimum Ag loading on (LSA)α-Al_2O_3 was found to be 12.5 wt.%, at which a maximum ethylene oxide selectivity of 12.9% was obtained at the optimum applied voltage and input frequency of 15 kV and 500 Hz, respectively. Under these optimum conditions, the power consumption was found to be 12.6×10^{-16} W s/molecule of ethylene oxide produced. In addition, a low oxygen-to-ethylene molar ratio and a low feed flow rate were also experimentally found to be beneficial for the ethylene epoxidation.

Keywords Ethylene epoxidation · Ethylene oxide · Corona discharge · Silver · Alumina

Introduction

The selective oxidation of ethylene, especially ethylene epoxidation, is currently the largest hydrocarbon partial oxidation process in industry because the desired product, ethylene oxide (C_2H_4O, EO), is a valuable chemical feedstock or intermediate product for many important applications, such as solvents, antifreeze agents, textiles, detergents, adhesives, polyurethane foam, and pharmaceuticals [1]. Besides, this is in good accordance with the

S. Chavadej (✉) · A. Tansuwan · T. Sreethawong
The Petroleum and Petrochemical College, Chulalongkorn University,
Soi Chula 12, Phyathai Road, Pathumwan, Bangkok 10330, Thailand
e-mail: sumaeth.c@chula.ac.th

Plasma Chem Plasma Process (2008) 28:643–662
DOI 10.1007/s11090-008-9150-2

ORIGINAL PAPER

Ethylene Epoxidation over Alumina-Supported Silver Catalysts in Low-Temperature AC Corona Discharge

Sumaeth Chavadej · Anothai Tansuwan · Thammanoon Sreethawong

Received: 6 May 2008 / Accepted: 11 August 2008 / Published online: 3 September 2008

Abstract In this paper, the epoxidation of ethylene over different catalysts—namely Ag/(low-surface-area, LSA)α-Al_2O_3, Ag/(high-surface-area, HSA)γ-Al_2O_3, and Au–Ag/(HSA)γ-Al_2O_3—in a low-temperature corona discharge system was investigated. In a comparison among the studied catalysts, the Ag/(LSA)α-Al_2O_3 catalyst was found to offer the highest selectivity for ethylene oxide, as well as the lowest selectivity for carbon dioxide and carbon monoxide. The selectivity for ethylene oxide increased with increasing applied voltage, while the selectivity for ethylene oxide remained unchanged when the frequency was varied in the range of 300–500 Hz. Nevertheless, the selectivity for ethylene oxide decreased with increasing frequency beyond 500 Hz. The optimum Ag loading on (LSA)α-Al_2O_3 was found to be 12.5 wt.%, at which a maximum ethylene oxide selectivity of 12.9% was obtained at the optimum applied voltage and input frequency of 15 kV and 500 Hz, respectively. Under these optimum conditions, the power consumption was found to be 12.6×10^{-16} W s/molecule of ethylene oxide produced. In addition, a low oxygen-to-ethylene molar ratio and a low feed flow rate were also experimentally found to be beneficial for the ethylene epoxidation.

Keywords Ethylene epoxidation · Ethylene oxide · Corona discharge · Silver · Alumina

Introduction

The selective oxidation of ethylene, especially ethylene epoxidation, is currently the largest hydrocarbon partial oxidation process in industry because the desired product, ethylene oxide (C_2H_4O, EO), is a valuable chemical feedstock or intermediate product for many important applications, such as solvents, antifreeze agents, textiles, detergents, adhesives, polyurethane foam, and pharmaceuticals [1]. Besides, this is in good accordance with the

S. Chavadej (✉) · A. Tansuwan · T. Sreethawong
The Petroleum and Petrochemical College, Chulalongkorn University,
Soi Chula 12, Phyathai Road, Pathumwan, Bangkok 10330, Thailand
e-mail: sumaeth.c@chula.ac.th

currently high global demand for ethylene oxide, which exceeds 40 billion pounds per annum [2], indicating high ethylene oxide consumption around the world.

Ordinarily, ethylene can be oxidized to ethylene oxide with a high selectivity over unique traditional silver catalysts supported on low-surface-area alpha-alumina (Ag/(LSA)α-Al_2O_3). Commercially, the addition of a few ppms of chloride to gaseous reactants as a moderator in the form of chlorine-containing hydrocarbon species, such as dichloroethane ($C_2H_4Cl_2$) and vinyl chloride (C_2H_3Cl), was reported to significantly increase the selectivity for ethylene oxide by 15–20% [3–6]. Alkali and alkali earth, such as Cs and Re, were also reported to provide an improvement of the selectivity toward ethylene oxide by 10% [7, 8]. In a recent work [9], a silver catalyst supported on high-surface-area gamma-alumina (Ag/(HSA)γ-Al_2O_3) was proved to exhibit a good selectivity toward ethylene oxide. Moreover, adding a small amount of Au to form Au–Ag bimetallic catalysts on the high-surface-area alpha-alumina support was found to favor the epoxidation reaction of ethylene to ethylene oxide. They reported that ethylene conversion obtained from these catalysts did not occur at temperatures below 220°C. Even though the reaction temperature was raised to 270°C, ethylene conversion was still low, around 1–4% [10]. Consequently, this limitation results in high energy consumption for the catalytic reaction at high temperatures, which becomes an obstruction in developing the process for industrial application. A non-traditional catalysis technique is, therefore, expected to overcome this constraint. One potential technique is to combine selective traditional catalysis and non-thermal plasma, which is believed to reduce the power consumption and/or increase the selectivity and yield for ethylene oxide production.

Non-thermal plasma is one kind of electric gas discharge [11]. In non-thermal plasmas, the electrons in electrodes gain energy from an external applied voltage until they possess enough energy to overcome the potential barrier of metal surface electrodes. Then, they can move from one electrode to the other, and these high-energy electrons will chemically excite or dissociate the gaseous species by colliding with the gaseous components present in the plasma zone. Typically, these excited or dissociated atoms or molecules have a much higher reactivity than neutral species at the ground state, and consequently they can easily lead to the formation of new chemical species. Furthermore, the most important characteristic of non-thermal plasma is that the electrons in the plasma zone have a higher energy, but the temperature of the bulk gas is still much lower [12]. Examples of chemical synthesis using plasma are oxidations of olefins, aromatics, and so on [13, 14]. The combined processes of catalysis and non-thermal plasma have been demonstrated to offer a number of advantages over conventional catalytic processes. One advantage is to require low operational temperatures close to room temperature and low pressure at near or slightly higher than atmospheric pressure, as described above. This implies comparatively that non-thermal plasma processes offer a lower energy consumption used for activating catalysts as compared with conventional catalytic processes. Hence, corona discharge was employed for this research because it is capable of operating at low temperature and atmospheric pressure [11].

A basic configuration of corona discharge is to use a pair of in-homogeneous metal electrode geometries, which can stabilize the discharge generated. There are many industrial applications involving the utilization of corona discharge, such as NO_x and SO_x reduction in flue gas, toxic compound destruction, and ozone production [15–17]. From literature review, the combination of corona discharge and heterogeneous catalysts has been used for many applications [18–30]. Recently in our previous works, it was also used with photocatalysts for the gaseous removal of benzene and ethylene [31, 32].

The objective of this work was, for the first time, to investigate a combined catalytic and corona discharge system for the epoxidation of ethylene using different catalysts:

Ag/(LSA)α-Al_2O_3, Ag/(HSA)γ-Al_2O_3, and Au–Ag/(HSA)γ-Al_2O_3. In this study, the effects of various operating parameters, including applied voltage, input frequency, molar ratio of oxygen to ethylene, and feed flow rate, on the activity of ethylene epoxidation were examined systematically. Moreover, the optimum conditions for maximum ethylene oxide production and minimum power consumption were determined.

Experimental

Materials and Reactant Gases

The two types of supports used were (LSA)α-Al_2O_3, supplied by A.C.S. Xenon Limited Partnership, and (HSA)γ-Al_2O_3, supplied by Aerosil®. Silver nitrate ($AgNO_3$), supplied by Carlo Erba, and hydrogen tetrachloroaurate (III) trihydrate ($HAuCl_4 \cdot 3H_2O$), supplied by Alfa Aesar, were employed as silver and gold catalyst precursors, respectively. All chemicals were used as received without further purification. Distilled water was used for catalyst preparation in this study. For the reactant gases, 99.995% helium (high purity grade), 40% ethylene balanced with helium, and 97% oxygen balanced with helium were obtained from Thai Industrial Gas (Public) Co., Ltd.

Catalyst Preparation Procedures

The incipient wetness impregnation method was used to prepare all catalysts according to literature [9, 10, 33]. For silver supported on (LSA)α-Al_2O_3, the alumina support was impregnated with aqueous solutions of silver nitrate to achieve various nominal Ag loadings ranging from 0 to 15 wt.% and then dried in air at 110°C overnight. These mixtures were calcined in air at 400°C for 12 h. After that, each impregnated catalyst was sieved in order to obtain the desired grain size range of 221–425 μm for the activity studies. For silver supported on (HSA)γ-Al_2O_3, the alumina support was impregnated with an aqueous solution of silver nitrate to achieve a nominal Ag loading of 13.18 wt.%, exhibiting superior activity in previous works [9, 10], and then dried in air at 110°C overnight. This mixture was calcined in air at 500°C for 5 h. After that, the impregnated catalyst was also sieved in order to obtain the desired grain size range of 221–425 μm for the reaction activity experiments, which will be described later. For bimetallic Au–Ag supported on (HSA)γ-Al_2O_3, a Ag catalyst on the alumina support with an optimum Ag loading of 13.18 wt.% was initially prepared and dried at 110°C for 2 h. This catalyst was then sequentially impregnated with an appropriate amount of an aqueous solution of tetrachloroaurate (III) trihydrate to achieve an optimum Au loading of 0.63 wt.% [9, 10]. This impregnated catalyst was then dried in air at 110°C overnight and calcined in air at 500°C for 5 h. After that, the catalyst was sieved in the same manner as explained above.

Catalyst Characterizations

The specific surface areas of all prepared catalysts were determined by a surface area analyzer (Quantachrom, Autosorb-1) using nitrogen adsorption analysis. A catalyst sample was dried and outgassed in a sample cell under vacuum at 150°C for 10 h to remove the humidity and any volatile components adsorbed on the catalyst surface before the analysis. The specific surface area of each catalyst was calculated from the 5-point adsorption isotherm. The results were analyzed by Autosorb ANAGAS software, version 2.10.

The actual contents of silver and gold in the prepared catalysts were determined by an atomic absorption spectroscope (AAS) (Varian Spectr, AA-300).

The crystalline phases of the prepared catalysts were investigated by an X-ray diffractometer (XRD, Rigaku RINT-2200) equipped with a graphite monochromator, a Cu tube for generating CuKα radiation ($\lambda = 1.5406$ Å) at a generator voltage of 40 kV and a generator current of 30 mA, and a nickel filter used as the filter for Kβ removal. The goniometer parameters were; divergence slit = 1°(2θ), scattering slit = 1°(2θ), and receiving slit = 0.3 mm. The catalyst sample was held in the hollow of a glass slide holder and was examined in the 2θ range of 20–90° at a scanning speed of 5°(2θ)/min and a scan step of 0.02°(2θ). The digital output of the proportional X-ray diffractometer and the goniometer angle measurements were sent to an online microcomputer to record the data and to perform subsequent analyses.

Transmission electron microscopy (TEM) was employed for investigating the average particle size of Ag particles and identifying the microstructures of the prepared catalysts. The catalyst sample was ground into a fine powder and ultrasonically dispersed in ethanol. A small droplet of the suspension was deposited on a copper grid, and the solvent was evaporated prior to loading the sample into the TEM. The TEM (JEOL, 2000 CX) was operated at an accelerating voltage of 200 kV in bright field mode.

Temperature-programmed oxidation (TPO) was employed to quantitatively investigate the coke formation on the spent catalysts. The TPO analysis was performed at a continuous flow of O_2/He (ratio 2:1) with a total flow rate of 40 ml/min. A spent catalyst was placed in the quartz tube, and it was secured with packing quartz wool. The sample temperature was linearly increased with a constant rate of 10°C/min to reach a maximum temperature of 850°C. The carbon fraction of the sample was completely oxidized to form carbon dioxide. After this reaction, the effluent gas was passed through a methanator containing a Ni/Al_2O_3 catalyst to convert the carbon dioxide to methane. Subsequently, the produced methane was detected with a flame ionization detector (FID). The area under the obtained curve was used to calculate carbon content in the spent catalyst sample. The amount of coke formed is reported based on the weight of spent catalyst.

Experimental Setup and Reaction Activity Experiments

The experimental study of ethylene epoxidation was conducted in an AC corona discharge reactor, which was operated at atmospheric pressure and ambient temperature, around 25–27°C (room temperature). A schematic of the corona discharge system is shown in Fig. 1a. The reactor comprised an 11.25-inch-long quartz tube with an outer diameter of 10 mm and an inner diameter of 8 mm. Plasma was generated in the reactor via pin-and-plate electrodes, which were located at the center of the reactor. The power used to generate plasma was alternating current, 200 V and 50 Hz, which was transformed to a high voltage current via a power supply unit. The output voltage and frequency was adjusted by a function generator, whereas the sinusoidal wave signal generated was monitored by an oscilloscope. Since the plasma generated in the reactor was found to have a very high fluctuation, it was not possible to measure the voltage across the electrodes of the reactor (high-side voltage). Therefore, the low-side voltage and current were measured instead, and the high-side voltage and current were then calculated by multiplying and dividing by a factor of 130, respectively. To investigate the effect of catalyst in the plasma reactor on the ethylene epoxidation, 0.24 g of each of the three studied catalysts was individually placed on the plate electrode and secured by a quartz wool layer, as shown in Fig. 1b. In this study, the gap distance between the two electrodes was fixed at 1 cm.

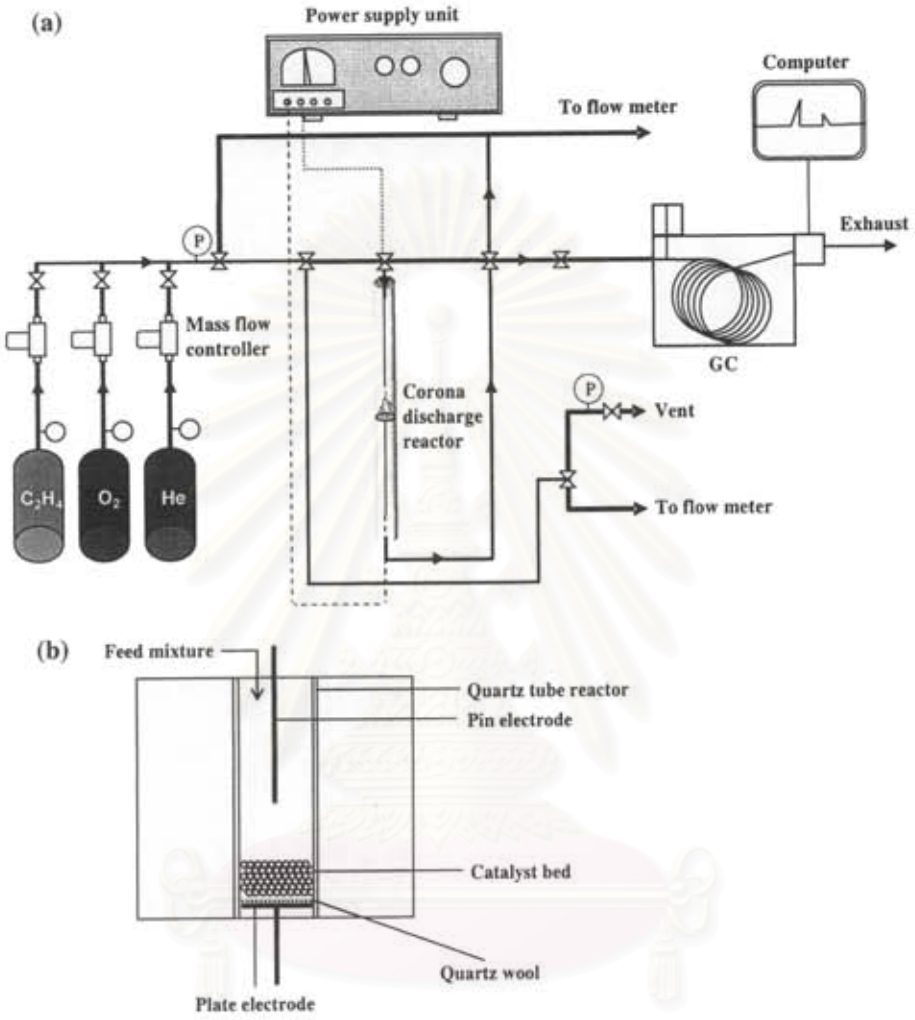

Fig. 1 (**a**) Schematic of experimental setup for ethylene epoxidation reaction in corona discharge plasma system and (**b**) configuration of the corona discharge reactor

Reactant gases (ethylene, oxygen, and helium) fed through the plasma reactor were controlled by a set of electronic mass flow controllers to obtain a feed gas mixture having different flow rates and molar ratios of oxygen to ethylene, while the ethylene concentration was fixed at 6%. All reactant lines had 0.7 μm in-line filters before being passed through the mass flow controllers in order to trap any foreign particles. When the composition of the feed remained constant, the power supply unit was turned on. After 60 min, the composition of the effluent gas was analyzed every 60 min until it was invariant, indicating the steady state condition. Reactor pressure was controlled by a needle valve, and the outlet of the reactor was either vented to the atmosphere via rubber tube exhaust or was connected to an on-line gas chromatograph for analysis of the product gases. Before being fed to the on-line gas chromatograph, the moisture in the effluent gas was removed by a water trap filter. The gas chromatograph used was a Perkin-Elmer AutoSystem GC equipped with both a thermal conductivity detector (TCD) and a flame ionization detector

(FID). For the TCD channel, a packed column (Carboxen 1000) was used for separating the product gases—oxygen (O_2), carbon monoxide (CO), carbon dioxide (CO_2), and ethylene (C_2H_4). For the FID channel, a capillary column (OV-Plot U) was used for analysis of the ethylene oxide (C_2H_4O), methane (CH_4), ethane (C_2H_6), acetylene (C_2H_2), and propane (C_3H_8). Since the gas volume was changed after the reactions, the flow rate of the outlet gas was also measured. The experimental data taken under steady state conditions were averaged, and these averages were used to evaluate the performance of the plasma system.

To evaluate the process performance, the conversions of ethylene and oxygen and the selectivities for products, including CO, CO_2, C_2H_4O, CH_4, C_2H_6, C_2H_2, and traces of C_3, were considered. The conversion of either ethylene or oxygen is defined as:

$$\%\text{Reactant conversion} = \frac{(\text{moles of reactant } in - \text{moles of reactant } out)}{(\text{moles of reactant } in)} \times 100 \quad (1)$$

The product selectivity is calculated from the following equation:

$$\%\text{Product selectivity} = \frac{(\text{number of carbon atom in product})(\text{moles of product produced})}{(\text{number of carbon atom in ethylene})(\text{moles of ethylene converted})} \times 100 \quad (2)$$

To determine the energy efficiency of the plasma system, the specific power consumption is calculated in a unit of W s per molecule of converted ethylene or per molecule of produced ethylene oxide using the following equation:

$$\text{Specific power consumption} = \frac{P \times 60}{\tilde{N} \times M} \quad (3)$$

where P is the power (W), $\tilde{N}$ is Avogadro's number $= 6.02 \times 10^{23}$ molecules/mol, M is the rate of converted ethylene molecules in feed or rate of produced ethylene oxide molecules (mol/min).

Results and Discussion

Catalyst Characterization Results

The nominal metal loadings, actual metal loadings, and BET surface areas of all the studied catalysts are shown comparatively in Table 1. The actual metal loadings of these three catalysts obtained from AAS were not significantly different from the nominal metal loadings. This implies that the incipient wetness impregnation technique used for loading metals on supports is reliably effective to control any desired catalyst loading.

The BET surface areas of the Ag/(LSA)α-Al_2O_3 family slightly increased with increasing silver loading, indicating that the silver particles are well dispersed on the support without the sintering effect during the preparation step. For the other catalysts supported on (HSA)γ-Al_2O_3, their surface areas were similar to those of the unloaded support in the range of 97–101 m^2/g. These results also imply that both Ag and/or Au were highly dispersed on the surface of this high-surface-area support [10].

Figure 2 shows the XRD patterns of the Ag catalysts on (LSA)α-Al_2O_3 at different silver loadings. For the unloaded support, only the α-Al_2O_3 phase was observed as a major phase. The silver phase was found at the diffraction peaks of approximately 38, 44, and 64° when silver loading increased up to 12.5 wt.% Ag. At 15 wt.% Ag, a silver nitrate phase

Table 1 Textural characteristics of all prepared catalysts

Catalyst	Nominal content (wt.%)		Actual content[a] (wt.%)		BET surface area[b] (m^2/g)
	Ag	Au	Ag	Au	
Ag/(LSA)α-Al_2O_3	0	0	0	0	0.44
	10	0	9.63	0	0.61
	12.5	0	12.54	0	0.74
	15	0	14.94	0	0.89
Ag/(HSA)γ-Al_2O_3	0	0	0	0	101
	13.18	0	12.98	0	98
Au–Ag/(HSA)γ-Al_2O_3	13.18	0.63	12.98	0.78	97

[a] Determined by AAS

[b] Determined by N_2 adsorption analysis

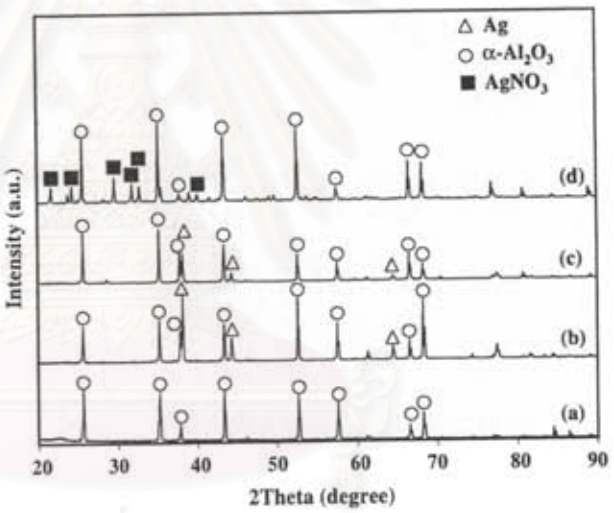

Fig. 2 XRD patterns of (a) (LSA)α-Al_2O_3, (b) 10 wt.% Ag/(LSA)α-Al_2O_3, (c) 12.5 wt.% Ag/(LSA)α-Al_2O_3, and (d) 15 wt.% Ag/(LSA)α-Al_2O_3

was additionally observed, probably due to overloading of the Ag precursor. As shown in Fig. 3, it can be observed from the XRD patterns that the γ-Al_2O_3 phase is a major phase of the (HSA)γ-Al_2O_3-supported catalysts. For the 13.18 wt.% Ag/(HSA)γ-Al_2O_3, the silver phase was found at the aforementioned diffraction peaks as well. When 0.63 wt.% Au was additionally loaded onto the 13.18 wt.% Ag/(HSA)γ-Al_2O_3, its XRD pattern was not significantly changed, without distinguishable diffraction peaks of gold phase due to their same positions as the diffraction peaks of silver phase.

Figure 4 shows the morphology and mean particle size of Ag on the surface of the studied catalysts observed by using TEM. The TEM results show that Ag particles are highly dispersed on the alumina supports. The TEM micrographs of a representative 12.5 wt.% Ag/(LSA)α-Al_2O_3, which exhibited superior activity toward ethylene epoxidation as explained later, are depicted in Fig. 4a, b (low and high magnifications, respectively). From the TEM results, the mean Ag particle size was found to be approximately 9.5 nm.

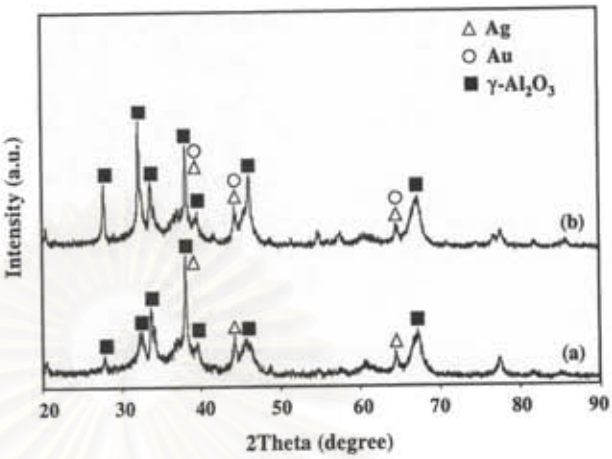

Fig. 3 XRD patterns of (a) 13.18 wt.% Ag/(HSA)γ-Al_2O_3 and (b) 0.63 wt.% Au-13.18 wt.% Ag/(HSA)γ-Al_2O_3

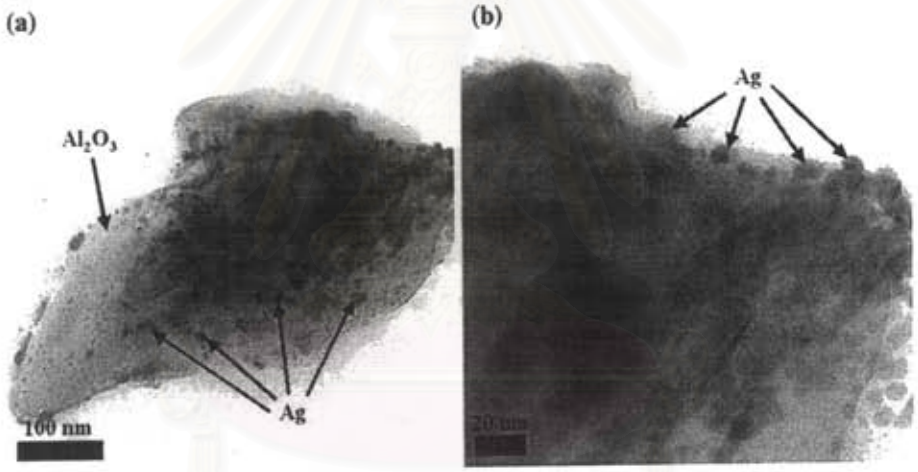

Fig. 4 TEM micrographs of 12.5 wt.% Ag/(LSA)α-Al_2O_3 at (a) low magnification and (b) high magnification

Reaction Activity Performance

All experiments were carried out at ambient temperature and atmospheric pressure in order to determine the effects of type of catalyst, silver loading, applied voltage, input frequency, molar ratio of O_2/C_2H_4, and feed flow rate on the epoxidation activity of ethylene. Under the studied conditions, the product gas contained carbon monoxide, carbon dioxide, ethylene oxide, methane, ethane, acetylene, and traces of C_3. Interestingly, hydrocarbons containing a carbon number greater than C_3 were not detectable.

Effect of Type of Catalyst

In the corona discharge system without a catalyst, most of the discharge energy is used to produce and accelerate electrons, which then react with gas molecules to generate highly

active species (metastable radicals and ions). Ethylene and oxygen are, therefore, chemically activated directly by electron collisions. For a combined catalytic-plasma system, a catalytic material in the plasma or discharge zone is used to enhance the selectivity and efficiency of the plasma process by surface reactions.

Figure 5a shows the ethylene and oxygen conversions and ethylene oxide yield over different catalysts. The ethylene conversion was always lower than the oxygen conversion in both the sole plasma and combined catalytic-plasma systems since the bond dissociation energy of ethylene (682 kJ/mol) is much higher than that of oxygen (498.38 kJ/mol). Under the studied oxygen-to-ethylene molar ratio of 1:1, both partial and complete oxidation to produce CO and CO_2 appear, as confirmed in Fig. 5b. As a result, the oxygen conversion was higher than the ethylene conversion. The plasma system without a catalyst provided the highest oxygen conversion. The oxygen conversion on the Ag/(HSA)γ-Al_2O_3 was higher than that on the Ag/(LSA)α-Al_2O_3 since the high-surface-area alumina support can provide higher silver dispersion than the low-surface-area one, therefore improving oxygen adsorption for the oxidation reaction, to result in a higher oxygen conversion. Interestingly, the bimetallic Au–Ag/(HSA)γ-Al_2O_3 gave a lower oxygen conversion than both Ag/(HSA)γ-Al_2O_3 and Ag/(LSA)α-Al_2O_3. A possible explanation is that if chemisorption-induced surface enrichment is operative, it will tend to enhance the concentration

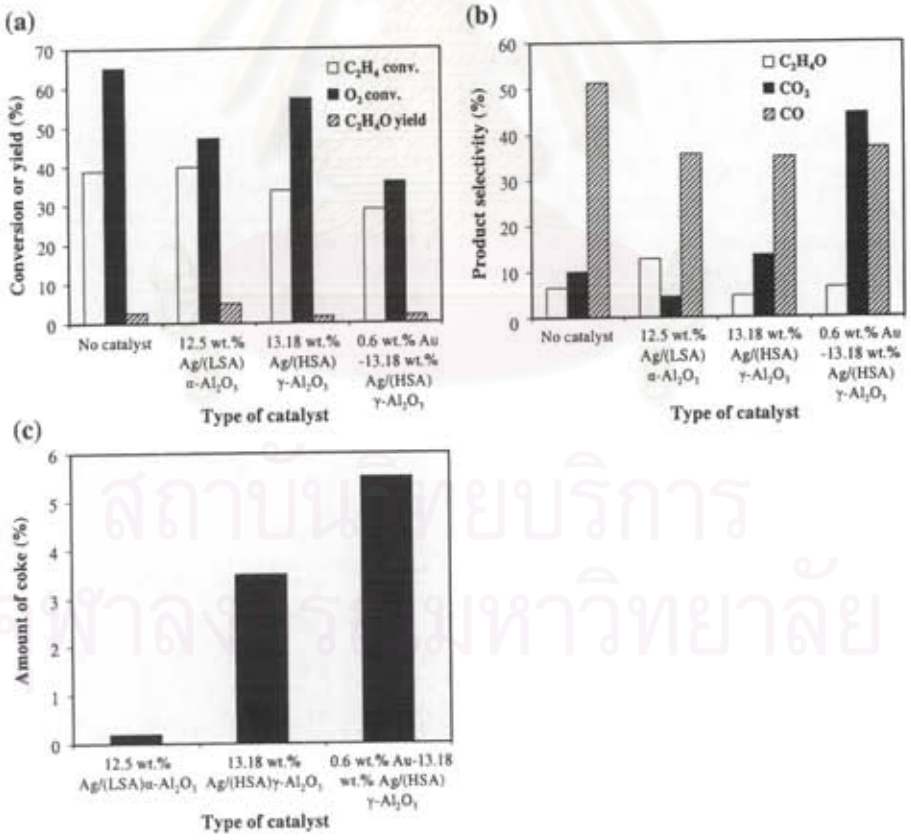

Fig. 5 (**a**) Ethylene and oxygen conversions and ethylene oxide yield, (**b**) product selectivities, and (**c**) amount of coke formed as a function of different catalysts (molar ratio of O_2/C_2H_4 = 1/1; feed flow rate = 50 ml/min; gap distance = 1 cm; frequency = 500 Hz; and voltage = 15 kV)

of Ag on the surface. This is due to the fact that oxygen forms strong chemisorption bonds with silver, while it does not chemically adsorb, to any appreciable extent, on gold. It is well known that the component that forms the strongest chemisorption bonds tends to segregate at the surface of the alloy particles [34], resulting in less oxygen chemisorption and consequent lower oxygen conversion in the case of the Au–Ag/(HSA)γ-Al_2O_3. Interestingly, the oxygen conversion in the sole plasma system was higher than that in the case of the combined catalytic and plasma systems. This result indicates that the activity of the plasma can be slightly retarded in the presence of catalysts, since they simply reduce the volume of the plasma zone, as well as act as an electrically resistant material. However, the ethylene conversion on the Ag/(LSA)α-Al_2O_3 was found to be comparatively the same as that in the sole plasma system, but not in the case of Ag/(HSA)γ-Al_2O_3. Since the Ag catalysts have been found to be the hydrogenation sites for acetylene [35], this might be another important reason to explain how the lower conversion of ethylene was obtained on the Ag catalyst supported on (HSA)γ-Al_2O_3. This can imply that despite the presence of the Ag catalyst, C_2H_2 hydrogenation does not favorably occur on the (LSA)α-Al_2O_3 support. Interestingly, the Ag/(LSA)α-Al_2O_3 was also found to provide the highest ethylene oxide yield, plausibly due to the comparatively high ethylene conversion and the highest ethylene oxide selectivity, as explained next.

By considering the product selectivities, as shown in Fig. 5b, it can be seen that the type of catalyst significantly affects the selectivities for main products, i.e. C_2H_4O, CO, and CO_2. Even though the bimetallic Au–Ag/(HSA)γ-Al_2O_3 combined with plasma was shown to favor the total oxidation reaction as compared to the other two catalysts, it still provided a moderate ethylene oxide selectivity, even higher than the Ag/(HSA)γ-Al_2O_3. The reason is that gold could behave as a diluting agent on the silver surface, resulting in the destruction of multiple silver sites, which favor atomic oxygen adsorption. As a result, the addition of gold simply creates new adsorption sites for molecular oxygen, which is also responsible for the ethylene epoxidation reaction [10]. The reason why the Au–Ag/(HSA)γ-Al_2O_3 showed the highest selectivity for carbon dioxide is that the O^{2-} species are separated from each other, and the adsorbed ethylene complex can consequently react with atomic oxygen to form carbon dioxide and water [34]. Obviously, the Ag/(HSA)γ-Al_2O_3 catalyst was shown to be more active for the total oxidation reaction than the Ag/(LSA)α-Al_2O_3 and the sole plasma system. In the plasma system, it was found to show the highest selectivity for carbon monoxide and a low selectivity for carbon dioxide.

It is generally accepted that non-thermal plasma changes the status of reactant molecules. Instead of neutral ground state molecules, a mixture of electrons, excited molecules, ions, and radicals predominantly occupies the plasma zone. The energized electrons and excited active species are in a thermodynamically initial state for subsequent reactions. Besides, the interactions among the active species and catalyst lead to unusual plasma catalytic reactions [36]. In comparisons of these three catalysts combined with plasma and the sole plasma system, it is clear that the presence of a suitable catalyst in corona discharge can enhance the selectivity for the desired product, ethylene oxide. In this experiment, the Ag/(LSA)α-Al_2O_3 catalyst was found to offer the highest ethylene oxide selectivity, the lowest carbon dioxide selectivity, and the highest ethylene oxide yield. Interestingly, as shown in Fig. 5c, the coke formed on the spent Ag/(LSA)α-Al_2O_3 was comparatively very low, as the amounts of coke formed on the spent Ag/(HSA)γ-Al_2O_3 and Au–Ag/(HSA)γ-Al_2O_3 were approximately 13 and 21 times higher than that on the Ag/(LSA)α-Al_2O_3. Hence, the Ag/(LSA)α-Al_2O_3 catalyst was selected for further studies.

Effect of Silver Loading

Figure 6a illustrates the conversions of C_2H_4 and O_2 and the C_2H_4O yield over the Ag/(LSA)α-Al_2O_3 as a function of silver loading. The catalyst having a Ag loading greater than 15 wt.% was found to produce a large amount of coke on the surface of the pin electrode and on the surface of the catalyst. The lowest ethylene and oxygen conversions were observed for the blank support, as compared to the Ag-loaded ones. This result indicates that the presence of silver on this support is necessary to enhance both C_2H_4 and O_2 conversions. The conversion of C_2H_4 increased with increasing Ag loading up to 10 wt.% and remained almost constant beyond 10 wt.% Ag, while the conversion of O_2 also increased with increasing the Ag loading up to 10 wt.%, but substantially decreased with further increasing the Ag loading. Interestingly, a Ag loading of 12.5 wt.% was found to give the highest ethylene oxide yield. Besides, as shown in Fig. 6b, it is worth noting that at high Ag loadings, especially higher than 12.5 wt.%, the amount of coke formed was observed to be relatively high, resulting in significant decreases in the O_2 conversion and the C_2H_4O yield.

The influence of silver loading on the selectivities for C_2H_4O, CO, CO_2, CH_4, C_2H_2, C_2H_6, and C_3H_8 is depicted in Fig. 6c. It is apparent that an increase in silver loading resulted in increases in both CO and CO_2 selectivities, especially with a Ag loading higher

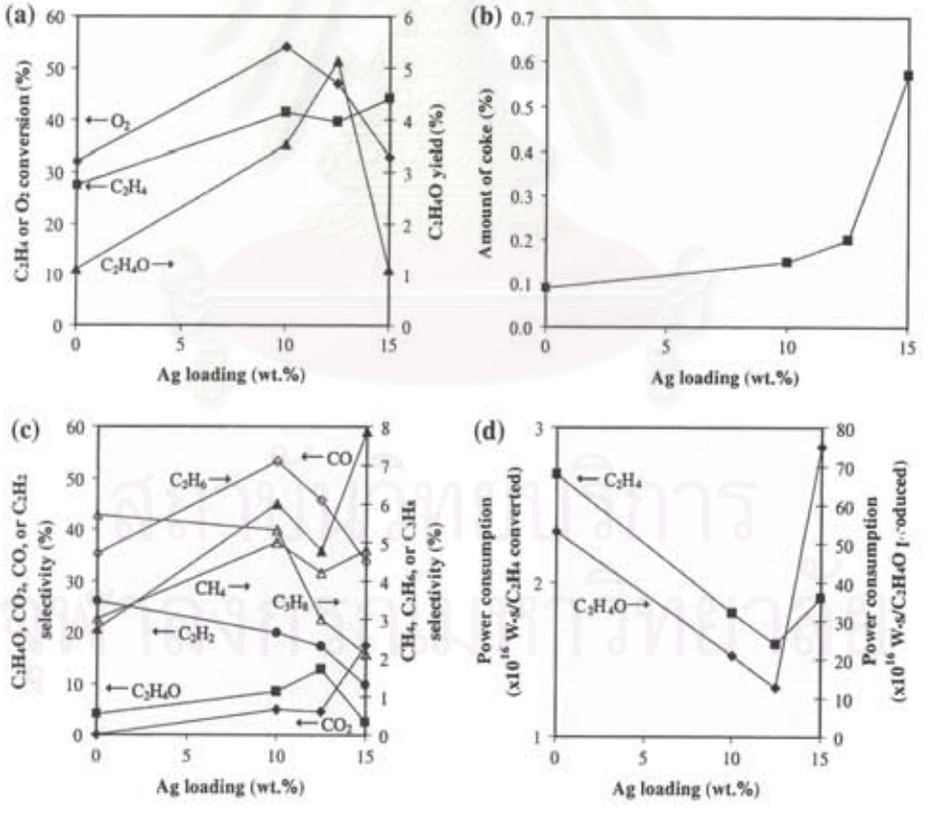

Fig. 6 (**a**) Ethylene and oxygen conversions and ethylene oxide yield, (**b**) amount of coke formed, (**c**) product selectivities, and (**d**) power consumptions as a function of Ag loading on (LSA)α-Al_2O_3 (molar ratio of O_2/C_2H_4 = 1/1; feed flow rate = 50 ml/min; gap distance = 1 cm; frequency = 500 Hz; and voltage = 15 kV)

than 12.5 wt.%; however, the selectivities for C_2H_4O increased with increasing Ag loading up to 12.5 wt.% and substantially declined with further increasing Ag loading. The results also show that the selectivities for C_2H_2 and C_3H_8 tended to decrease as the Ag loading increased. The selectivities for CH_4 and C_2H_6 first increased and then decreased with increasing Ag loading. By comparing the activity of the catalysts with various Ag loadings, 12.5 wt.% Ag was considered to be the optimum value because it provided the highest C_2H_4O selectivity and yield with relatively low CO and CO_2 selectivities.

Figure 6d shows the effect of silver loading on the power consumption for ethylene conversion and ethylene oxide production. The results show that the power consumption per molecule of C_2H_4 converted was much lower than the power consumption per molecule of C_2H_4O produced. With increasing the silver loading, the power consumption per molecule of C_2H_4 converted or per molecule of C_2H_4O produced substantially decreased and reached the minimum at a Ag loading of 12.5 wt.%. Beyond this optimum Ag loading, the power consumption dramatically increased with further increasing the Ag loading. The increase in the power consumption at above the 15 wt.% Ag loading resulted from the increase in coke formation. The optimum Ag loading of 12.5 wt.% on (LSA)α-Al_2O_3 was selected for further investigation since it gave the highest ethylene oxide selectivity, the highest ethylene oxide yield, and the lowest power consumption. This optimum Ag loading was in good agreement with our previous study [10].

Effect of Applied Voltage

Based on the preliminary tests on the voltage range that could be applied to the studied system, the break-down voltage, or the lowest voltage (onset voltage), to generate plasma was found to be about 7 kV, and at an applied voltage higher than 15 kV, the plasma system became unstable due to a large amount of coke formation. Therefore, the reaction experiments were conducted in the voltage range of 7–15 kV in order to determine the effect of applied voltage. The effect of applied voltage on the C_2H_4 and O_2 conversions and the C_2H_4O yield is illustrated in Fig. 7a. The oxygen conversion and ethylene oxide yield tended to increase with increasing applied voltage in the range of 7–15 kV, whereas the ethylene conversion remained almost unchanged. One plausible explanation for the converted oxygen increase is that a higher voltage results in a higher generated current, as shown in Fig. 7b, leading to more available electrons that, in turn, increase an opportunity for collision with reactant molecules. Moreover, an increase in the O active species generated in the plasma zone results in their more opportunities to adsorb on the surface of the catalyst for further subsequent reactions, especially to yield the desired ethylene oxide product. In contrast, it was unexpected that C_2H_4 conversion remained nearly constant with increasing applied voltage. This indicates that the converted C_2H_4 species in the plasma zone may be recombined to form C_2H_4 as a secondary reaction in the catalytic zone. More discussion will be given in the next paragraph.

The effect of applied voltage on the selectivities for C_2H_4O, CO, CO_2, CH_4, C_2H_2, C_2H_6, and C_3H_8 is shown in Fig. 7c. The selectivity for C_2H_4O obviously increased, but only slightly for the CO_2 selectivity, with increasing applied voltage, in contrast to the selectivity for C_2H_2, whereas the selectivities for CH_4 and C_2H_6 first increased and then decreased. The selectivity for C_3H_8 remained almost unchanged in the studied range of voltage. When the applied voltage increased, corresponding to the increasing O active species as mentioned above, active hydrocarbon species are further oxidized to form CO and C_2H_4O on the surface of the catalyst, but CO is not further oxidized to CO_2, as confirmed by a sharp drop with increasing applied voltage from 13 to 15 kV. These results

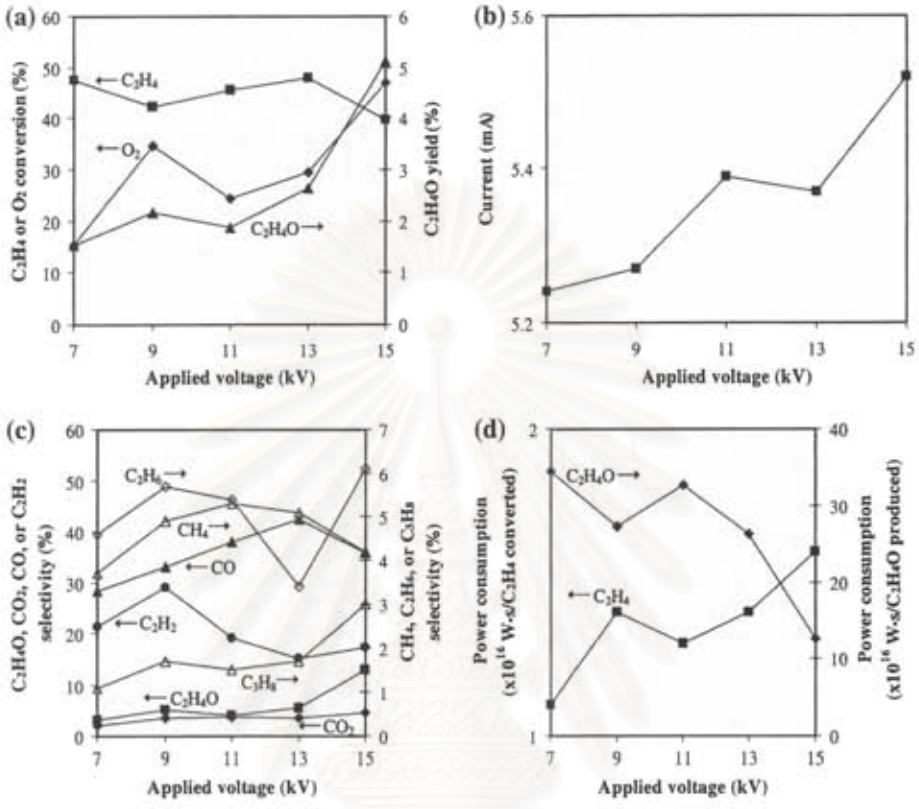

Fig. 7 (**a**) Ethylene and oxygen conversions and ethylene oxide yield, (**b**) generated current, (**c**) product selectivities, and (**d**) power consumptions as a function of applied voltage in the presence of 12.5 wt.% Ag on (LSA)α-Al_2O_3 (molar ratio of O_2/C_2H_4 = 1/1; feed flow rate = 50 ml/min; gap distance = 1 cm; and frequency = 500 Hz)

suggest that a higher number of O active species at a higher applied voltage is more favorable for C_2H_4O production than complete combustion. Interestingly, the amount of C_2H_2, a product from the C_2H_4 dehydrogenation in the plasma zone, tended to decrease with increasing applied voltage due to the simultaneous hydrogenation reaction of C_2H_2 on the Ag catalyst [35], which may compensate for the amount of C_2H_4 converted in the plasma zone, consequently resulting in almost unchanged C_2H_4 conversion.

Figure 7d shows the effect of applied voltage on the power consumption. With increasing applied voltage, the power consumption per molecule of converted C_2H_4 increased, whereas the power consumption per molecule of produced C_2H_4O substantially decreased. As shown above concerning the almost unchanged ethylene conversion, the rising average electron energy and the increasing number of electrons in the plasma zone could not enhance the conversion of ethylene, probably due to the C_2H_2 hydrogenation to reform C_2H_4 on the surface of the silver catalyst in the catalytic zone, resulting in an insignificant increase in energy consumption per molecule of C_2H_4 converted when increasing the applied voltage. In contrast, an increase in the selectivity for C_2H_4O was comparatively much higher when increasing the applied voltage, resulting in lower power consumption per molecule of produced C_2H_4O. From the results, the optimum voltage of 15 kV, which produced reasonably high C_2H_4 and O_2 conversions, the highest ethylene

oxide selectivity, and the highest ethylene oxide yield with the lowest power consumption per C_2H_4O molecule produced, was selected for further experiments.

Effect of Input Frequency

Input frequency is another important parameter greatly affecting the plasma characteristics in terms of stability and efficiency performance. In order to investigate the effect of input frequency, the studied plasma system was operated in the 300–800 Hz frequency range since a large amount of coke was found to deposit on the electrode surface at a frequency lower than 300 Hz, and the plasma could not exist at a frequency higher than 800 Hz. The effect of input frequency on the C_2H_4 and O_2 conversions and the C_2H_4O yield is illustrated in Fig. 8a. When the input frequency increased, the O_2 conversion decreased, whereas the C_2H_4 conversion remained almost constant. The explanation is that, as shown in Fig. 8b, a higher frequency results in lower current, which corresponds to the reduction of the number of electrons generated. Consequently, the opportunity for collision between electrons and O_2 or C_2H_4 molecules declines with decreasing current. Therefore, it was expected that the conversions of both C_2H_4 and O_2, and the C_2H_4O yield, should decrease with increasing input frequency; however, the conversion of C_2H_4 did not follow this expectation, which is similar to the case of increasing applied voltage. As mentioned

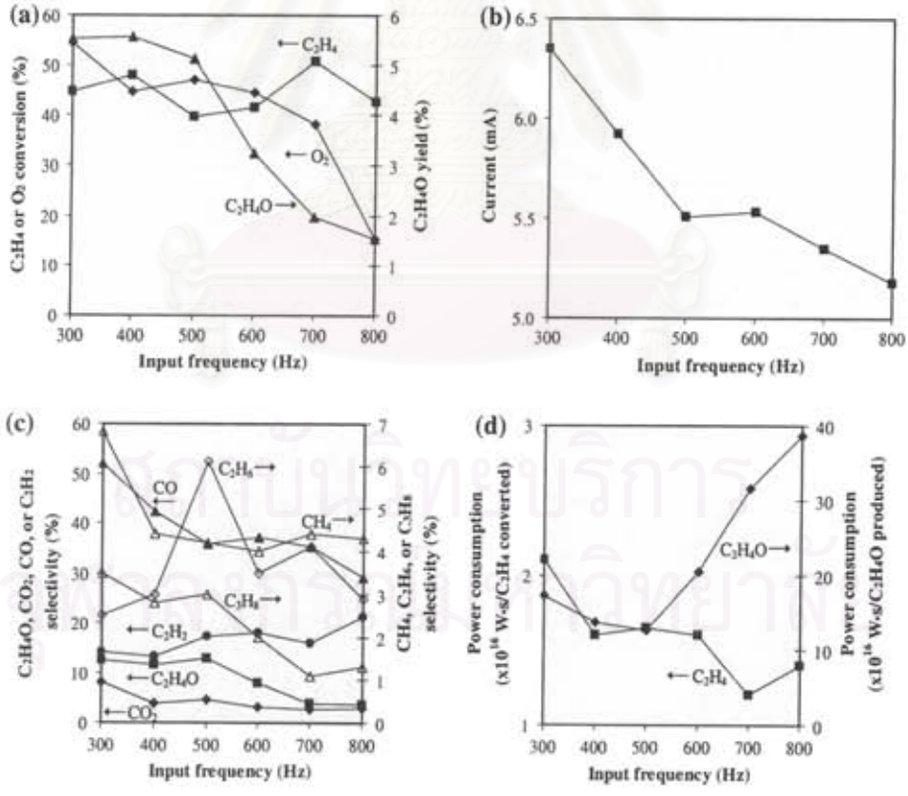

Fig. 8 (**a**) Ethylene and oxygen conversions and ethylene oxide yield, (**b**) generated current, (**c**) product selectivities, and (**d**) power consumptions as a function of input frequency in the presence of 12.5 wt.% Ag on (LSA)α-Al_2O_3 (molar ratio of O_2/C_2H_4 = 1/1; feed flow rate = 50 ml/min; gap distance = 1 cm; and applied voltage = 15 kV)

earlier, the invariant conversion of C_2H_4 is the trade off between the C_2H_4 dehydrogenation in the plasma zone and the C_2H_2 hydrogenation on the surface of the silver catalyst in the catalytic zone. Moreover, in the frequency range of 300–500 Hz, the C_2H_4O yield was found to remain almost unchanged, but beyond 500 Hz, it significantly decreased, probably due to the dramatic decrease in O_2 conversion.

The effect of input frequency on the product selectivities is shown in Fig. 8c. The selectivity for C_2H_4O remained nearly unchanged when the frequency was varied in the range of 300–500 Hz. Beyond 500 Hz, the selectivity decreased substantially with increasing frequency. Since the decrease in the input frequency from 800 to 500 Hz results in increased current, there are accordingly more O active species available to adsorb on the surface of the silver catalyst for the epoxidation reaction, leading to the higher selectivities for all products, including C_2H_4O. At a frequency lower than 500 Hz, the selectivity for C_2H_4O did not further increase with decreasing frequency, despite a higher amount of generated electrons, because of the coke formation. The selectivities for CO and CO_2 also tended to increase with decreasing input frequency. This is because more O active species at lower input frequency could lead to the increase in the selectivities for CO and CO_2. Therefore, an input frequency of 500 Hz was considered to be a potentially optimum condition, exhibiting reasonably high C_2H_4O selectivity with relatively low CO and CO_2 concentrations.

The effect of frequency on the power consumption to break down each C_2H_4 molecule or to create each C_2H_4O molecule is shown in Fig. 8d. The result shows that the power consumption per C_2H_4 molecule converted tended to gradually decline with increasing input frequency. Interestingly, the power consumption to create each C_2H_4O molecule decreased with increasing the input frequency up to 500 Hz; beyond this frequency, the power consumption dramatically increased. This is because a higher frequency gives a lower current, resulting in lowering the number of electrons to initiate the plasma reactions. At a frequency lower than 500 Hz, both power consumptions increased considerably with decreasing frequency. This is because the coke formation simply decreases the power efficiency. Based upon a relatively high ethylene oxide selectivity and ethylene oxide yield, as well as the lowest power consumption per molecule of ethylene oxide produced, an optimum input frequency of 500 Hz was selected for further experiments.

Effect of Molar Ratio of O_2/C_2H_4

To determine the influence of the feed gas composition on the ethylene epoxidation reaction under a corona discharge environment, the feed O_2/C_2H_4 molar ratio was varied in the range of 1/1 to 5/1, while the applied voltage and input frequency were kept constant at 15 kV and 500 Hz, respectively. An increase in the O_2/C_2H_4 molar ratio significantly enhanced only the C_2H_4 conversion, while the O_2 conversion increased and then decreased with further increasing the molar ratio higher than 3/1, as shown in Fig. 9a. The explanation is that an increase in the molar ratio of O_2/C_2H_4 results in having more O_2 available to react with ethylene molecules, leading to higher C_2H_4 conversion. Interestingly, the maximum conversion of O_2 was found to approximately be at the molar ratio of 3/1, which is the theoretical ratio for the C_2H_4 complete combustion. When considering the C_2H_4O yield, as also shown in Fig. 9a, it was interestingly found to drastically decrease with increasing the molar ratio from 1/1 to 2/1; and beyond the molar ratio of 2/1, the yield tended to slightly decrease to almost zero at the molar ratio of 5/1.

The effect of O_2/C_2H_4 molar ratio on the product selectivities is shown in Fig. 9b. In this corona discharge system, the selectivities for C_2H_4O, C_2H_2, C_2H_6, and C_3H_8

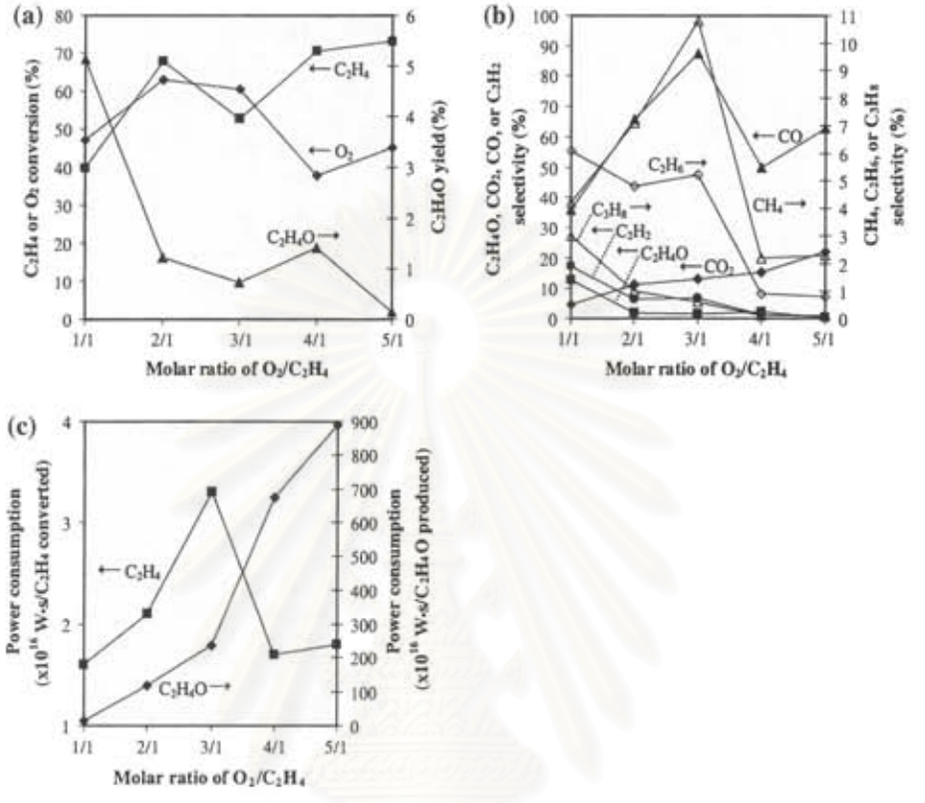

Fig. 9 (**a**) Ethylene and oxygen conversions and ethylene oxide yield, (**b**) product selectivities, and (**c**) power consumptions as a function of molar ratio of O_2/C_2H_4 in the presence of 12.5 wt.% Ag on (LSA)α-Al_2O_3 (feed flow rate = 50 ml/min; gap distance = 1 cm; applied voltage = 15 kV; and input frequency = 500 Hz)

decreased, but, in contrast, the selectivity for CO_2 increased with increasing O_2/C_2H_4 molar ratio. Interestingly, the selectivities for CO and CH_4 increased up to the O_2/C_2H_4 molar ratio of 3/1; however, beyond this ratio, their selectivities rapidly declined. At the O_2/C_2H_4 molar ratio of 3/1, O_2 was contributed to form the highest amount of CO. At a molar ratio higher than 3/1, known as an excess O_2 condition, CO is further oxidized to form CO_2, as confirmed by an increase in the CO_2 selectivity. Moreover, at an O_2/C_2H_4 molar ratio of 5/1, the selectivity for C_2H_4O reached zero, suggesting that C_2H_4O can be formed under a deficient O_2 condition. The highest C_2H_4O selectivity was found at an O_2/C_2H_4 molar ratio of 1/1, which is in good agreement with our previous study [10].

Figure 9c shows the power consumption needed to convert ethylene and to produce ethylene oxide at different O_2/C_2H_4 molar ratios. The power consumption per molecule of converted ethylene reached a maximum at an O_2/C_2H_4 molar ratio of 3/1. At an O_2/C_2H_4 molar ratio higher than 3/1, the power consumption rapidly decreased. However, there was an extremely significant increase in the power consumption per molecule of produced ethylene oxide with increasing the O_2/C_2H_4 molar ratio, especially at a molar ratio of 5/1. An O_2/C_2H_4 molar ratio of 1/1 was selected for further experiments because it provided the highest ethylene oxide selectivity, the highest ethylene oxide yield, and the lowest power consumption, in spite of having the lowest ethylene conversion.

Effect of Feed Flow Rate

The feed flow rate has a significant effect on the residence time of gas molecules within both the plasma and catalytic zones, affecting the performance of the plasma system. The experiments were performed by varying the feed flow rates from 50 to 150 ml/min at an O_2/C_2H_4 molar ratio of 1/1. The optimum applied voltage of 15 kV and the input frequency of 500 Hz were still applied to control the plasma system. Figure 10a illustrates the influence of the feed flow rate on the C_2H_4 and O_2 conversions and the C_2H_4O yield. The conversions of C_2H_4 and O_2 and the C_2H_4O yield decreased almost linearly with increasing feed flow rate from 50 to 150 ml/min, corresponding to decreasing the residence time from 0.6 to 0.2 s. An increase in the feed flow rate reduces the gas residence time in the reaction zone, resulting in a shorter contact time for ethylene and oxygen molecules to collide with electrons. As a result, a reduction in the feed flow rate enhanced the conversions of both C_2H_4 and O_2. The feed flow rate dependence for product selectivities is depicted in Fig. 10b. It is apparent that the selectivities for C_2H_4O, CO, CO_2, and other by-products tended to decrease with increasing feed flow rate. As explained above, this is because a higher feed flow rate reduces the opportunity for collision between electrons and reactant/intermediate molecules, as well as subsequent secondary reactions.

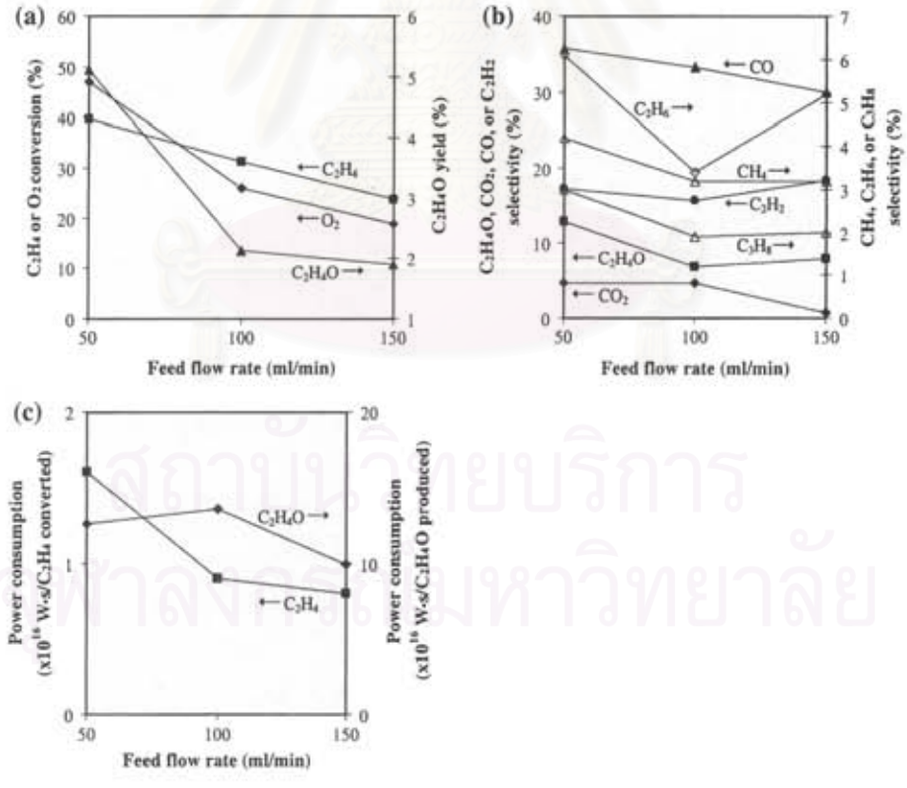

Fig. 10 (**a**) Ethylene and oxygen conversions and ethylene oxide yield, (**b**) product selectivities, and (**c**) power consumptions as a function of feed flow rate in the presence of 12.5 wt.% Ag on (LSA)α-Al_2O_3 (molar ratio of O_2/C_2H_4 = 1/1; gap distance = 1 cm; applied voltage = 15 kV; and input frequency = 500 Hz)

Figure 10c shows the effect of feed flow rate on the power consumption. Even though the power consumption per molecule of converted ethylene and per molecule of produced ethylene oxide slightly decreased when increasing feed flow rate, a lower feed flow rate could provide much higher reactant conversions and desired ethylene oxide selectivity. This is possibly because the power consumption per molecule of produced ethylene oxide at different feed flow rates is not varied much in the studied range, and its change is relatively small compared to those for all previous operating parameters.

From all experimental results obtained above, it was found that the ethylene epoxidation preferably occurred in the combined catalytic and corona discharge plasma system using Ag/(LSA)α-Al_2O_3 as a catalyst under a deficient O_2 condition with an O_2/C_2H_4 molar ratio of 1/1, as compared with the sole plasma system. The chemistry of the combined catalytic and plasma system is considerably complicated, and further investigation is needed to obtain a better understanding of the interaction between plasma and catalysts on simultaneously occurring chemical reactions including ethylene epoxidation. Based on the current knowledge, for the corona discharge system without the catalyst, various oxygen and hydrocarbon active species can be mostly generated by electron collision. The oxygen active species can mainly react with ethylene molecules/radicals in the bulk gas phase to form ethylene oxide. When the combined catalytic and corona discharge is used, the ethylene oxide can be additionally produced by the partial oxidation of ethylene molecule with oxygen molecularly adsorbed at the catalyst surface [10]. Therefore, the ethylene oxide formed in the combined system can be plausibly produced via the combination of gaseous discharge mechanism and catalytic surface chemistry.

Durability of Catalyst

To study the durability of the 12.5 wt.% Ag/(LSA)α-Al_2O_3 catalyst, the activity test was performed in two consecutive runs without any intermediate treatment. The studied plasma reactor packed with the catalyst was operated about 3 h for each run to reach the steady state. Figure 11 shows the comparison of the process performance of the two consecutive runs under the optimum conditions. The results show that the process performance of the

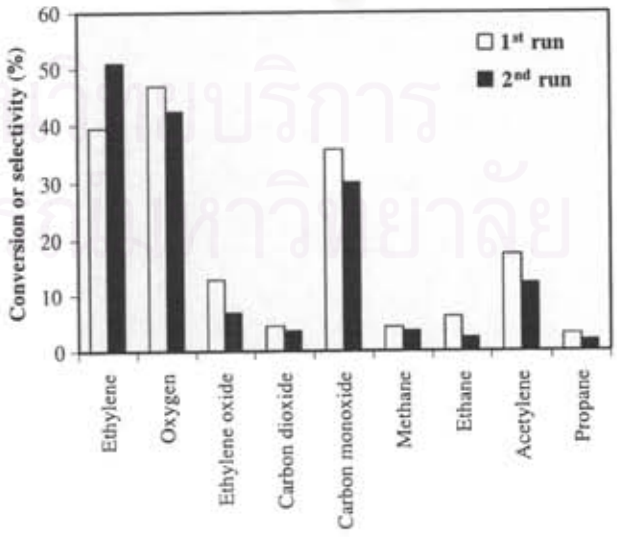

Fig. 11 Reactant conversions and product selectivities obtained by catalytic-plasma system at the optimum conditions for two consecutive runs (molar ratio of O_2/C_2H_4 = 1/1; feed flow rate = 50 ml/min; gap distance = 1 cm; frequency = 500 Hz; and voltage = 15 kV)

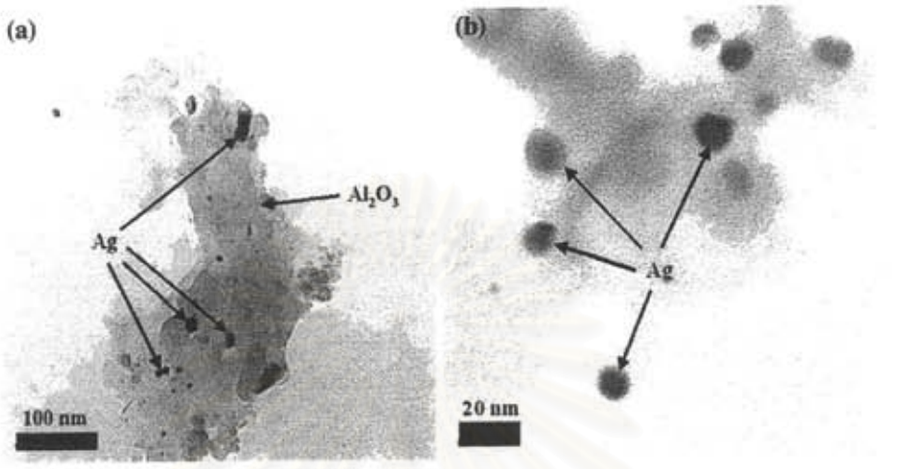

Fig. 12 TEM micrographs of spent 12.5 wt.% Ag/(LSA)α-Al_2O_3 at (**a**) low magnification and (**b**) high magnification

second run was lower than that of the first run in terms of the oxygen conversion and all product selectivities except the ethylene conversion. This lower activity could possibly be due to the coke formation on the spent catalyst, observed by TPO, as mentioned previously, as well as the Ag agglomeration verified by the TEM micrographs, as shown in Fig. 12. When comparing the TEM micrographs of the fresh catalyst (Fig. 4) and of the spent catalyst (Fig. 12), the mean particle size of Ag increased from 9.5 to 15 nm after the activity experiment. The Ag agglomeration on the catalyst surface is believed to result from the high energy intensity of the corona discharge used in this study. For non-thermal AC plasma, the bulk gas temperature is comparatively low; however, the energetic electrons may have energy ranging from 1 to 10 eV, which corresponds to extremely high temperatures of about 10,000 to 100,000 K [12]. Therefore, the catalyst surface has high probability to be collided intermittently with these high-temperature electrons, causing the increase in temperature on scattering micro-sized spots in a very short period throughout the catalyst surface and subsequently resulting in the Ag agglomeration. The measured temperature of the bulk gas was low in the range of 100–200°C, whereas the temperature of these aforementioned spots was expected to be significantly higher. In our future study, a dielectric barrier discharge (DBD), which can produce microdischarge with much lower energy intensity, will also be tested for the ethylene epoxidation reaction without causing the sintering effect of Ag nanoparticles.

Conclusions

In this work, the epoxidation reaction of ethylene under AC low-temperature corona discharge was investigated in the presence of catalysts; Ag/(LSA)α-Al_2O_3, Ag/(HSA)γ-Al_2O_3, and Au–Ag/(HSA)γ-Al_2O_3. In comparisons among the studied catalysts, Ag/(LSA)α-Al_2O_3 was experimentally found to be the best catalyst to provide the highest ethylene oxide selectivity. The optimum Ag loading on the (LSA)α-Al_2O_3 was found to be 12.5 wt.%, at which a maximum ethylene oxide selectivity of 12.9% was obtained at the optimum applied voltage and input frequency of 15 kV and 500 Hz, respectively. Under

these optimum conditions, the power consumption was found to be 12.6×10^{-16} W s/molecule of ethylene oxide produced. In addition, decreases in the oxygen-to-ethylene molar ratio and feed flow rate were also experimentally found to provide better ethylene epoxidation activity.

Acknowledgments The authors would like to gratefully acknowledge the Ratchadapisek Somphot Endowment Fund (Contract/Grant No. R019-2550), Chulalongkorn University, Thailand, the Research Unit of Petrochemical and Environmental Catalysis under the Ratchadapisek Somphot Endowment Fund, Chulalongkorn University, Thailand, and the National Excellence Center for Petroleum, Petrochemicals, and Advanced Materials under the Ministry of Education, Thailand, for their partial financial support and for providing all research facilities.

References

1. http://www.osha.gov/OshDoc/data_General_Facts/ethylene-oxide-factsheet.pdf. Accessed 1 April 2008
2. http://www.dow.com/ethyleneoxide/news/20050405b.htm. Accessed 1 April 2008
3. Law GH, Chitwood HC (1942) US Patent 2,279,470
4. Campbell CT, Paffett MT (1984) Appl Surf Sci 19:28–42
5. Tan SA, Grant RB, Lambert RM (1986) J Catal 100:383–391
6. Yeung KL, Gavriilidis A, Varma A, Bhasin MM (1998) J Catal 174:1–12
7. Iwakura G (1985) Japan Patent 63-126552
8. Bhasin MM (1988) US Patent 4,908,343
9. Rojluechai S, Chavadej S, Schwank JW, Meeyoo V (2007) Catal Commun 8:57–64
10. Rojluechai S, Chavadej S, Schwank JW, Meeyoo V (2006) J Chem Eng Jpn 39:321–326
11. Eliasson B, Kogelschatz U (1991) IEEE Trans Plasma Sci 19:1063–1077
12. Rosacha LA, Anderson GK, Bechtold LA, Coogan JJ, Heck HG, Kang M, McCulla WH, Tennant RA, Wantuck PJ (1993) NATO ASI Series, Part B 34
13. Suhr H (1983) Plasma Chem Plasma Process 3:1–61
14. Patiño P, Ropero M, Iacocca D (1995) Plasma Chem Plasma Process 16:563–575
15. Chang JS, Lawless PA, Yamamoto T (1991) IEEE Trans Plasma Sci 19:1152–1166
16. Yan K, Hui H, Cui M, Miao J, Wu X, Bao C, Li R (1998) J Electrostat 44:17–39
17. Bröer S, Hammer T (2000) Appl Catal B: Environ 28:101–111
18. Marafee A, Liu C, Xu G, Mallinson R, Lobban L (1997) Ind Eng Chem Res 36:632–637
19. Liu C, Marafee A, Mallinson R, Lobban L (1997) Appl Catal A: Gen 164:21–33
20. Liu C, Mallinson R, Lobban L (1998) J Catal 179:326–334
21. Liu C, Mallinson R, Lobban L (1999) Appl Catal A: Gen 178:17–27
22. Francke KP, Miessner H, Rudolph R (2000) Plasma Chem Plasma Process 20:393–403
23. Wen Y, Jiang X (2001) Plasma Chem Plasma Process 21:665–678
24. Li D, Yakushiji D, Kanazawa S, Ohkubo T, Nomoto Y (2002) J Electrostat 55:311–319
25. Sobacchi MG, Saveliev AV, Fridman AA, Kennedy LA, Ahmed S, Krause T (2002) Int J Hydrogen Energ 27:635–642
26. Gordon CL, Lobban LL, Mallinson RG (2003) Catal Today 84:51–57
27. Dors M, Mizeraczyk J (2004) Catal Today 89:127–133
28. Kušić H, Koprivanac N, Locke BR (2005) J Hazard Mater 125:190–200
29. Li MW, Liu CP, Tian YL, Xu GH, Zhang FC, Wang YQ (2006) Energ Fuel 20:1033–1038
30. Van Durme J, Dewulf J, Sysmans W, Leys C, Van Langenhove H (2007) Appl Catal B: Environ 74:161–169
31. Chavadej S, Kiatubolpaiboon W, Rangsunvigit P, Sreethawong T, Mol J (2007) Catal A: Chem 263:128–136
32. Chavadej S, Saktrakool K, Rangsunvigit P, Lobban LL, Sreethawong T (2007) Chem Eng J 132:345–353
33. Linic S, Jankowiak JT, Barteau MA (2004) J Catal 224:489–493
34. Geenen PV, Boss HJ, Pott GT (1982) J Catal 77:499–510
35. Sárkány A, Révay Zs (2003) Appl Catal A: Gen 243:347–355
36. Malik MA, Malik SA (1999) Platinum Metals Rev 43:109–113

G Model
CEJ-6489; No. of Pages 8

Chemical Engineering Journal xxx (2009) xxx–xxx

Contents lists available at ScienceDirect

Chemical Engineering Journal

journal homepage: www.elsevier.com/locate/cej

Ethylene epoxidation in low-temperature AC corona discharge over Ag catalyst: Effect of promoter

Thammanoon Sreethawong[a,b], Thanapoom Suwannabart[a], Sumaeth Chavadej[a,b,*]

[a] The Petroleum and Petrochemical College, Chulalongkorn University, Soi Chula 12, Phyathai Road, Pathumwan, Bangkok 10330, Thailand
[b] Center for Petroleum, Petrochemicals, and Advanced Materials, Chulalongkorn University, Bangkok 10330, Thailand

ARTICLE INFO

Article history:
Received 19 May 2009
Received in revised form 29 July 2009
Accepted 31 July 2009

Keywords:
Epoxidation
Ethylene oxide
Corona discharge
Ag catalyst
Promoter

ABSTRACT

In this work, the epoxidation of ethylene using a low-temperature corona discharge system was investigated with various reported catalytically active catalysts: Ag/α-Al_2O_3, Cs–Ag/α-Al_2O_3, Cu–Ag/α-Al_2O_3, and Au–Ag/α-Al_2O_3. It was experimentally found that the investigated catalysts could improve the ethylene conversion and the ethylene oxide (EO) yield and selectivity for the corona discharge system, particularly 1 wt.% Cs–12.5 wt.% Ag/α-Al_2O_3 and 0.2 wt.% Au–12.5 wt.% Ag/α-Al_2O_3. The power consumption per EO molecule produced in the corona discharge system, combined with the superior bimetallic catalysts, was much lower than that of the sole corona discharge system and that of the corona discharge system combined with the monometallic Ag catalyst.

1. Introduction

Ethylene epoxidation is an important process in the petrochemical industry for producing a versatile ethylene oxide (C_2H_4O, EO) molecule. The most widely used technique for ethylene oxide production is catalytic processes using silver-based catalysts. Silver catalysts supported on low-surface area α-alumina (Ag/(LSA)α-Al_2O_3) provide high EO selectivity [1–4]. Some previous research has revealed that alkali and transition metals, especially cesium (Cs) [5–11], copper (Cu) [12–15], and gold (Au) [16–21], also provide the improvement of the EO selectivity. However, the conventional catalytic processes are generally facilitated by a high temperature operation, implying high energy consumption. The normal temperature used for such processes is at least 200 °C. In addition, the use of high temperatures for ethylene epoxidation inevitably causes operational problems, i.e., catalyst deactivation, catalyst regeneration, and catalyst replacement. To develop and apply a new low-temperature plasma technique for ethylene epoxidation would be attractive for lowering the energy consumption and alleviating the catalytic problems.

Non-thermal plasma is considered to be an interesting potential replacement for the conventional catalytic processes for ethylene epoxidation. It is one kind of electric gas discharge, in which electrons gain enough energy from an external applied voltage to overcome the potential barrier of metal surface electrodes [22]. Subsequently, these energetic electrons can move from one electrode to the other and instantaneously collide with gaseous molecules in the plasma zone to generate highly active atoms, molecules, and radicals by excitation and dissociation reactions. The excited and dissociated species can rapidly bring about the formation of new chemical species. A great advantage of non-thermal plasma is that the generated electrons have a high temperature of approximately 10^4–10^5 K, while the bulk gas still has a much lower temperature, close to room temperature [23–25], leading to a lower energy requirement as compared to the conventional catalytic processes. Moreover, the low-temperature operation of non-thermal plasma is expected to enable its combined use with a catalyst, without the aforementioned catalytic problems.

In our previous work, ethylene epoxidation using a low-temperature corona discharge system was, for the first time, studied both in the absence and in the presence of various powder catalysts, including Ag/(LSA)α-Al_2O_3, Ag/(high-surface area, HSA)γ-Al_2O_3, Au–Ag/(HSA)γ-Al_2O_3, and Au/TiO_2 [26]. The results showed that the combination of corona discharge and the reported highly active Ag/(LSA)α-Al_2O_3 catalyst with an optimum Ag loading of 12.5 wt.% offered the highest EO selectivity. Furthermore, ethylene epoxidation was investigated using a low-temperature dielectric barrier discharge (DBD) system [27]. Because the large-surface area parallel plate electrodes of the DBD reactor (as compared to that of the pin and circular plate electrodes of corona discharge reactors) led to a difficulty in packing the powder catalysts between them, the DBD system was only operated without

* Corresponding author at: The Petroleum and Petrochemical College, Chulalongkorn University, Soi Chula 12, Phyathai Road, Pathumwan, Bangkok 10330, Thailand. Tel.: +66 2 218 4139; fax: +66 2 218 4139.
E-mail address: sumaeth.c@chula.ac.th (S. Chavadej).

1385-8947/$ – see front matter © 2009 Elsevier B.V. All rights reserved.
doi:10.1016/j.cej.2009.07.056

catalysts. However, it can be concluded from the experimental results of the previous work that both low-temperature corona discharge and DBD systems are highly potential candidates to be used for ethylene epoxidation. In this extended work, the effect of promoter (Cs, Cu, and Au) on the ethylene epoxidation activity over a 12.5 wt.% Ag/(LSA)α-Al_2O_3 catalyst using a low-temperature corona discharge system was investigated.

2. Experimental

2.1. Materials and reactant gases

In this work, the support used was (LSA)α-Al_2O_3 (A.C.S. Xenon). Silver nitrate ($AgNO_3$, Carlo Erba), cesium nitrate ($CsNO_3$, Merck), copper nitrate trihydrate ($Cu(NO_3)_2{\cdot}3H_2O$, Merck), and hydrogen tetrachloroaurate trihydrate ($HAuCl_4{\cdot}3H_2O$, Alfa Aesar) were employed as silver, cesium, copper, and gold catalyst precursors, respectively. All chemicals were used as received without further purification. For the reactant gases, 99.995% helium (high purity grade), 40% ethylene balanced with helium, and 97% oxygen balanced with helium were used and were supplied by Thai Industrial Gas (Public) Co., Ltd.

2.2. Catalyst preparation procedure

All bimetallic catalysts were prepared by the sequential incipient wetness impregnation method using (LSA)α-Al_2O_3 as the catalyst support. First, a Ag catalyst on the (LSA)α-Al_2O_3 support was prepared by using a $AgNO_3$ aqueous solution at a nominal loading of 12.5 wt.% Ag, which was found to provide the maximum EO selectivity with relatively high ethylene and oxygen conversions [26]. After the mixture had been dried at 110 °C for 2 h, it was sequentially impregnated with an appropriate amount of a Cs, Cu, or Au promoter by using an aqueous solution of $CsNO_3$, $Cu(NO_3)_2{\cdot}3H_2O$, or $HAuCl_4{\cdot}3H_2O$. For each bimetallic catalyst, i.e., Cs–Ag/(LSA)α-Al_2O_3, Cu–Ag/(LSA)α-Al_2O_3, and Au–Ag/(LSA)α-Al_2O_3, the loadings of Cs, Cu, or Au were 0.2 and 1 wt.% for each. After that, these impregnated catalysts were dried in air at 110 °C overnight and then calcined in air at 400 °C for 12 h. Finally, all the prepared catalysts were sieved in order to obtain the desired grain size range of 221–425 μm for the reaction activity experiments.

2.3. Catalyst characterization techniques

The specific surface areas of all prepared catalysts were determined by a surface area analyzer (Quantachrom, Autosorb-1) using nitrogen adsorption analysis. A catalyst sample was dried and outgassed under vacuum at 150 °C for 10 h to remove the humidity and any volatile components adsorbed on the catalyst surface before the analysis. The crystalline phases of the prepared catalysts were investigated by an X-ray diffractometer (XRD, Rigaku RINT-2200) equipped with a graphite monochromator, a Cu tube for generating CuKα radiation (λ = 1.5406 Å) at a voltage of 40 kV and a current of 30 mA, and a nickel filter used as the filter for Kβ removal. The catalyst sample was examined in the 2θ range of 30–60° at a scan-

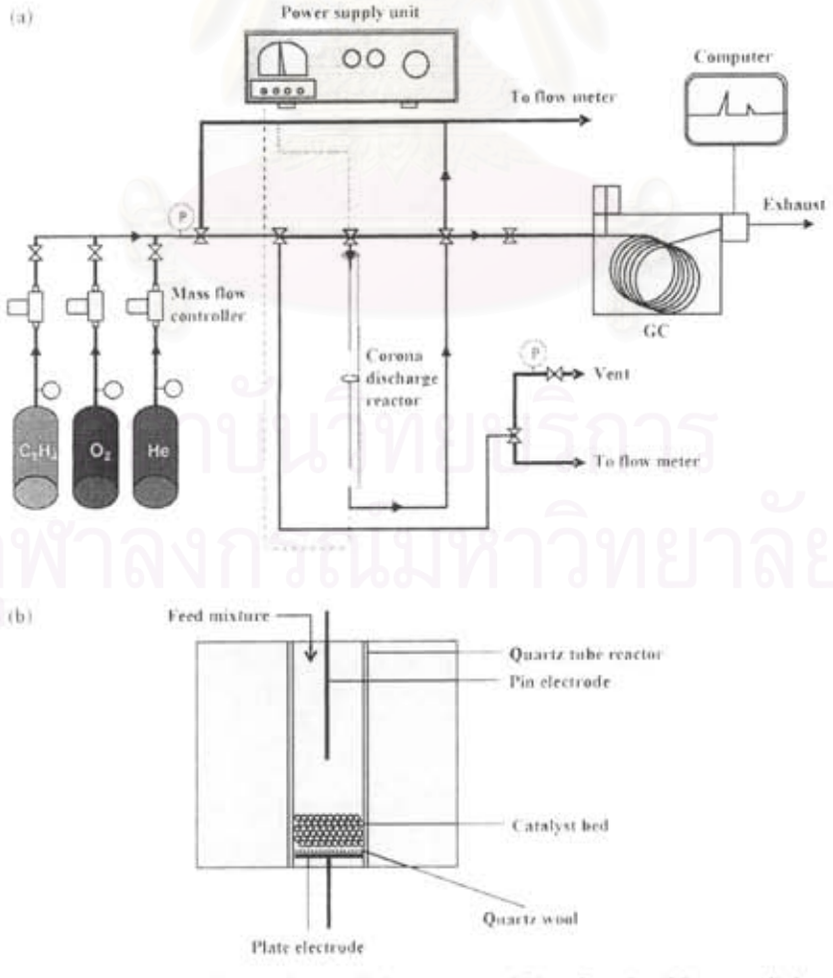

Fig. 1. (a) Schematic of experimental setup of corona discharge system and (b) configuration of the corona discharge reactor.

Please cite this article in press as: T. Sreethawong, et al., Ethylene epoxidation in low-temperature AC corona discharge over Ag catalyst: Effect of promoter, Chem. Eng. J. (2009), doi:10.1016/j.cej.2009.07.056

ning speed of 5°(2θ)/min. Transmission electron microscopy (TEM, JEOL 2000 CX) was employed for investigating the average particle size of the Ag particles on the prepared catalysts. The catalyst sample was ground into a fine powder and ultrasonically dispersed in ethanol. A small droplet of the suspension was placed on a copper grid, and the solvent was evaporated prior to loading the sample into the TEM. The TEM was operated at an accelerating voltage of 200 kV. Temperature-programmed oxidation (TPO) was employed to quantitatively investigate the coke deposition on the spent catalysts. The TPO analysis was performed at a continuous flow of O_2/He (ratio 2:1) with a total flow rate of 40 cm^3/min. A spent catalyst was placed in the quartz tube and was secured with packing quartz wool. The sample temperature was linearly increased to reach a maximum temperature of 850 °C in order to completely oxidize the carbon fraction of the deposited coke to CO_2. The effluent gas was passed through a methanator containing a Ni/Al_2O_3 catalyst to convert the CO_2 to methane at 400 °C. Subsequently, the produced methane was detected with a flame ionization detector (FID, SRI model 110). The area under the obtained curve was used to calculate the carbon content in the spent catalyst sample. In addition, the amount of coke deposited on the catalyst surface was also confirmed by the weight change of spent catalyst after the TPO analysis.

2.4. Reaction testing experiments

The ethylene epoxidation experiments were conducted in a corona discharge system, which was operated at ambient temperature and atmospheric pressure. The schematic of experimental setup of the corona discharge system and the configuration of the corona discharge reactor are shown in Fig. 1. The input power used to generate plasma was alternating current (AC) power, 200 V and 50 Hz, which was transmitted to a high voltage current via a power supply unit. The output voltage was adjusted by a function generator, whereas the sinusoidal wave signal was controlled and monitored by an oscilloscope. A quantity of 0.24 g of each studied catalyst was individually placed on the plate electrode and secured by a quartz wool layer. The base reaction conditions used for the comparative investigation were an O_2/C_2H_4 molar ratio of 1/1, a total feed gas flow rate of 50 cm^3/min, an applied voltage of 19 kV, an input frequency of 500 Hz, and an electrode gap distance of 10 mm. The flow rates of reactant gases (ethylene, oxygen, and helium) fed through the plasma reactor were controlled by a set of electronic mass flow controllers and transducers, supplied by SIERRA® Instrument Inc. A 7-μm in-line filter was placed upstream of each mass flow controller in order to trap any solid particles. A check valve was placed downstream of each mass flow controller to prevent any back flow of the reactant gases. All of the reactant gases were mixed inside a single line before being introduced into the plasma reactor. Prior to the reaction start-up, the feed gas mixture was first introduced into the plasma system without turning on the power supply unit. After the composition of outlet gas was invariant with time, it was turned on. The outlet of the reactor was either vented to the atmosphere via a rubber tube exhaust or was connected to an on-line gas chromatograph (GC, PerkinElmer, AutoSystem) for analysis of the product gases. The moisture in the product gas stream was removed by a water trap filter before entering a heated stainless steel line to the on-line GC. The GC was equipped with both a thermal conductivity detector (TCD) and an FID. For the TCD channel, a packed column (Carboxen 1000) was used for separating the product gases, which were H_2, O_2, CO, CO_2, and C_2H_4. For the FID channel, a capillary column (OV-Plot U) was used for the analysis of EO and other by-product gases, i.e., CH_4, C_2H_2, C_2H_6, and C_3H_8. However, there were some unknown products with small quantities produced during the reaction, which could not be analyzed. The composition of the product gas stream was determined by the GC every 20 min. After the system reached steady state, an analysis of the outlet gas composition was taken at least a few times. The experimental data taken under steady state conditions were averaged, and these averages were used to evaluate the performance of the plasma system.

To evaluate the process performance, the conversions of C_2H_4 and O_2 and the selectivities for products, including EO, CO, CO_2, H_2, CH_4, C_2H_2, C_2H_6, and traces of C_3, were considered. The conversion of either C_2H_4 or O_2 is defined as:

$$\%\text{reactant conversion} = \frac{(\text{moles of reactant in} - \text{moles of reactant out})(100)}{(\text{moles of reactant in})}$$

The product selectivity is calculated from the following equation:

$$\%\text{product selectivity} = \frac{[(\text{number of C or H atom in product})(\text{moles of product produced})](100)}{(\text{number of C or H atom in } C_2H_4)(\text{moles of } C_2H_4 \text{ converted})}$$

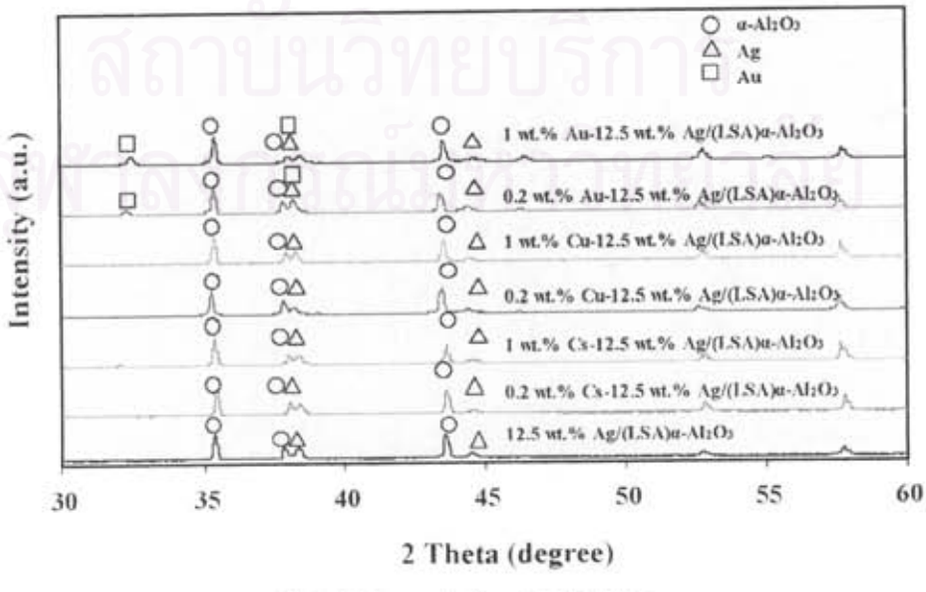

Fig. 2. XRD patterns of all investigated catalysts.

Please cite this article in press as: T. Sreethawong, et al., Ethylene epoxidation in low-temperature AC corona discharge over Ag catalyst: Effect of promoter, Chem. Eng. J. (2009), doi:10.1016/j.cej.2009.07.056

All the product selectivities, except H_2 selectivity, are calculated based on the numbers of C atom in C_2H_4 and product, and moles of C_2H_4 converted and product produced.

The EO yield is calculated from the following equation:

$$\%\text{EO yield} = \frac{(\%\ C_2H_4\text{conversion})\,(\%\text{EO selectivity})}{(100)}$$

To determine the energy efficiency of each plasma system, the specific power consumption is calculated in a unit of Ws per molecule of converted C_2H_4 or per molecule of produced EO using the following equation:

$$\text{specific power consumption} = \frac{(P)(60)}{(N)(M)}$$

where P, Power (W); N, Avogadro's number = 6.02×10^{23} molecules/mol, and M, rate of converted C_2H_4 molecules in the feed or the rate of produced EO molecules (mol/min).

Table 1
Specific surface area and amount of coke formed for all investigated catalysts used for the corona discharge system.

Catalyst	Specific surface area (m^2/g)	Coke formation (%)
12.5 wt.% Ag/(LSA)α-Al_2O_3	0.28	0.26
0.2 wt.% Cs–12.5 wt.% Ag/(LSA)α-Al_2O_3	0.33	0.11
1 wt.% Cs–12.5 wt.% Ag/(LSA)α-Al_2O_3	0.44	0.16
0.2 wt.% Cu–12.5 wt.% Ag/(LSA)α-Al_2O_3	0.39	0.14
1 wt.% Cu–12.5 wt.% Ag/(LSA)α-Al_2O_3	0.74	0.22
0.2 wt.% Au–12.5 wt.% Ag/(LSA)α-Al_2O_3	0.33	0.75
1 wt.% Au–12.5 wt.% Ag/(LSA)α-Al_2O_3	0.42	1.07

3. Results and discussion

In this work, four types of catalysts – Ag/(LSA)α-Al_2O_3, Cs–Ag/(LSA)α-Al_2O_3, Cu–Ag/(LSA)α-Al_2O_3, and Au–Ag/(LSA)α-Al_2O_3 – were used for investigating the ethylene epoxidation activity in the combined catalytic and corona discharge system.

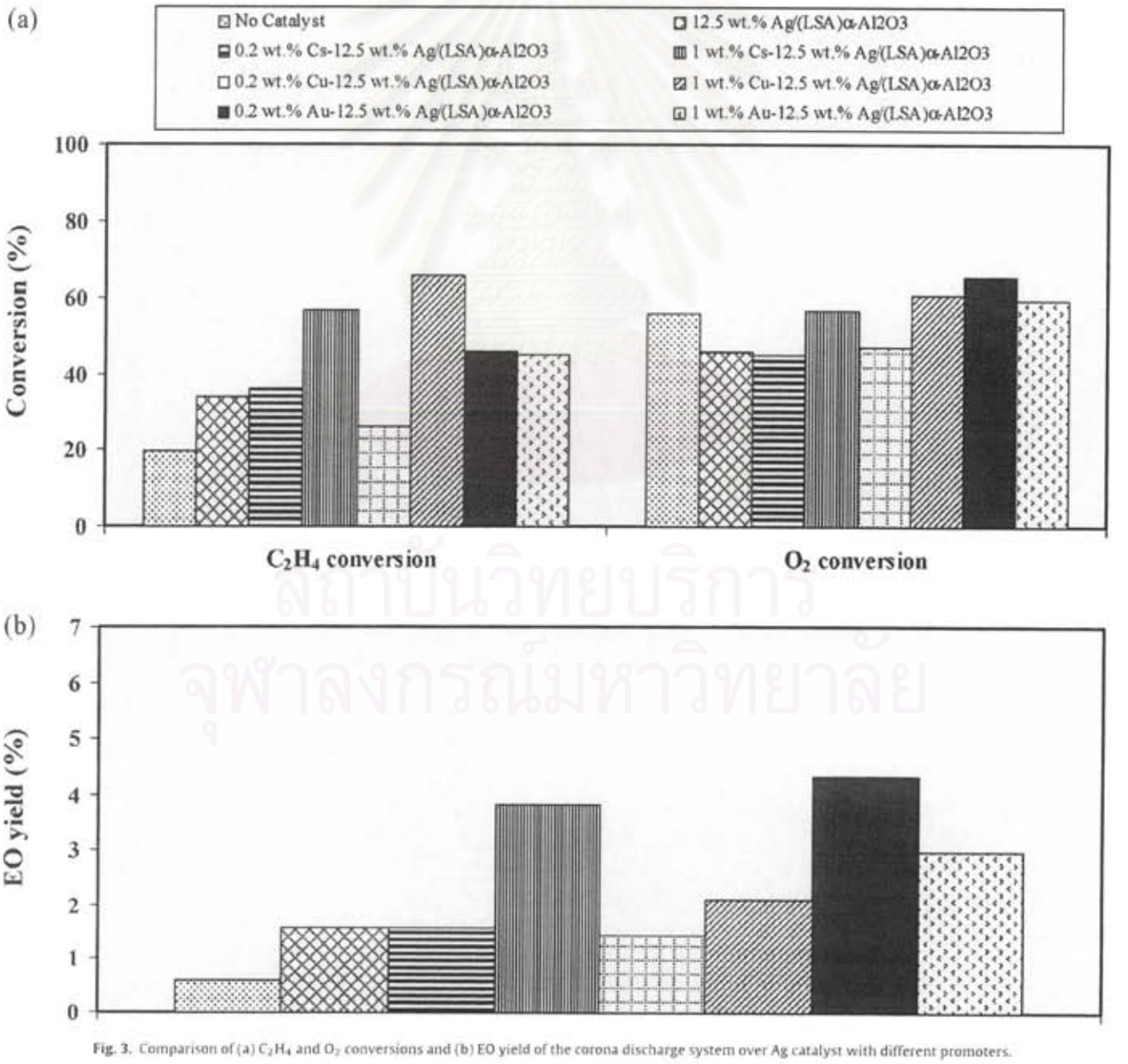

Fig. 3. Comparison of (a) C_2H_4 and O_2 conversions and (b) EO yield of the corona discharge system over Ag catalyst with different promoters.

Please cite this article in press as: T. Sreethawong, et al., Ethylene epoxidation in low-temperature AC corona discharge over Ag catalyst: Effect of promoter, Chem. Eng. J. (2009), doi:10.1016/j.cej.2009.07.056

The specific surface areas of all investigated Ag/(LSA)α-Al_2O_3-based catalysts are shown in Table 1. The results indicate that when the three, second metals (Cs, Cu, and Au) were sequentially loaded on the Ag/(LSA)α-Al_2O_3 catalyst, the specific surface areas of all bimetallic catalysts slightly increased. This implies that all the loaded second metals showed good dispersion on the Ag/(LSA)α-Al_2O_3 catalyst. Because of the insignificantly different specific surface areas of all the catalysts, it can be hypothesized that the specific surface area plays a less significant role than the property of the metals themselves on the epoxidation activity.

XRD patterns of all the studied catalysts were obtained (Fig. 2), and all of the bimetallic catalysts show the same XRD patterns as the monometallic Ag/(LSA)α-Al_2O_3 catalyst, mainly consisting of α-Al_2O_3 and Ag phases. For the Au–Ag/(LSA)α-Al_2O_3 catalyst, the peaks corresponding to the Au phase were clearly observed. For both the Cs–Ag/(LSA)α-Al_2O_3 and the Cu–Ag/(LSA)α-Al_2O_3 catalysts, however, there was no clear evidence of any peaks corresponding to Cs and Cu. This is possibly due to their light mass as compared to that of Au at the same wt.% loadings.

Under the plasma environment, the gas phase reactions induced by the discharge mainly contribute to the reactant conversions. In the corona discharge system used in this work, most of the discharge energy is used to produce and accelerate electrons, which instantaneously react with gas molecules (C_2H_4 and O_2) to generate several highly active species (metastable radicals and ions) [26]. It was experimentally found that the C_2H_4 and O_2 conversions and the EO yield were significantly enhanced by using all the bimetallic catalysts with a suitable second metal loading, as compared to the monometallic Ag catalyst and the system without catalyst (Fig. 3). Among the investigated catalysts, the 1 wt.% Cs–12.5 wt.%

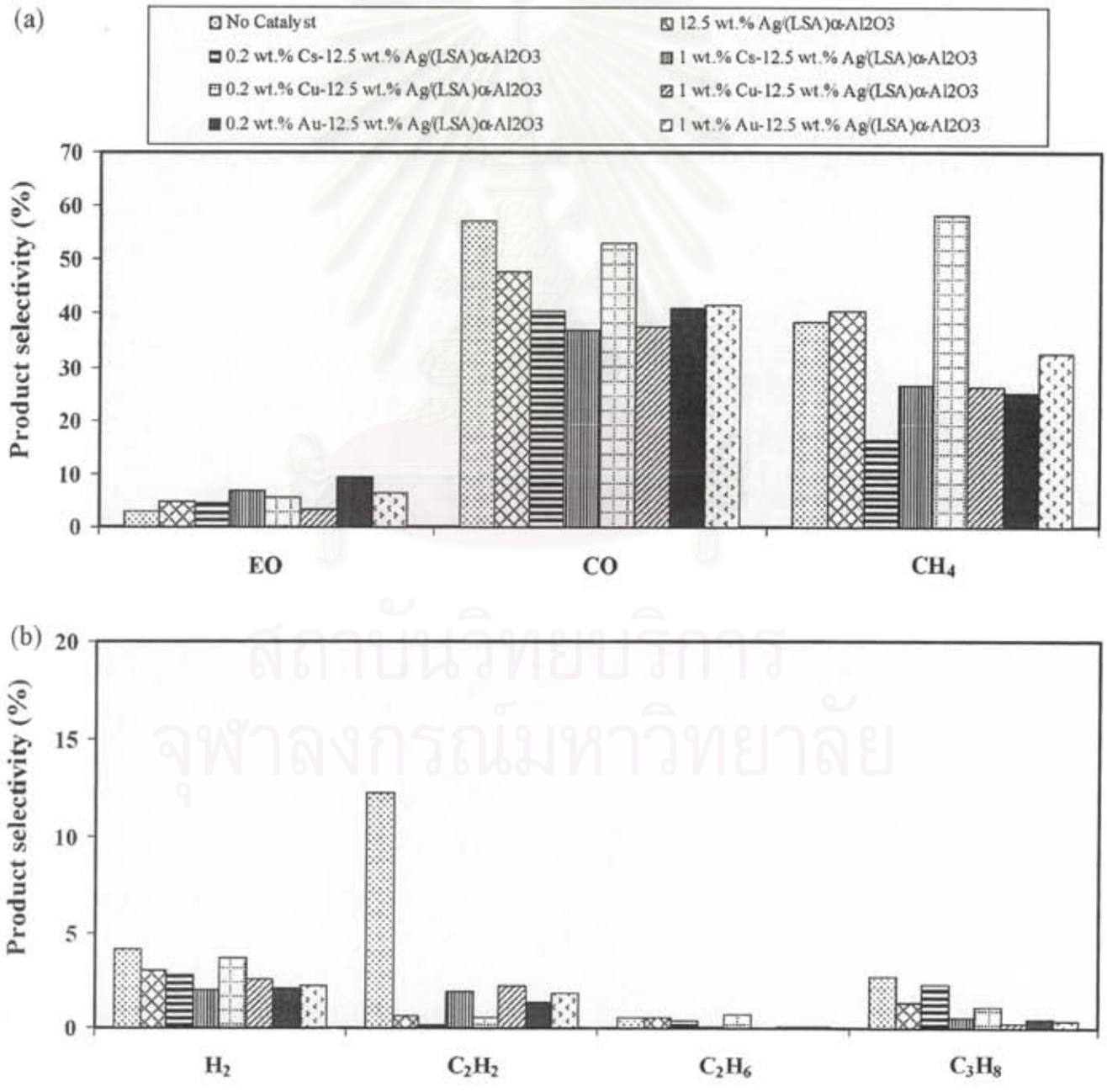

Fig. 4. Comparison of product selectivities for (a) EO, CO, and CH_4, and (b) H_2, C_2H_2, C_2H_6, and C_3H_8 of the corona discharge system over Ag catalyst with different promoters.

Please cite this article in press as: T. Sreethawong, et al., Ethylene epoxidation in low-temperature AC corona discharge over Ag catalyst: Effect of promoter, Chem. Eng. J. (2009), doi:10.1016/j.cej.2009.07.056

Ag/(LSA)α-Al_2O_3 and the 0.2 wt.% Au–12.5 wt.% Ag/(LSA)α-Al_2O_3 catalysts provided a comparatively high EO yield. The use of Cu as the promoter, however, slightly increased the EO yield only at the high loading of 1 wt.%, while 0.2 wt.% Cu showed no improvement of the EO yield as compared to the monometallic Ag catalyst.

The main products of the studied plasma system with different bimetallic catalysts were EO, CO, CH_4, and H_2 with trace amounts of C_2H_2, C_2H_6, and C_3H_8 (Fig. 4). No CO_2 was observed from ethylene epoxidation in the studied corona discharge system. It can be seen that the type of catalysts significantly affected the selectivities for the main products. Particularly, the bimetallic 1 wt.% Cs–12.5 wt.% Ag/(LSA)α-Al_2O_3 and the 0.2 wt.% Au–12.5 wt.% Ag/(LSA)α-Al_2O_3 catalysts combined with plasma were found to be favorable for the ethylene epoxidation reaction, compared to the other catalysts. Moreover, they provided a relatively low amount of CO, as well as low selectivities for H_2, C_2 products, and C_3H_8. From the results, it can be concluded that for the sole corona discharge system, both the EO selectivity and yield were relatively low because most reactions occur in the gas phase, and C_2H_4 is mostly split into CH_4 and is partially oxidized to CO. In the presence of the monometallic Ag catalyst, the C_2H_4 conversion and both the EO selectivity and yield greatly increased, compared to the sole corona discharge system; this is because the system provided the additional Ag active sites for molecular oxygen adsorption to consequently favor ethylene epoxidation [28]. The Cs promoter added on the Ag catalyst, moreover, neutralizes acid sites on the catalyst surface, which are active for the further isomerization and oxidation of EO [29], and adjusts the surface electron density to reduce the binding strength of EO to the catalyst surface, resulting in less oxidized product formation [30]. In addition, Cs plays a role in increasing the adsorption probability of oxygen on the Ag active sites [31]; whereas, the Au promoter affects the electronic properties of Ag by weakening the Ag–O bond strength, which, in turn, promotes ethylene epoxidation [19,28]. It was experimentally found that in the presence of small amounts of Au (lower than 0.54 wt.%) on the Ag catalyst, the interaction between the Au and Ag significantly enhanced the oxygen adsorption for the ethylene epoxidation; however, a higher Au addition (greater than 0.54 wt.%) caused the Au–Ag alloy formation, instead of Au–Ag bimetallic formation, which was proved to be disadvantageous for ethylene epoxidation [28]. It can also be seen from the present work, using the combined catalytic–corona discharge system, that a low Au addition of 0.2 wt.% showed much better epoxidation performance than a high Au addition of 1 wt.%, probably by a consequence of the Au–Ag bimetallic formation as aforementioned. In other words, when the Au addition increased from 0.2 (small amount) to 1 wt.% (sufficiently large amount), it can possibly form alloy with Ag (12.5 wt.%). This Au–Ag alloy formation negatively affected the epoxidation performance. Therefore, a suitable addition of each promoter should be used.

In general observation, it was found that the power consumptions per EO molecule produced and per C_2H_4 molecule converted were greatly reduced in the presence of all the studied catalysts (Fig. 5). The power consumption per EO molecule produced was much higher than that per C_2H_4 molecule converted. For a comparison among the promoters, both Cs and Au added on the Ag catalyst significantly helped reduce the power consumption per EO molecule produced, and the lowest power consumption per EO molecule produced was found with the 1 wt.% Cs–12.5 wt.% Ag/(LSA)α-Al_2O_3 and the 0.2 wt.% Au–12.5 wt.% Ag/(LSA)α-Al_2O_3 catalysts, which exhibited good epoxidation performance (Figs. 3 and 4).

After the plasma reaction testing experiments, the spent catalysts were analyzed to determine the amount of coke deposited on the catalyst surface (Table 1), and the Ag partcle size. It can be clearly seen in the table that there were, overall, extremely low amounts of coke formed on all the studied catalysts. However, the Au–Ag/(LSA)α-Al_2O_3 catalysts, which exhibited the comparatively good epoxidation performance, tended to induce slightly higher coke formation. TEM was employed to observe the mean particle size of the Ag nanoparticles on the surface of the investigated catalysts (Fig. 6). The results from the high resolution TEM (HRTEM) analysis show that Ag nanoparticles are highly dispersed on the alumina support for the freshly prepared catalysts. As exempli-

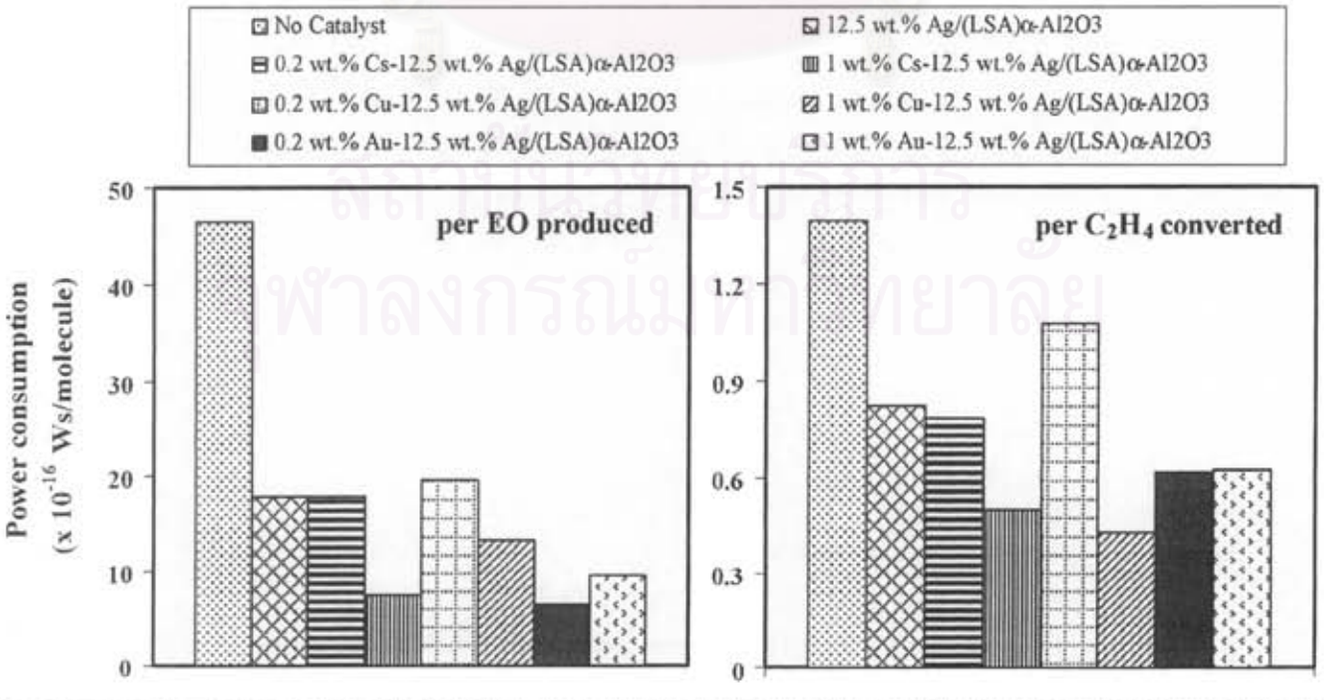

Fig. 5. Comparison of power consumptions per EO molecule produced and per C_2H_4 molecule converted of the corona discharge system over Ag catalyst with different promoters.

Please cite this article in press as: T. Sreethawong, et al., Ethylene epoxidation in low-temperature AC corona discharge over Ag catalyst: Effect of promoter, Chem. Eng. J. (2009), doi:10.1016/j.cej.2009.07.056

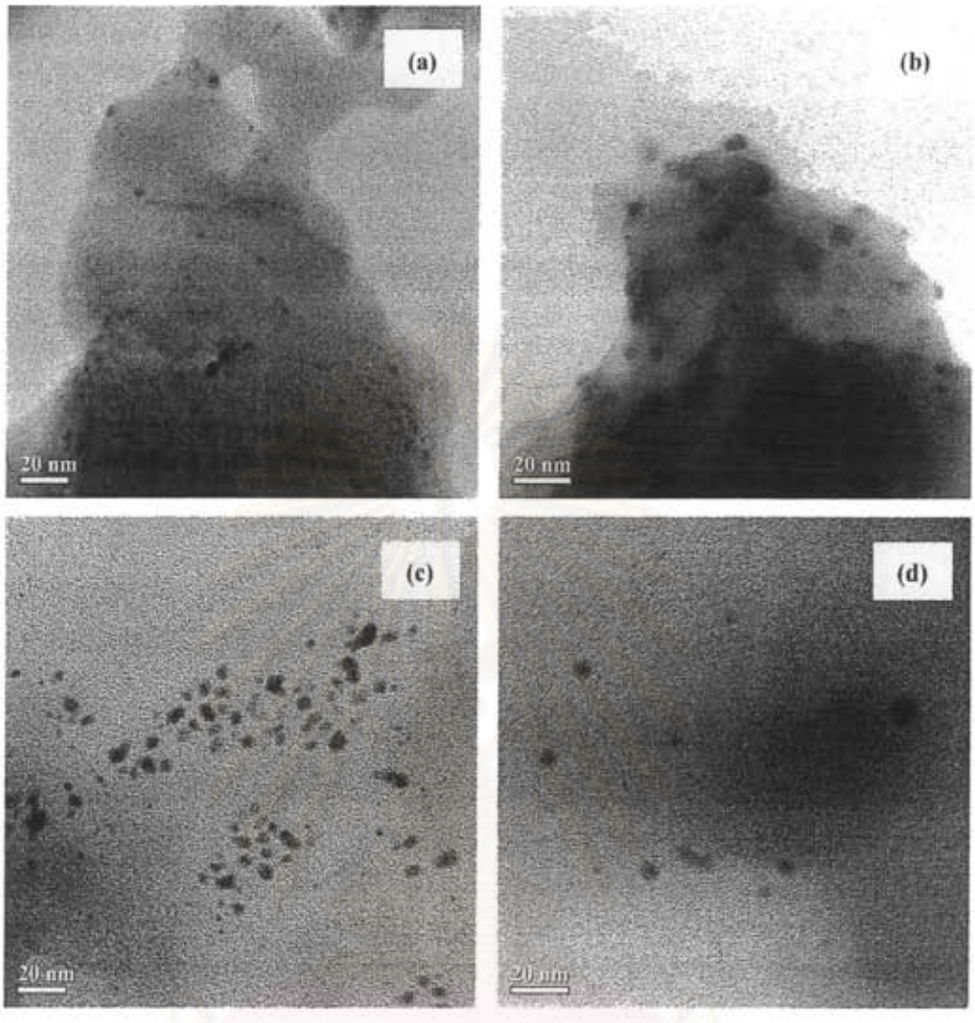

Fig. 6. HRTEM micrographs of Ag nanoparticles on (a) fresh and (b) spent 1 wt.% Cs–12.5 wt.% Ag/(LSA)α-Al_2O_3 catalyst, and (c) fresh and (d) spent 0.2 wt.% Au–12.5 wt.% Ag/(LSA)α-Al_2O_3 catalyst.

fied in Fig. 6, the HRTEM micrographs of the 1 wt.% Cs–12.5 wt.% Ag/(LSA)α-Al_2O_3 and the 0.2 wt.% Au–12.5 wt.% Ag/(LSA)α-Al_2O_3 catalysts, which exhibited superior activity toward ethylene epoxidation, as explained above, show average Ag particle sizes of approximately 5–7 nm for both of the fresh catalysts and approximately 9–12 nm for both of the spent catalysts, suggesting that the Ag agglomeration occurred after the activity testing under the corona discharge environment. This Ag agglomeration on the surface of the spent catalysts possibly results from the high energy intensity from the corona discharge with the pin and plate electrodes used in this work. For the corona discharge used in this work, the bulk gas temperature is comparatively low; however, the energetic electrons may have energy ranging from 1 to 10 eV, corresponding to extremely high temperatures of about 10^4–10^5 K [23–25]. This intense electron collision can induce a significant increase in the temperature of a number of micro-sized spots on the whole catalyst surface, inevitably leading to the Ag agglomeration. Even though the Ag agglomeration occurs on the catalyst surface, the Ag particle sizes are still very tiny, in the nanometer range (below 15 nm), and the Ag nanoparticles are still highly dispersed on the alumina support. To solve this Ag agglomeration, an ongoing research is being conducted with other types of plasma reactors, such as DBD, in our group. If this problem is resolved, the durability of the catalyst is also necessary to be investigated in our future work.

4. Conclusions

In this work, ethylene epoxidation was investigated in a combined catalytic–corona discharge system. The catalysts used were (LSA)α-Al_2O_3-supported 12.5 wt.% Ag with a 0.2 or 1 wt.% Cs, Cu, or Au promoter. The addition of the promoter on the Ag catalyst helps enhance the ethylene conversion and the EO yield and selectivity when combined with the corona discharge, especially for the 1 wt.% Cs–12.5 wt.% Ag/(LSA)α-Al_2O_3 and the 0.2 wt.% Au–12.5 wt.% Ag/(LSA)α-Al_2O_3 catalysts. The corona discharge system, combined with these catalysts, also consumed relatively low power to produce the EO molecule.

Acknowledgements

The authors would like to thank the Ratchadapisek Somphot Endowment Fund, Chulalongkorn University, Thailand; the Sustainable Petroleum and Petrochemicals Research Unit, Center for Petroleum, Petrochemicals, and Advanced Materials, Chulalongkorn University, Thailand; and the Petrochemical and Environmental Catalysis Research Unit under the Ratchadapisek Somphot Endowment Fund, Chulalongkorn University, Thailand.

References

[1] P.P. McClellan, Ind. Eng. Chem. 42 (1950) 2402.

Please cite this article in press as: T. Sreethawong, et al., Ethylene epoxidation in low-temperature AC corona discharge over Ag catalyst: Effect of promoter, Chem. Eng. J. (2009), doi:10.1016/j.cej.2009.07.056

[2] S. Matar, M.J. Mirbach, H.A. Tayim, Catalysis in Petrochemical Processes, Kluwer Academic Publishers, Dordrecht, The Netherlands, 1989.
[3] J.G. Serafin, A.C. Liu, S.R. Seyedmonir, J. Mol. Catal. A: Chem. 131 (1998) 157.
[4] K.L. Yeung, A. Gavriilidis, A. Varma, M.M. Bhasin, J. Catal. 174 (1998) 1.
[5] W.S. Epling, G.B. Hoflund, D.M. Minahan, J. Catal. 171 (1970) 490.
[6] S.N. Goncharova, E.A. Paukshtis, B.S. Bal'zhinimaev, Appl. Catal. A: Gen. 126 (1995) 67.
[7] M.A. Peña, D.M. Carr, K.L. Yeung, A. Varma, Chem. Eng. Sci. 53 (1998) 3821.
[8] D. Lafarga, A. Varma, Chem. Eng. Sci. 55 (2000) 749.
[9] E.A. Podgornov, I.P. Prosvirin, V.I. Bukhtiyarov, J. Mol. Catal. A: Chem. 158 (2000) 337.
[10] A. Ayame, Y. Uchida, H. Ono, M. Miyamoto, T. Sato, H. Hayasaka, Appl. Catal. A: Gen. 244 (2003) 59.
[11] M.C.N. Amorim de Carvalho, F.B. Passos, M. Schmal, J. Catal. 248 (2007) 124.
[12] S. Linic, J. Jankowiak, M.A. Barteau, J. Catal. 224 (2004) 489.
[13] J.T. Jankowiak, M.A. Barteau, J. Catal. 236 (2005) 366.
[14] J.T. Jankowiak, M.A. Barteau, J. Catal. 236 (2005) 379.
[15] J.C. Dellamorte, J. Lauterbach, M.A. Barteau, Catal. Today 120 (2007) 182.
[16] P.V. Geenen, H.J. Boss, G.T. Pott, J. Catal. 77 (1982) 499.
[17] N. Toreis, X.E. Verykios, J. Catal. 108 (1987) 161.
[18] R. Herrera, A. Varma, E. Martínez, Stud. Surf. Sci. Catal. 55 (1990) 717.
[19] D.I. Kondarides, X.E. Verykios, J. Catal. 158 (1996) 363.
[20] S. Rojluechai, S. Chavadej, J.W. Schwank, V. Meeyoo, Catal. Commun. 8 (2007) 57.
[21] S. Chavadej, S. Rojluechai, J.W. Schwank, V. Meeyoo, Mechanisms in Homogeneous and Heterogeneous Epoxidation Catalysis, Elsevier, 2008, p. 283.
[22] B. Elissson, U. Kogelschatz, IEEE Trans. Plasma Sci. 19 (1991) 1063.
[23] H. Suhr, H. Pfreundschuh, Plasma Chem. Plasma Process. 8 (1988) 67.
[24] L.A. Rosacha, G.K. Anderson, L.A. Bechtold, J.J. Coogan, H.G. Heck, M. Kang, W.H. McCulla, R.A. Tennant, P.J. Wantuck, NATO ASI Ser. Part B (1993) 34.
[25] P. Patiño, F.E. Hernández, S. Rondón, Plasma Chem. Plasma Process. 15 (1995) 159.
[26] S. Chavadej, A. Tansuwan, T. Sreethawong, Plasma Chem. Plasma Process. 28 (2008) 643.
[27] T. Sreethawong, T. Suwannabart, S. Chavadej, Plasma Chem. Plasma Process. 28 (2008) 629.
[28] S. Rojluechai, S. Chavadej, J.W. Schwank, V. Meeyoo, J. Chem. Eng. Jpn. 39 (2006) 321.
[29] W.S. Epling, G.B. Hoflund, D.M. Minahan, J. Catal. 171 (1997) 490.
[30] S.A. Tan, R.B. Grant, R.M. Lambert, J. Catal. 106 (1987) 54.
[31] M. Kitson, R.M. Lambert, Surf. Sci. 109 (1981) 60.

Please cite this article in press as: T. Sreethawong, et al., Ethylene epoxidation in low-temperature AC corona discharge over Ag catalyst: Effect of promoter, Chem. Eng. J. (2009), doi:10.1016/j.cej.2009.07.056